Elucidating the mechanism of action of novel small molecule activators of differentiation in acute myeloid leukemic cells



Purnima Kumar

St Hugh's College

University of Oxford

Thesis submitted for the degree of Doctor of Philosophy in Pharmacology

January 2020

Declaration of Authorship

The work presented in this thesis is my own, except where otherwise stated. No part of this thesis has been submitted for any other degree at this or any other university.

Purnima Kumar

January 2020

Dedication

For my father Anil Kumar and mother Rita Kumar who always thought I was going to be a Doctor and supported me throughout.

Acknowledgement

First and foremost, I must extend my most sincere thanks to **Prof Angela Russell** for allowing me to be a part of the AJR group and for making this whole thing possible. For guiding me through my DPhil and for encouraging me throughout. My warmest thanks to **Prof Thomas Milne** for guiding me in this project with his expertise.

Dr Laia Josa Culleré, I cannot thank you enough for your commitment to supervise for the past three and a half years. I have learnt so much from you both inside and outside the lab. Thank you for your invaluable advice throughout this project and for your diligence in proofreading this thesis. Thank you for being the excellent mentor- without you this wouldn't have been possible.

Dr Thomas Jackson, thank you for your valuable contribution to this project. For helping me with the RNA sequencing analysis, for guiding me through most of the new techniques and for always agreeing to share the batch of cells.

Thank you to everyone in the Paresh group for making me a part of the group and for letting me enjoy the tea and cake Mondays. Special thank you to **Hedia** for introducing me to western blot and for always pushing me to have a prettier looking blot. Thank you to **Nick** in the Milne group for all your suggestions with the HDAC recombinant assays.

Thank you to everyone in the AJR group for making it such a fun place to work and for providing all the help in need. Thank you to **Graham, Carole** and **Maria** for their helpful advice over the years. Thank you**, Carole,** for providing the BMP plate used in the phenotypic screening.

Thank you to the most amazing DPhil group. You girls made it possible to survive the gloomy days with the amazing coffee and cake chats. **Isabel**, the most fun loving and hard working. Thank you for encouraging and inspiring me throughout. **Alice** you are the most hard-working chemist AJR group has. I am sure you would do amazingly well in this and whatever comes

ahead. **Rachel**, besides being an amazing scientist, you are a lovely friend. Thank you for listening to my RNA sob stories and for coming to my rescue all the time. **Ria,** an excellent chemist, biologist and the best baker the two departments can ever have, thank you for bringing those delicious cupcakes and cakes for us. Thank you all for giving me the best time I had in UK. My best wishes and love with you girls.

Thank you to my lovely Pharmacology friends, for being the second family to me in Oxford and for all the fun and laughter over the past five years.

To my wonderful friends **Agota** and **Jelena,** thank you for having my back since I stepped in Oxford. Thank you for always sharing my happiness, and for being such an inspiration. I certainly wouldn't have made it through without you both.

Thank you to my amazing **family** in Delhi, for encouraging me throughout and for all the love and support. Thank you for my meal reminders and for taking such good care of me.

Thank you to my parents **Mr. Anil** and **Rita Kumar** without whose love, support and sacrifices I wouldn't have been able to live the dream of coming to Oxford or becoming a Doctor. Your hard work and love inspire me to become a better scientist and excel in whatever I choose to do.

Lastly, a big thank you to my husband **Rishabh** whose been a constant support through thick and thin. Thank you for helping me sail through this and for believing in me always. Thank you for patiently helping me format this thesis. Your love and support inspire me to bring out the best in me. Thank you for being the one to come on this journey with me.

Abstract

Acute Myeloid Leukaemia (AML) is a haematopoietic malignancy which comprises of different genetic subtypes with a common hallmark of differentiation arrest. In abnormal haematopoiesis, overcoming the differentiation blockade has emerged as an attractive therapeutic strategy. While current approaches target specific genetic mutations, herein we were interested in identifying novel agents which may be effective in multiple patient populations. In a small phenotypic screen, compounds were identified which increased the expression of CD11b- a cell surface receptor known to indicate differentiation of myeloid lineages. In an assay with six genetically distinct AML cell lines, clinical histone deacetylase inhibitors (HDACi) and some novel derivatives were observed to cause an upregulation in CD11b expression. These were further validated by a change in cell morphology and a block in proliferation, with a cell cycle arrest at G1 phase. The novel derivatives were successfully resynthesized along with potential inactive ones devoid of the zinc ion active site binding motif. Recombinant HDAC inhibitory assays and *in situ* HDAC inhibitory assays were performed which allowed to understand the profile of all the derivatives synthesized and be distinguished as HDACi and non HDACi. To elucidate the mechanism of action of these novel HDACi in detail, we explored various cell cyclins and cell cyclin inhibitors related to G1 arrest. By western blot it was seen that the novel HDACi causing G1 arrest did not cause the concomitant increase of cell cyclin inhibitor p21 unlike mocetinostat, suggesting a potential secondary downstream target for some of the effects observed. Further work using RNA sequencing allowed us to better understand the molecular events that underpin these responses and helped us confirm the selectivity of our novel HDACi. It was interesting to observe that the derivatives serving as mechanistic probes devoid of zinc ion active site binding motif were not HDACi but still initiated differentiation, further confirmed by the observed block in proliferation and the

change in morphology and were recognised as non HDACi. However, the cell cycle arrest with these non HDACi was observed at G2 phase in HL60 cells. Moreover, the sequencing results of these derivatives highlighted the role of cell cycle regulatory kinases leading to G2 arrest and the concomitant increase in CD11b expression suggesting these may be future therapeutic targets for differentiation agents in AML.

Table of Contents

List of Abbreviations 1

Chapter 1: Introduction 5

1.1 Acute Myeloid Leukaemia 5

1.2 Therapy of AML 13

1.2.1 Targeted Therapy of AML 13

1.2.1.1 IDH1/2 inhibitors 14

1.2.1.2 FLT3 Inhibitor 15

1.2.1.3 DOT1L inhibitors 16

1.2.2 Epigenetic Modifiers 17

1.3 Differentiation Therapy in AML 18

1.3.1 ATRA for targeted treatment of AML 18

1.3.2 Understanding of the clonal heterogeneity in AML 20

1.3.3 Inhibition of Dihydroorotate Dehydrogenase (DHODH) as a new therapeutic approach to overcome AML differentiation Blockade 22

1.4 Histones and their altered states 24

1.4.1 Histone Deacetylase Inhibitors 26

1.4.2 The Role of HDACi in AML 28

1.5 Cell Cycle 31

1.5.1 Cell cycle arrest during differentiation 32

1.5.2 The role of cell cyclins and their inhibitors in the cell cycle process 32

1.5.3 The cell cyclins involved in G1 arrest and G2 arrest 33

1.6 HDACi and cell cycle arrest 34

1.7 Background of the project 35

Chapter 2: Materials and Methods 38

2.1 Biological Materials and Methods 38

2.2 Chemistry Experimental Procedure 52

2.2.1 General Experimental Section 52

Chapter 3: Screening 62

3.1 CD11b upregulation in OCI- AML3, HL60, THP1 and KG-1 64

3.1.1 Hits across different cell lines 64

3.2 Isotype Control 68
3.3 Morphology analysis and block in proliferation 69
3.4 Cell Cycle analysis 73
3.5 Synthesis 75
3.5.1 Synthesis of mocetinostat (PK022) and its *meta* analogue (PK026) 77
3.5.2 Synthesis of the novel compound D6 (D6) and its *meta* analogue (PK040) 78
3.6 Dose response curves in HL60 cell line 79
3.6.1 Dose response curve in OCI-AML3 and THP1 80
3.7 Western blot 81
3.8 CD11b Time point study- HL60 cell line 82
3.8.1 Western blot timepoint study 85
3.9 Discussion 86
Chapter 4: Compound Profiling 88
4.1 Pan HDAC inhibitory assays 89
4.1.1 Optimising the protein amount from HL60 cells for the assay 91
4.2.1 *In situ* HDAC activity assessment 94
4.3 Recombinant Enzyme Assays 97
4.3.1 HDAC1 97
4.3.1.2 HDAC2 98
4.3.1.3 HDAC 6 99
4.3.1.4 HDAC11 100
4.4 Apoptosis Assay 101
4.5 Rescue Experiment 104
4.5.1 Transient Transfection with HDAC1- GFP plasmid 106
4.5.2 Transfection with only HDAC1 plasmid 111
4.6 Discussion 117
Chapter 5: Cell Cycle analysis and Target Validation 119
5.1 G1 arrest in AML cell lines 120
5.3 G2 arrest and differentiation 123
5.4 Cell cyclins 126

5.5 Microtubule Inhibition assay 130
5.6 RNA samples 131
5.7 Discussion 139
Chapter 6: Conclusion and Future Work 141
6.1 Conclusion 141
6.1.1 Summary of the work 141
6.1.2 Significance of this work 145
6.2 Future Plans 146
Appendices 148
Bibliography 175

List of Abbreviations

2 HG	alpha hydroxy glutaric acid
AML	acute myeloid leukaemia
APL	acute promyelocytic leukaemia
ATO	arsenic trioxide
ATRA	all trans retinoic acid
BM	bone marrow
Brq	brequinar
CDKs	cyclin dependent kinases
CLPs	common lymphoid progenitors
CML	chronic myelocytic leukaemia
CMPs	common myeloid progenitors
CoR	co-repressors
CR	complete remission
DHODH	dihydroorotate dehydrogenase
DNMT3A	DNA (cytosine-5)-methyltransferase 3A
FAB	French American British

FLT3	fms like tyrosine kinase 3
HDACi	histone deacetylase inhibitor
HLA	human leukocyte antigen
HSCs	hematopoietic stem cells
HSCT	hematopoietic stem cell treatment
IDH1/2	isocitrate dehydrogenase 1 and 2
ITD	internal tandem duplication
MLL	mixed lineage leukaemia
NADPH	reduced nicotinamide adenine dinucleotide phosphate
NGS	next generation sequencing
NPM1	nucleophosmin
PKMT	protein lysine methyltransferases
PML-RAR	promyelocytic leukaemia/retinoic acid receptor
SAHA	suberoylanilide hydroxamic acid
TCA	tricarboxylic acid cycle
TET2	tet methylcytosine dioxygenase 2
TSA	trichostatin

Ubq	ubiquitylation
VPA	valproic acid
αKG	alpha ketoglutaric acid

Chapter 1: Introduction

1.1 Acute Myeloid Leukaemia

Acute myeloid leukaemia refers to a disease of the blood and the bone marrow. It is a well characterised haematological malignancy that is marked by uncontrolled proliferation of leukemic cells, decreased apoptosis and a block in differentiation leading to an increase of immature cells (Longo et al., 2015). These immature cells accumulate in the blood affecting the formation of other normal cells, thereby influencing the normal functions of the cells in the blood system. The various types of leukemia are identified by the target cell that undergoes transformation. When the cancer develops in the lymphocytes it is called lymphocytic leukemia, when it is of the granulocytes or monocytes it is called myelogenous leukemia. The rate of disease progression also defines the type of leukemia. In the chronic phase the hematopoietic cells mature slowly, thus the disease progression is slow. On the other hand, in acute leukemia the progenitors proliferate rapidly, and mature hematopoietic cells decrease in number causing rapid disease progression. The current therapies for AML largely involves chemotherapy and hematopoietic stem cell transplantation both of which are not well tolerated by elderly patients (Mughal et al., 2010).

According to a recent statistic, in the United States (U.S.) there are 62,130 new cases of leukaemia recorded in 2017 out of which 24,500 are the estimated deaths (Jemal et al., 2007). Recently, a survey examined the incidences and deaths of leukaemia and overall cancer in the U.S. from 1998 to 2018. The acute myeloid leukaemia (AML) and chronic myeloid leukaemia (CML) incidences remained constant prior to 2011 but have climbed up substantially since then; the chronic lymphocytic leukaemia (CLL) incidence has increased continuously since 1998. The significant increase of myeloid leukaemia and CLL incidences was strongly correlated with the U.S. population aging. The incidence of all cancers was increased in

correlation with a small increase in aging population prior to 2011, but surprisingly has changed marginally since 2011, which was not significantly correlated with the accelerated population aging. It was also observed that the most substantial decline of deaths was with CML, whereas AML deaths continued to rise in the past 20 years. In conclusion, the overall cancer incidence was not increased as fast as previously feared with aging Americans; however, the incidences of myeloid leukaemia and CLL significantly outpaced that of all cancers (Hao et al., 2019).

For understanding AML, it is important to understand the normal hematopoietic system. The haematopoietic system has well characterised normal stem cells. In a normal haematopoietic system, there is a downshift from being pluripotent to multipotent and finally unipotent. Haematopoietic stem cells or HSCs can be subdivided into long-term self-renewing HSCs, short-term self-renewing HSCs and multipotent progenitors. They give rise to common lymphoid progenitors (CLPs; the precursors of all lymphoid cells) and common myeloid progenitors (CMPs; the precursors of all myeloid cells) (Metcalf, 2007). Figure 1.1 describes the normal cell hierarchy with two major progenitor cell lineages.

However, cancer of the haematopoietic system or leukaemia provides the best evidence that normal stem cells are targets of transforming mutation and that cancer cell proliferation is driven by cancer stem cells. In leukaemia, there is an increase in the proliferative capabilities and decrease in the differentiation capabilities.

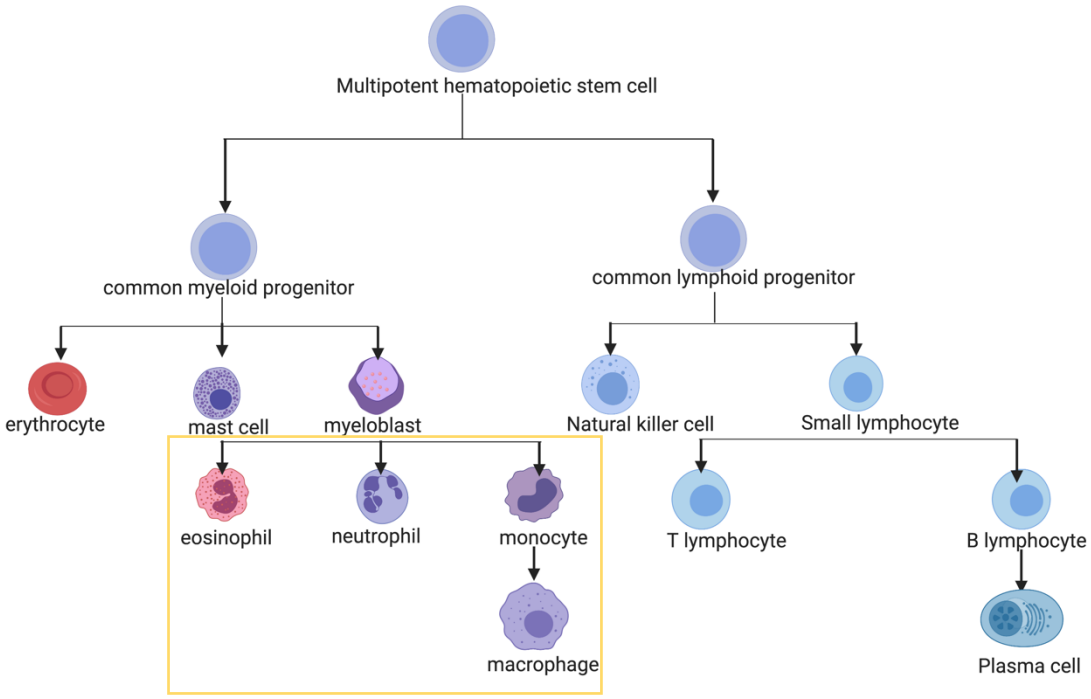


Figure 1.1: Normal Hematopoietic stem cell: in AML there is maturational myeloblast arrest (denoted by yellow box). They do not fully differentiate and have uncontrolled proliferation ability.

French American British Classification (FAB) classifies AML from M0 to M7, based on the type of cell from which leukaemia develops and the maturity of the cells (Table1.1) (Schiffer et al., 2003).

FAB subtype	Name	Cytogenetics	Adult AML patients (%)
M0	Undifferentiated acute myeloblastic leukemia		5%
M1	Acute myeloblastic leukemia with minimal maturation		15%
M2	Acute myeloblastic leukemia with maturation	t(8;21)(q22;q22), t(6;9)	25%
M3	Acute promyelocytic leukemia	t(15;17)	10%
M4	Acute myelomonocytic leukemia	inv(16)(p13q22), del(16q)	20%
M4eos	Acute myelomonocytic leukemia with eosinophilia	inv(16), t(16;16)	5%
M5	Acute monocytic leukemia	del (11q), t(9;11), t(11;19)	10%
M6	Acute erythroid leukemia		5%
M7	Acute megakaryocytic leukemia	t(1;22)	5%

Table 1.1: FAB classification of AML subtypes with its cytogenetics and percentage of patients affected (Grimwade et al., 2017).

M0 is the most common among adult patients. It accounts for 5-10% in all AML patients. The most common characteristics of this type of AML includes blasts with small to medium sized cells and eccentric nucleus. The nucleus is flattened and contains fine chromatin with several distinct nucleoli. The cytoplasm does not have granules.

M1is found in all age groups but highest incidence is seen in adults and infants. Cells have poorly differentiated myeloblast with finely reticulated chromatin and distinct nucleoli. Auer rods are present.

M2 abnormal maturation of neutrophils with the presence of segmentation and auer rod distinguishes AML-M2 subtype from AML-M1.

M3 results from fusion of truncated retinoic acid receptor alpha gene on chromosome 17 to a transcription unit called (t8;21) and PML for promyelocytic leukemia on chromosome 15. The

blasts are large with abundant cytoplasm and the nucleus is usually irregular. The cytoplasm is completely occupied by closely packed large granules. ATRA has significantly reduced the early mortality rate associated with AML-M3, also discussed later in the chapter in section 1.2.2.

M4 is also known as acute myelomonocytic leukemia as it has an increased proportion of leukemia monocytic cells than M1, M2 and M3. It can sometimes also be characterized by increase in marrow eosinophils. It has been reported to have inv (16), (p13; q22) and del (16) (q22).

M5 is also known as acute monoblastic leukemia. It is characterized by 80% or more of monocytic cells. It has two distinct forms with maturation index of less than 4% known as 5a and 5 b form with maturation index of more than 5%.

M6 is a rare form of leukaemia that primarily affects the peripheral cells. Nucleated red cells demonstrate abnormal nuclear configuration. The erythroblast is abnormal with its morphologic features. Giant multilobular or multinucleated forms are common.

M7 is also known as acute megakaryoblastic leukemia. It is one of the rare forms of leukemia often characterized by micromegakaryocytes and undifferentiated blasts. Chromosomal abnormality of t (1;22) (p13;q13) has been reported in this subtype (Abdul-Hamid).

The FAB classification system can be useful, but it does not take into account many of the factors that are now known to affect prognosis. The World Health Organization (WHO) system, most recently updated in 2016, includes some of these factors to try to better classify AML (Arber, 2017) .

The WHO system divides AML into several groups based on the genetic abnormalities and chromosomal changes.

- AML with a translocation between chromosomes 8 and 21 [t(8;21)]
- AML with a translocation or inversion in chromosome 16 [t(16;16) or inv(16)]
- APL with the *PML-RARA* fusion gene
- AML with a translocation between chromosomes 9 and 11 [t(9;11)]
- AML with a translocation between chromosomes 6 and 9 [t(6:9)]
- AML with a translocation or inversion in chromosome 3 [t(3;3) or inv(3)]
- AML (megakaryoblastic) with a translocation between chromosomes 1 and 22 [t(1:22)]
- AML with the *BCR-ABL1* (*BCR-ABL*) fusion gene
- AML with mutated *NPM1* gene
- AML with biallelic mutations of the *CEBPA* gene (that is, mutations in both copies of the gene) (Arber, 2017).

These along with the FAB classification allow us to broadly categorize different types of leukaemia with both altered morphological changes and with genetic abnormalities. Genetic heterogeneity refers to the mutation at two or more genetic loci that produce the same or similar phenotypic effects and the epigenetic heterogeneity arises as a result of these mutations in the genome affecting the downstream proteins/enzymes (Mcginniss et al.). However, the understanding of genetic and epigenetic heterogeneity of leukaemia has been an evolutionary process driven by clonal selection. The next generation sequencing (NGS) has also allowed the discovery of the genetic mutations that lead to the cause and progression of AML. In NGS, DNA polymerase adds fluorescent nucleotides one by one onto a growing DNA template strand and each incorporated nucleotide is identified by its fluorescent tag. This allows for massive

parallel sequencing with each fragment being sequenced per run. On the other hand, exosome sequencing which uses the technique for sequencing all the protein coding regions in the genes of a genome has also enabled to analyse the epigenetic factors responsible for the progression of AML. At least 70% of patients with AML display at least one mutation in an epigenetic modifier (Riva et al., 2012).

The in-depth studies of genome sequencing highlight this heterogeneity as being multi-layered involving both genome and epigenome complexity. Furthermore, this heterogeneity, contributes to the understanding of this disease from a clinical point of view. In a model system proposed by Woalder et. al, AML with high genetic and epigenetic heterogeneity has been proposed to have a poor prognosis, whereas AML with low genetic and epigenetic heterogeneity has been proposed to have a better prognosis.

These mutations are multifaceted and include recurrent somatic mutations which can be divided into two classes. These include mutations in genes from receptor tyrosine kinase family including *FLT3, KIT, V-Ras* and *NRAS*. . These mutations mainly enhance proliferation and survival of the hematopoietic progenitors through activation of signalling pathways. The second class of mutations are in transcription factors such as *RUNX1, CEBPA* and *RARA* (Woalder, 2017). Mutations or translocations affecting these factors hinder cell differentiation and create an accumulation of immature progenitors. Interestingly these mutations are found in the subclonal cellular fractions indicating that these are late clonal events in the disease progression (Di Nardo and Cortes, 2016). The co-occurrence of these two mutations together or a change in transcriptional program as a result of either mutation alone is necessary for the onset of leukaemia (Woalder, 2017).

The disruption of epigenetic patterning with mutations in epigenetic modifiers such as *DNMT3A, IDH1/2* and *TET2* (explained in Section 1.2) also initiate AML. In a study by Welch

and colleagues it has been shown that the mutation of *NPM1* gene encoding aberrant *NPM1c* protein is an initial hit. Their data suggests that most of the somatic events in AML genomes appear to be random, pre-existing, background mutations in the hematopoietic cell that acquired the key initiating mutation (Welch et al., 2012). Also, clonal analysis of AML relapse patients outlines how in cases with *DNMT3A+NPM1*, *DNMT3A* may persist even if *NPM1* mutation is lost. Slush et al. have also found that *DNMT3A* and *IDH2* mutations exist in pre leukemic HSCs and also precede *NPM1*and *FLT3-ITD* mutations (Shlush et al., 2014). The complexity of clonal architecture and the vast heterogeneity between the genetic and epigenetic landscape has therefore vastly affected the success of clinical outcome in AML. This has been expanded upon in Section 1.4 with the example of understanding clonal heterogeneity in AML patients when treated with IDH2 inhibitor enasidenib.

There is a continuous attempt made to understand the complexity of AML. Studies conducted in the recent years have emphasized to move to NGS which provides detailed genetic abnormalities, base substitutions, small indels, copy number variations and translocations based on the parallel sequencing done of the millions of small DNA fragments ultimately sequencing the whole genome in a single day (Riva et al., 2012). Out of the above-mentioned techniques, whole genome sequencing has successfully recognized a good number of mutations in AML. The technique is designed to identify mutations in coding regions and also recognize structural abnormalities such as translocations and inversions. The understanding of novel somatic mutations mentioned before such as *IDH1/2, DNMT3A, MY888* and *MLL2* have been discovered using this approach and are helping substantially to change the clinical management and therapeutic decisions. This is of utmost importance in chemo resistant cases where novel genes or pathways can be targeted with alternative drug combinations. The challenge therefore lies in a successful transition from genetic discovery to therapeutic intervention.

1.2 Therapy of AML

Current AML treatment is largely based on intensive chemotherapy and hematopoietic stem cell transplantation (HSCT). Chemotherapy involves destruction of the leukemic cells. The two most common drugs used in the treatment include cytarabine and daunorubicin which primarily work by inhibiting the DNA synthesis. Along with these treatments being extremely cytotoxic for elderly patients, refractory AML and early relapse are issues which still need to be addressed (Mughal et al., 2010). The HSCT treatment involves the use of human stem cells with self-renewable properties which are responsible for the formation of the adult blood cells. HSCs can be harvested from peripheral blood, bone barrow, and umbilical cord blood and used in transplantation techniques and efficient therapies for haematological diseases; however, it is currently not possible to generate therapeutically viable HSCs for human patients. It is difficult to find matched human leukocyte antigen (HLA) donors which in turn makes it difficult to take advantage of the clinical benefits of HSCT (Kumar et al., 2019).

1.2.1 Targeted Therapy of AML

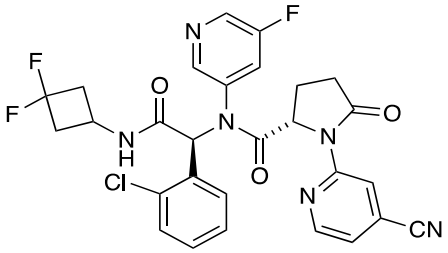
In the late twentieth century, targeted therapy was proposed for AML which focussed on cancer cells to differentiate (Sachs, 1987). Following this, several *in vitro* analyses made in 1970s and 1980s showed a number of compounds having anti-proliferative and pro-differentiating properties towards AML cells. For example, (Breitman et al., 1981) showed granulocytic differentiation of HL60 leukemic cells with all trans retinoic acid or ATRA (explained in detail in section 1.2.2).

However, over the past 2 years the amount of FDA approved frontline treatment for patients with AML have increased. Some of the recent approvals are IDH1/2 inhibitors, FLT3 inhibitors and DOT1L inhibitors which are all examples of targeted therapy for AML.

1.2.1.1 IDH1/2 inhibitors

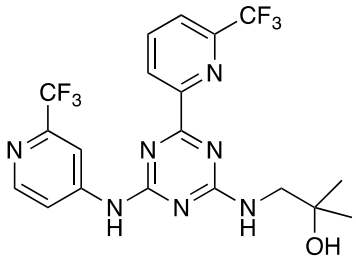
IDH1 and *IDH2* genes, located at 2q33.3 and 15q26.1, encode two isoforms of isocitrate dehydrogenase ($NADP^+$), the enzyme associated with the tricarboxylic acid (TCA) cycle. IDH1 and IDH2 are $NADP^+$ catalytic enzymes that normally catalyse the interconversion of isocitrate into alpha-ketoglutarate (αKG). In malignancies, mutation of the IDH enzyme leads to further reduction of αKG into the oncometabolite 2-hydroxyglutarate (2HG) which impairs cellular differentiation (Dang et al., 2009; Ward et al., 2010). Recent epigenetic studies have shown that aberrant DNA methylation is a key feature of AML, however other studies have also shown that DNA hypermethylation is a consequence of mutant IDH protein expression and that *IDH1/2* mutant mediated epigenetic effects contribute to AML pathogenesis (Figueroa et al., 2010). Inhibitors of mutant *IDH1* and *IDH2* are currently in Phase 1/2 clinical trials (Stein et al., 2015). Some drugs currently used for mutant *IDH1/IDH2* inhibition are as follows:

AG-120 or Ivosidenib: It is a first of its class, orally available, selective, potent inhibitor of mutated IDH1 protein currently in phase 1 clinical trial (Popovici-Muller et al., 2018).



AG120

AG-221or Enasidenib: *IDH2* mutant inhibitor. It is an oral, selective, potent inhibitor of IDH2 mutated protein (Stein et al., 2015).



AG221

1.2.1.2 FLT3 Inhibitor

Previous studies have shown a role of *FLT3/ITD* in myeloid differentiation (Radomska et al., 2006).

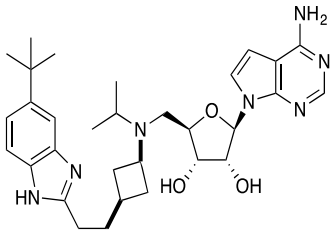
Quizartinib*:* In a study conducted by Sexauer et al., 2012 it was shown that among 14 patients who were treated with quizartinib there was a rapid clearance of peripheral blasts, which is also shown in other FLT3 inhibitors. BM aspirates collected from a representative patient, 1 week before and on days 15 and 29 of treatment with quizartinib also showed changes in the cellular morphology, with an increase in the mature myeloid cells (which increased from 9% to 57%). The presence of *CEBP-α* mutation offered an explanation as to why one patient had a lack of differentiation in response to the *FLT3* inhibition. They showed that the release of the differentiation block is an on-target effect of FLT3 inhibitor, because differentiation was induced successfully with sorafenib and with quizartinib.

Crenolanib: Point mutations of *FLT3* at aspartate 835 are observed in patients at a frequency of 7%. The mutation causes the receptor to become resistant to the FLT3 inhibitor such as sorafenib and sunitinib and is associated with the disease progression. When MOLM-14 and MV411 cell lines and FLT3 WT cell lines were treated with crenolanib for one hour and analysed by immunoblotting, it showed crenolanib inhibited *FLT3* activity. Crenolanib

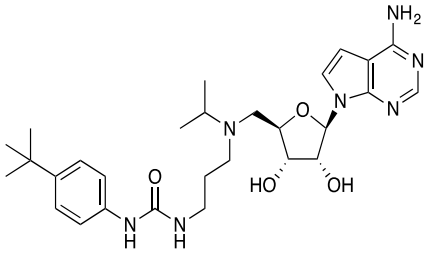
inhibited autophosphorylation of both WT and ITD mutated *FLT3* with an IC_{50} of 2nM (Galanis et al., 2014).

1.2.1.3 DOT1L inhibitors

DOT1L is a histone methyltransferase enzyme that targets the lysine 79 in the globular domain of histone H3 (H3K79) that is required for the development of MLL leukemia in model systems. Inhibitors of DOT1L like EPZ004777 and EPZ5676 can disrupt leukemia progression. All these inhibitors are at various stages of clinical development.



EPZ5676



EPZ004777

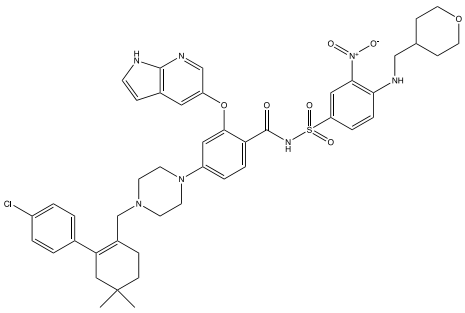
Study by Rau et al. has shown that the pharmacological inhibition of *DOT1L* with EPZ5676 resulted in a decreased expression of oncogenic genes and dose and time dependent inhibition of proliferation, induction of apoptosis and terminal differentiation in *DNMT3A* mutant cell lines *in vitro*. Treatment with EPZ004777 induced differentiation of *DNMT3A* mutant samples shown by increased expression of mature monocyte marker CD14, compared with vehicle treated controls (Rau et al., 2016) .

1.2.2 Epigenetic Modifiers

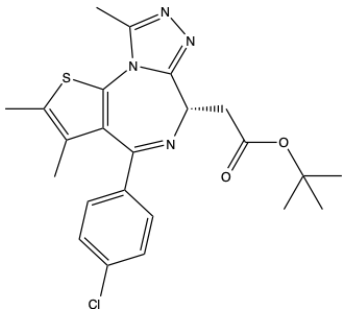
Certain agents disrupt key mutations or cell maintenance pathway of which examples include epigenetic modifier for *EZH2, ASXL1* or BCL2 inhibitors.

EZH2 augments leukemogenicity by reinforcing differentiation blockage in AML. The compounds used for inhibition of *EZH2* are EPZ005687 and GSK343 which perturb the disease progression and promote differentiation of AML cells (Tanaka et al., 2012).

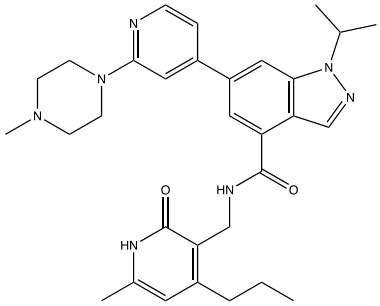
ASXL1 has functions to maintain both activation and suppressor of *HOX* genes. Studies have shown that *ASXL1* phenotype is characterized by differentiation defects in myeloid and lymphoid progenitors (Fisher et al., 2010). The BCL-2 family members interact to regulate initiation of apoptosis and are proapoptotic proteins. Inhibitors of BCl2 such as ABT-199 (Venetoclax) and ABT-263 (Navitoclax) initiate apoptosis and are thus clinically explored in cancer types including AML (Pan et al., 2014)(Knight et al., 2019).



ABT 199



JQ1



GSK343

1.3 Differentiation Therapy in AML

As explained previously, leukemic cells often have been shown to inhibit differentiation to genetic abnormalities or even epigenetic changes such as DNA hypermethylation. Overcoming the differentiation block seemed an attractive approach. It could overcome the disadvantages such as high toxicities from chemotherapy and the development of resistance from "targeted therapy". The first reports by Breitman, Collins, and Keene (1981) showed granulocytic differentiation of HL60 leukemic cells with all trans retinoic acid (ATRA) which was later approved by FDA in November 1995 for the treatment of acute promyelocytic leukaemia (APL). The next section discusses in detail, how ATRA was able to revolutionize the therapeutic approach in leukaemia.

1.3.1 ATRA for targeted treatment of AML

All trans retinoic acid (ATRA) led to a remarkable achievement by differentiating HL-60 cells with a terminal differentiation of 90% with 10 μM ATRA (Breitman et al., 1980).

This was however successful in acute promyelocytic leukaemia (APL) not in other AML subtypes. With the cloning of the receptor for retinoic acid in 1987, genetic approaches established the critical role of the retinoic acid-signalling pathway in regulation of myeloid differentiation. For instance (Tsai et al., 1992), showed that transfection of a dominant-negative *RARα* blocked myeloid differentiation of the FDCP1 cell line, the one which lacks FGF receptors and depends on interleukin 3 (IL-3) or granulocyte/macrophage colony-stimulating factor (GM-CSF) for its proliferation and survival. Surprisingly, murine knock-out models of *RARα* did not show a dramatic reduction in myelopoiesis. This was thought to be attributed to redundancy between the three isoforms of *RAR–α, β, and γ*, as double knockout of both *RARα* and *RARγ* is necessary to show impaired myelopoiesis. The strongest evidence for the involvement of *RAR* in myelopoiesis has come from detailed studies of *PML-RAR*, the fusion

protein expressed as a result of t(15;17) (q22;q21) in APL (Ablain et al., 2011). A balanced translocation between chromosome 15 and 17 leads to the formation of a fusion of promyelocytic leukaemia protein (PML) and *RARα* which was in 98% of APL patients (Redner, 2002; Rego et al., 2006). The *PML RARα* may inhibit normal function of PML protein and act as a tumour suppressor.

Pharmacological concentration of ATRA leads to a confirmation change of multifunctional molecule complex around *PML-RARα.* As shown in Figure 1.3 corepressors are released, normal regulation of *RAR-α* responsive genes is restored and terminal differentiation of APL cells is induced (Gianní et al., 2000).

Although in the first major study it had been shown that use of ATRA to treat APL was successful in all 24 patients. All the patients from this initial group relapsed due to the development of ATRA resistance (Niu et al., 1999).

To overcome the ATRA resistance, arsenic trioxide (ATO) emerged as an option for relapsed patients (Soignet et al., 1998; Niu et al., 1999). In a recent study, comparison of ATRA plus chemotherapy (idarubicin, mitoxantrone, methotrexate and 6-mercaptopurine) with ATRA plus ATO in patients with APL, showed 2-year event free survival rate of 97% in ATRA-ATO group and 86% in ATRA chemotherapy group (Lo-Coco et al., 2013; Lo-Coco and Cicconi, 2014).

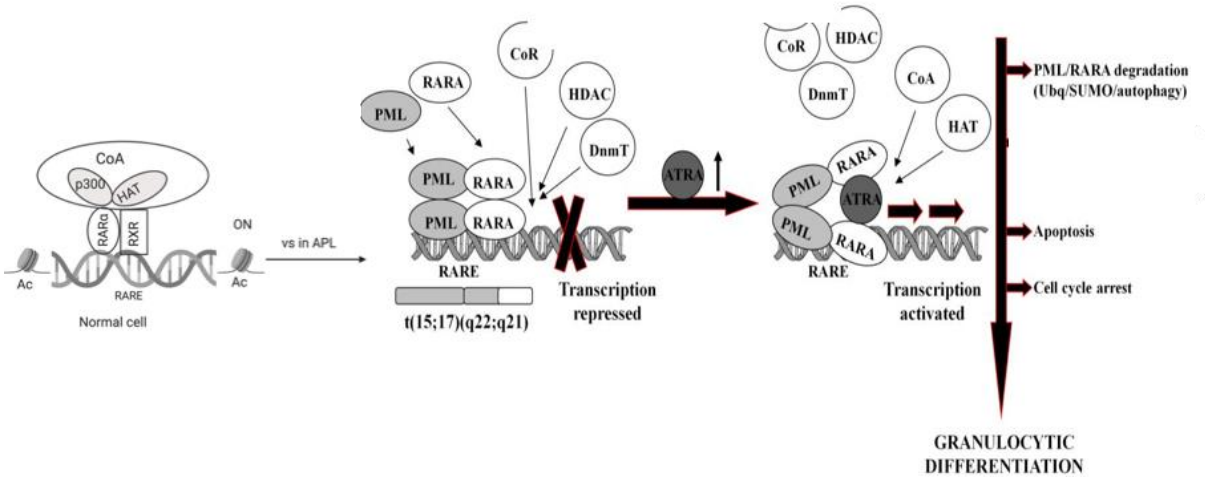


Figure 1.3: In APL cells, *PML-RARA* hereodimerization leads to the sequestration of co-repressor (CoR) complex, DNA hypermethylation and histones deacetylation, resulting in transcriptional repression. In the presence of high dose of ATRA the CoR is replaced by co-activator (CoA), allowing transcriptional activation and terminal differentiation of the APL cells into granulocytes. *PML-RARA* fusion protein undergoes degradation by several ways, including ubiquitination, sumoylation or authophagy. (PML: promyelocytic leukaemia; RARA: retinoic acid receptor; RARE: retinoid acid response elements; CoR: co-repressor; HDAC: histone deacetylase; DnmT: DNA methyltransferases; CoA: co-activators; HAT: histone acetyltransferase; Ubq ubiquitin) (Adapted from Gocek and Marcinkowska 2011).

Based on the understanding from these studies, new ways of treating the other 90% subtypes of AML need to be considered. It was possible to understand how small molecules target single clonal mutation in AML patients. The response to co mutation was not as successful, and it became important to understand how multiple mutation was limiting the clinical outcome in relapsed/refractory AML cases.

1.3.2 Understanding of the clonal heterogeneity in AML

As discussed above, differentiation arrest is a common feature of AML cells. Enasidenib, an *IDH2* mutant inhibitor, induced differentiation and is currently in clinical trials. In a phase 1/2

clinical trial, enasidenib monotherapy induced a clinical response in 40.3% patients with relapsed/refractory AML by inducing differentiation of the leukemic cells. In most of those responding patients terminally mature blood cells were *IDH2* mutant. However, in 12.6% of those responding patients *IDH2* mutant cells were eliminated and there was no response to enasidenib treatment. The patients that had initially responded also developed enasidenib resistance which was attributed to comutational burden and *NRAS* mutation (Quek et al., 2016). This study, however, did not assess the clones undergoing differentiation with enasidenib treatment or the clonal mechanism of enasidenib resistance. To understand this better, a subset of patients was selected, the majority of which were enasidenib responders. Enasidenib caused a clone specific differentiation response from ancestral (all nonterminal clones) or terminal clones. There was an acquired resistance due to a clonal evolution and clonal selection leading to the reestablishment of differentiation arrest. Clonal evolution at relapse highlighted variants in gene including *NFKB1*, *DDX1*, *DHX15* and *DEAF1*, some of them not being studied for AML before. Acquisition of additional *DHX15* and *DEAF1* mutation was known to be associated with the differentiation arrest. The study genotyped 110 single cells, at pretherapy and at CR. The results revealed an initiating *DNMT3A* clone (clone D) that acquired an *IDH2* mutation (clone DI). Subsequently, there was a branching clonal structure with two terminal clones; one acquired an *XPO1* mutation (clone *DIX*), whereas the other acquired two mutations (a second *DNMT3A* mutation and an *ASXL1* mutation; clone *DIdA*). This study demonstrates how any cancer therapy alters clonal structure across a fully transformed and premalignant cellular hierarchy. By defining clonal structures and mapping where clones were arrested across differentiation in purified hematopoietic compartments, this study helped to understand previously unavailable view of the same (Quek et al., 2018). However, the implications for future therapy are not yet clear.

1.3.3 Inhibition of dihydroorotate dehydrogenase (DHODH) as a new therapeutic approach to overcome AML differentiation blockade

An attractive approach of phenotypic screening for compounds to overcome myeloid differentiation has been conducted in AML. This approach offers the opportunity to discover new differentiation inducing therapies that are efficacious across multiple AML subtypes/mutations. Recently, a study identified compounds C03 and C07 to trigger differentiation as monitored by the CD11b expression in Lys-GFP-ER-HoxA9 cells (Sykes et al., 2016). HoxA9 was used in the model system as previous studies in the group have shown HoxA9 transcription factor to be commonly upregulated in a variety of AML cell lines (Lewis et al., 2016). The estrogen receptor ER helps to activate HoxA9. The lysosome is a myeloid marker for differentiation and GFP is positive upon maturation of the cells. They investigated the mechanism of the hits through the development of resistant GFP-ER-HoxA9 cells and U937 leukemic cell line, which were treated with increasing concentrations of their initial hit compounds C03 and C07. It was noticed that even after stopping the treatment, cells retained their resistance for more than six weeks. A detailed RNAseq analysis to discover the mechanism revealed eight upregulated genes in the resistant cell line, one of them being *DHODH* which encodes the metabolic enzyme DHODH and is used in the fourth enzymatic step that helps in the ubiquinone mediated oxidation of dihydroorotate to orotate in *de novo* pyrimidine biosynthesis (Figure 1.4). However, the low solubility and bioavailability of the above compound limited its use further; therefore, brequinar (BRQ) (a known DHODH inhibitor with clinical use) was taken forward. BRQ inhibited DHODH activity *in vitro* with an IC_{50} of 20 nM. Although a greater understanding needs to be developed for the mechanism of *DHODH* inhibition leading to myeloid differentiation, this approach opens up the possibility for targeting the genetic variability along with finding the new targets that cause the disease progression. It also helps to design a phenotypic screen that does not target just a specific

mutation or genetic lesion but also helps to find novel molecular mechanism of action which works in a broad group of patients (Lewis et al., 2016; Sykes et al., 2016).

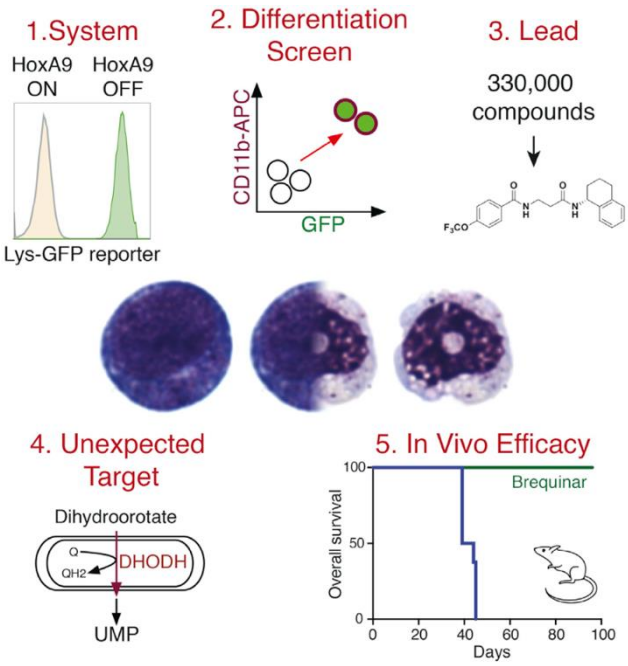


Figure 1.4: A phenotypic screen identifies *DHODH* as a target of AML. DHODH represents a metabolic vulnerability across a range of AML subtypes. DHODH inhibitors show potential in preclinical AML models (Adapted from Sykes et al., 2016).

This study has helped us to understand how the phenotypic screening using this approach can allow us to also target the clonal heterogeneity over a variety of AML cell lines.

Furthermore, using whole genome sequencing and NGS several epigenetic modifiers have been identified in the progression of AML. These epigenetic modifiers include proteins that chemically modify DNA or catalyse post-translational modifications on histones. Abnormal epigenetic patterns caused by these mutations can lead to aberrant gene expression in AML (Greenblatt and Nimer, 2014). This has resulted in several epigenetic modifier molecules to

enter clinical trials for AML (Pastore and Levine, 2016). Some of these epigenetic modulators include PKMT inhibitors, bromodomain inhibitors, lysine demethylase inhibitors, HAT modulators and HDAC inhibitors. However, we were in particular interested in HDAC inhibitors.

1.4 Histones and their altered states

Histones are a class of proteins that arrange DNA into nucleosomes, which become the repeating structures of the chromatin (Figure 1.5). The nucleosome contains 146 pairs of DNA bases wrapped around the histone core. The histone core contains two units each of H2A, H2B, H3 and H4. Each of these histone octamer cores is rich in lysine residue with *N*-terminal chains which are sites for post translational modifications including acetylation, deacetylation, ubiquitylation (Marks et al., 2001). The histones are altered in their state of acetylation by two set of enzymes known as HATs (histone acetyltransferases) and HDACs (histone deacetyltransferases). The state of acetylation of the histones is responsible for the alteration of the chromatin structure which in turn is responsible for the gene expression.

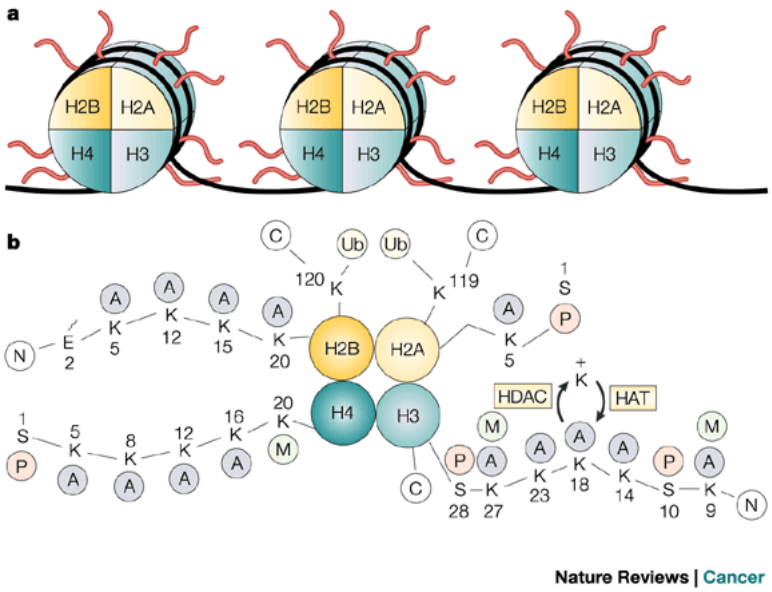


Figure 1.5 a: The core proteins of nucleosomes are designated H2A (histone 2A), H2B (histone 2B), H3 (histone 3) and H4 (histone 4). Each histone is present in two copies, so the DNA (black) wraps around an octamer of histones the core nucleosome. **b:** The amino-terminal tails of core histones. Lysines (K) in the amino-terminal tails of histones H2A, H2B, H3 and H4 are potential acetylation/deacetylation sites for histone acetyltransferases (HATs) and histone deacetylases (HDACs). Acetylation neutralizes the charge on lysines. A, acetyl; C, carboxyl terminus; E, glutamic acid; M, methyl; N, amino terminus; P, phosphate; S, serine; Ub, ubiquitin (Adapted from Davie 1998).

Since the acetylation of histones plays a key role in gene expression or repression, it is important to know that HDACs supress the gene expression. They are known to remove the charge neutralising acetyl groups from the lysine tails, which promotes a more condensed structure of the chromatin. HDACs have been divided into classes Class I, II and III. Class I have homology to yeast HDAC Rpd3 and includes HDAC 1, 2, 3 and 8. Class II HDACs include HDAC 4, 5, 6 and 7. Each of these HDACs identify different chromosomal sites and are hence reported to be involved in different transcriptional pathways. Class III of HDACs

shares homology with mouse and yeast Sir2. The Sir 2 is dependent on NAD^+ for activity and are hence insensitive to inhibition by any of the HDAC inhibitors (Figure 1.6)(Xu et al., 2007).

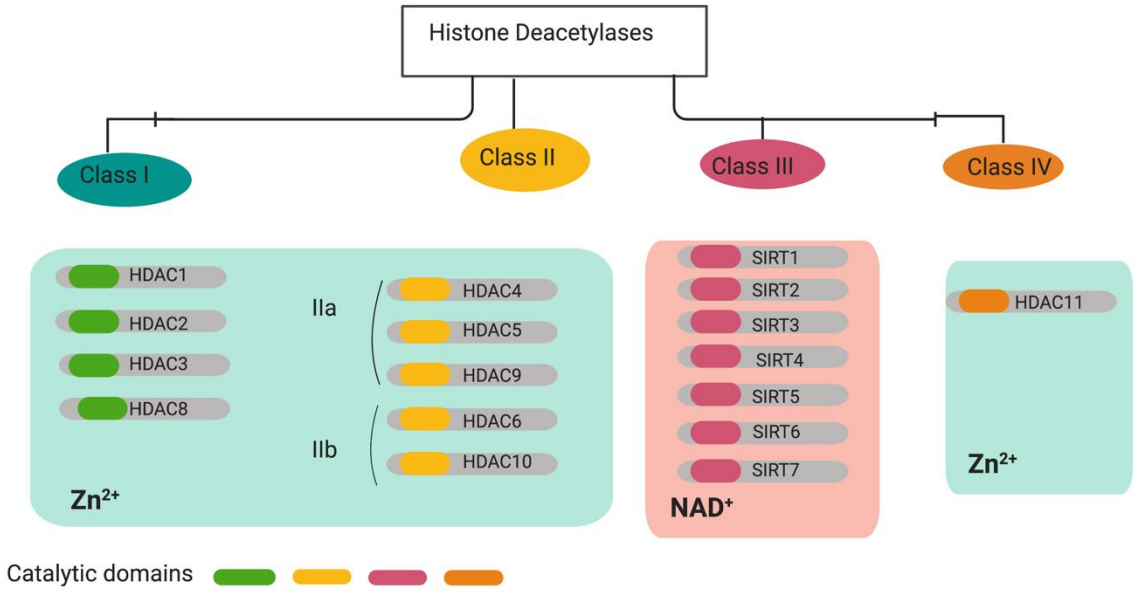


Figure 1.6: Different classes of HDACs. Four different classes of HDACs were identified in mammalian cell based on their sequence homology to corresponding yeast HDACs. Class 1 includes HDAC1,2,3 and 8. Class II can be divided into class IIa and IIb consisting of HDAC4,5,9 and 6 and 10 respectively. Class III is also known as sirtuins consisting of SIRT1-7. Class IV has its own structural similarity to class I and II.

1.4.1 Histone Deacetylase Inhibitors

HDAC inhibitors (HDACis) have been identified as a class of compounds which have a regulatory role in cell differentiation, apoptosis and growth arrest. There are different classes of HDACis. Firstly, short-chain fatty acids such as 4-phenylbutyrate and valproic acid. This class of compounds has not been explored a lot for structure activity relationship, but they are important in studying the effects of HDACs both *in vitro* and in clinical trials (Elmallah and

Micheau, 2019). These class of compounds have off-target effects which limit their specificity and therapeutic potential (Clawson, 2016).

HDAC inhibitors containing hydroxamic acids (such as SAHA, pyroxamide, TSA, oxamflatin and CHAPs) have been postulated to interact with the catalytic site of HDACs via a hydroxamic acid group, thereby blocking substrate access to the active zinc ion at its base, as shown by X-ray crystallographic studies (Figure 1.7 a, (Wagner et al., 2013)).

Another important class of HDACis is with a benzamide group. The benzamide group enters the catalytic site and binds to the active zinc atom. This class of HDACi includes mocetinostat, MS-275, CI-994 which all inhibit HDACs at nanomolar concentration (Xu et al., 2007).

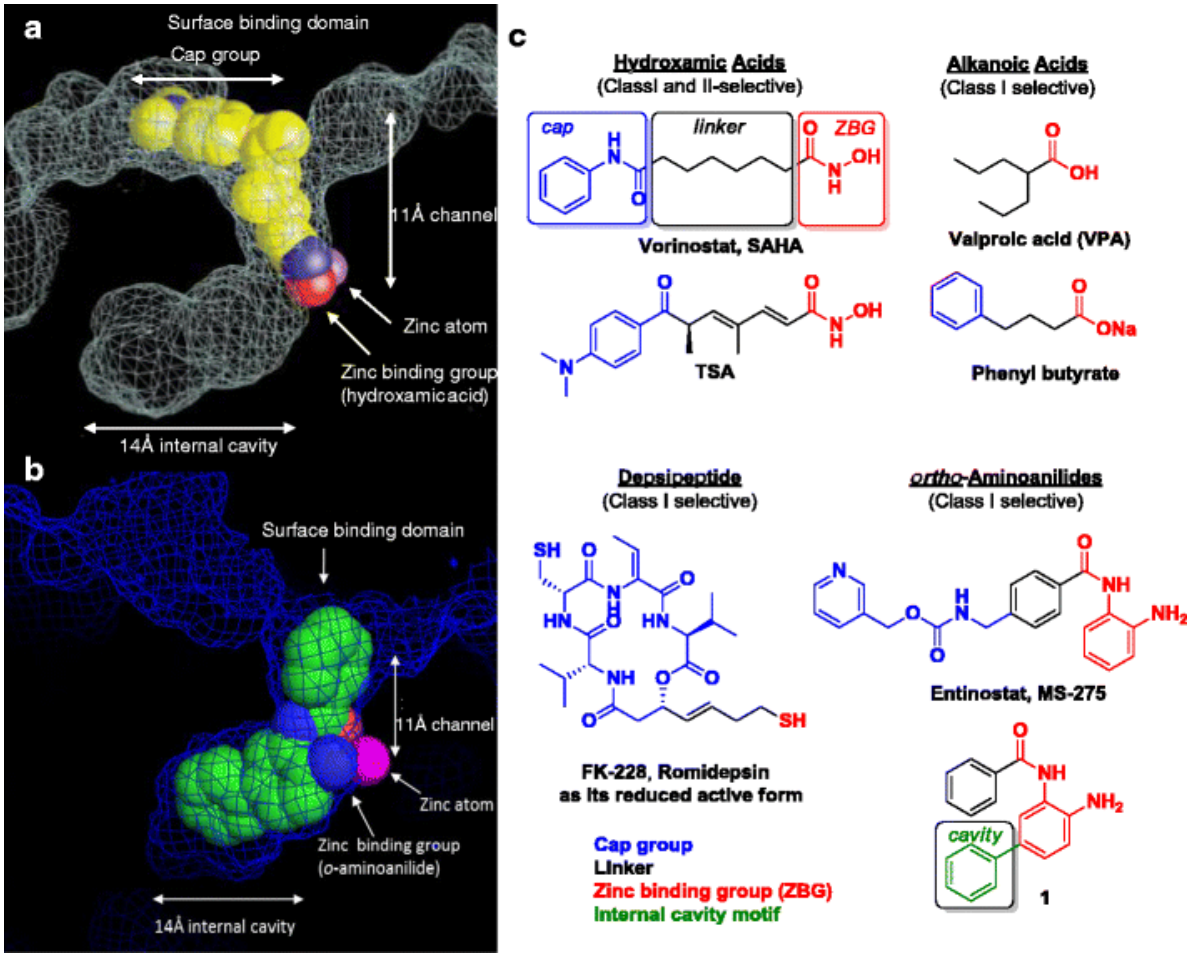


Figure 1.7: a) X-ray crystal structure of bacterial histone deacetylase-like protein and Trichostatin A (TSA). **b)** X-ray crystal structure of human histone deacetylase (HDAC) 2 and compound 1. **c)** Prototypical HDAC inhibitors (Adapted from Wagner et al. 2013).

1.4.2 The Role of HDACi in AML

HDACs are often overexpressed in AML cells. Some of the common HDACi such as romidepsin, belinostat, vorinostat are at various stages of clinical development and are often used in combination therapies for relapsed/refractory T cell lymphoma. However, HDACi comes with a complex mechanism of action which has only started to be unravelled recently. In particular, HDACi have been shown to increase the expression of CDK1 gene via the

upregulation of $p21^{(WAF1/Cip1)}$. This upregulation of p21 has been seen associated with G1 phase cell cycle arrest (Traore et al., 2005)(Rosato et al., 2003b).

HDACi can lead to cell death by activating apoptosis by both intrinsic and extrinsic pathways. HDACi increase levels of the death receptor ligands FasL and TRAIL (tumor necrosis factor-related apoptosis-inducing ligand), as well as of death receptors Fas and DR5 in leukemic cells and activate the extrinsic apoptotic pathway. However, this increase is unique to cancer cells (Figure 1.8). Increase in the acetylation of the histones located at the TRAIL gene promotor causes an increase in the expression of TRAIL mediated by the transcription factors Sp1 and Sp3. Interestingly, blocking TRAIL expression does not abrogate apoptosis in response to HDACis in leukemic cells, indicating the additional mechanisms of apoptosis which are responsible for cell death observed with these compounds (Santos, 2011). Some of the studies also confirm the upregulation of intrinsic apoptotic pathway dependent on the mitochondria via HDACi. This leads to the increase of proapoptotic factors such as BCl2 proteins (Xu et al., 2007).

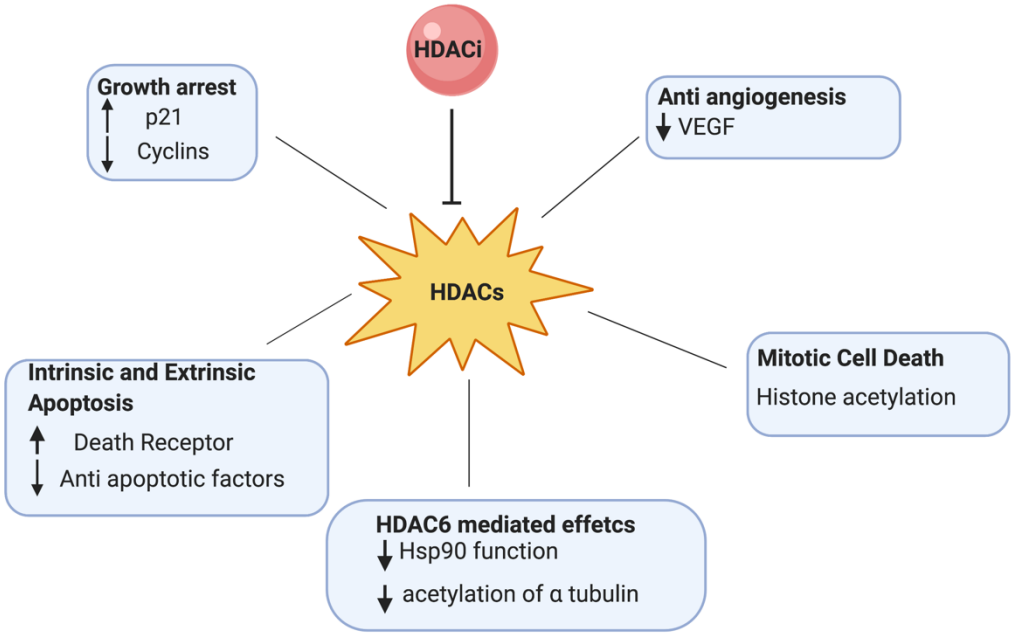


Figure 1.8: The role of HDAC inhibitors on cellular mechanisms and pathways.

MS-275 is one such HDACi known for its role of causing differentiation and anti-proliferation in leukemic cell lines U937 and K562. The studies by Rosato et al. revealed that the effects mediated by this compound were dose dependent and lower doses of MS-275 caused differentiation via an upregulation of p21 cell cyclin inhibitor and also a down regulation of cell cyclin D1. However, higher concentration of MS-275 in both leukemic cells and primary AML patient cell blasts confirmed the potent upregulation of cell death signalling pathway accompanied by the increase in ROS generation species and decrease in cell cyclin proteins such as p21, p27, BCL-2 and pRb (Rosato et al., 2003a).

It has also been reported that in the AML cell line U937, MS-275 and other HDACi such as SAHA and VPA show antitumor activity by the induction of TRAIL and more specifically its death receptor ligand DR5. RNA interference studies have shown that p21 causes G1 arrest

and confirmed TRAIL as the cause of rapid MS-275 induced cell death. It was also worth noting that p21 mediated G1 arrest and the TRAIL induced cell death were independent mechanisms as the knockdown of one did not affect the other (Nebbioso et al., 2005a).

1.5 Cell Cycle

The cell cycle phase is divided into four major phases G1, S, G2 and M phase. Each of the phase has different checkpoints which contribute towards the different progression of the cell (Figure 1.9).

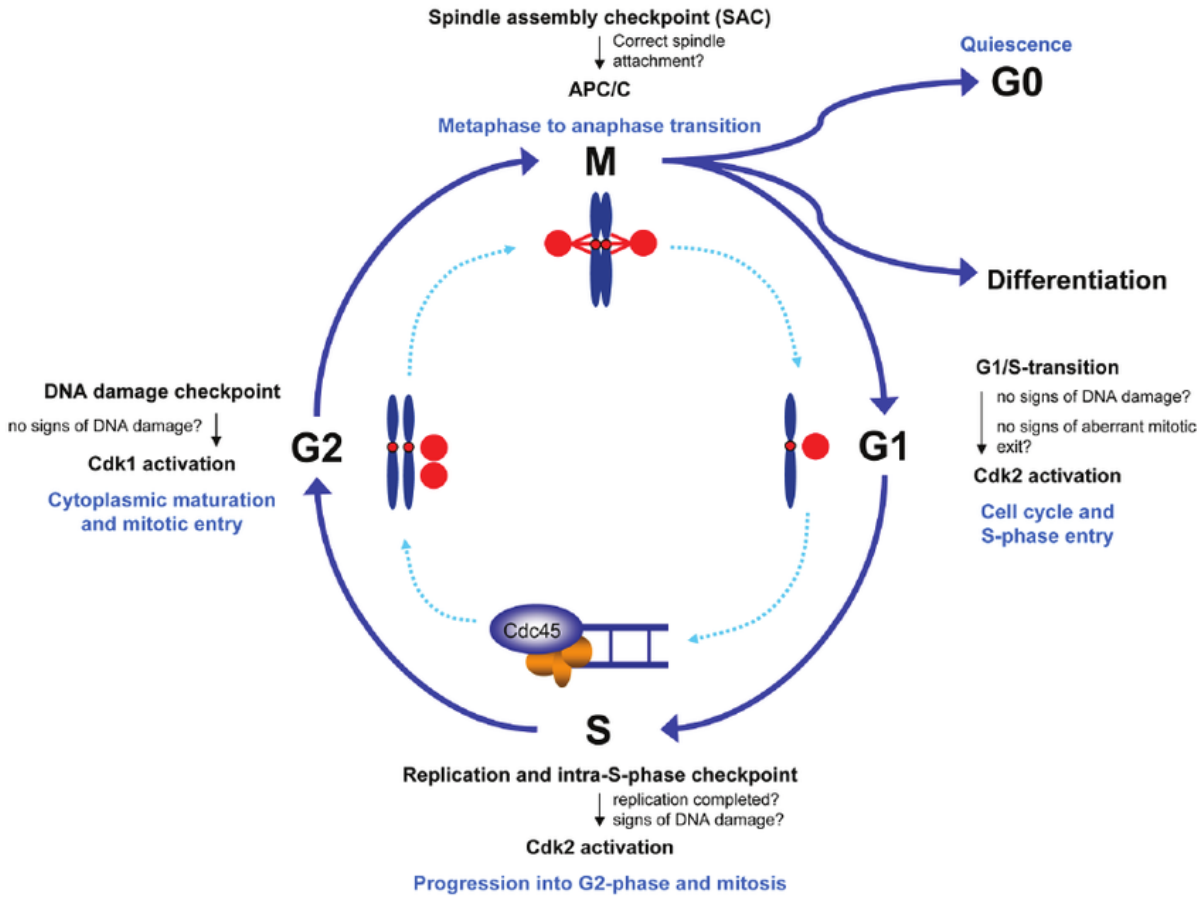


Figure 1.9: Normal cell cycle progression and its checkpoints. The human cell cycle can be divided into four phases - G1-phase, S- phase, G2-phase and M-phase (mitosis). The requirements for cell cycle progression are tightly regulated by the checkpoints (Adapted from Schnerch et al. 2012).

In leukaemia, DNA damage and weakened cell cycle checkpoint adds to the progression of the disease by enhancing the genetic aberration. Thus, to fully understand leukaemia it is important to understand clearly the various oncogenic factors that affect the cell cycle progression and promote the malignancy.

1.5.1 Cell cycle arrest during differentiation

Exit from G1 phase is associated with terminal differentiation. It begins with an upregulation of cyclin-dependent kinases (CDKs) ensuring inhibition suppressor protein family which serves to repress the E2F target genes for further cell cycle activity. The CDK inhibitors p21 and p27 are involved in the activation of terminal myogenic events which eventually leads to cell cycle arrest by suppressing the CDKs (Soufi and Dalton, 2016). The increase in G1 phase has also been characterised with epigenetic changes such as H3K4 trimethylation (Singh et al., 2013). Transcriptional genes become competent along with changes in H3K27me3 in G1 phase. However, in G2 and S phase pluripotency state is maintained by high levels of NANOG and OCT4 (She et al., 2017).

1.5.2 The role of cell cyclins and their inhibitors in the cell cycle process

Cyclin dependent kinases are proteins which contain a serine/threonine catalytic core and regulatory subunits which control the activity of the kinase and the specificity of the substrate. Currently there are over 20 members of the CDK recognised, each known for their role in DNA damage repair, epigenetic regulation, metabolism, stem cell renewal and proteolytic degradation (Lim and Kaldis, 2013). These cell cycle proteins have multifaceted roles. CDK4/cyclin D and CDK2/ cyclin E have shown to phosphorylate pRB that leads to activation of E2F and expression of E2F genes. The cell cyclin CDK2/cyclin A and CDK1/cyclin B

phosphorylate FoxM1 which causes it to recruit histone deacetylase p300/CREB activating the expression of FoxM1 target genes (Lim and Kaldis, 2013).

1.5.3 The cell cyclins involved in G1 arrest and G2 arrest

Cell cycle regulators have an important role in the transcription process. Table 1.2 and 1.3 shows the listed examples linked to the cell cycle control. One of the most commonly linked pathway is Rb/E2F where the hypophosphorylated state of Rb proteins (RbI, Rb II, Rb I2) bind to the E2F family of transcription factors. CDK4/6 and 2 along with cyclins D and E alleviate the inhibition of E2F by phosphorylating Rb, which in turn activates the genes for entering the S phase and initiate DNA synthesis (Lim and Kaldis, 2013).

Cyclin	**Established Function**
Cyclin A	Control of S phase in complex with CDK1 and CDK2
Cyclin B	Control of M phase in complex with CDK1
Cyclin D	Control of G1 phase in complex with CDK4/6; Rb/E2F transcription
Cyclin E	Control of G1-S phase with CDk2
p21 and p27	Inhibition of CDK and cyclin complexes

Table 1.2: Cell Cyclins and its inhibitors and their established role in various cell lines.

Protein	Established Function
CDK1	Control of M phase through cyc A and cyc B
	Myeloblast Proliferation through inhibition of MyoD
CDK2	Control of G1-S phase through cyc E and cyc A; RB/E2F transcription
	Myeloblast Proliferation through inhibition of MyoD
CDK4	Control of G1 phase of cell cycle in complex with cyc D; Rb/E2F transcription
CDK5	Neuronal function in complex with p35 and p39
CDK6	Control of G1 phase in complex with cycD and Rb/E2F transcription

Table 1.3: CDKs and their established role in various cell lines.

1.6 HDACi and cell cycle arrest

The increase in acetylation of histones is associated with increased transcriptional activity which in turn leads to the dysregulation of genes involved in differentiation, cell cycle control and apoptosis (Newbold et al., 2016).

Pan-HDACis such as TSA have shown to induce G1 arrest via the induction of p21, p27 and p53 and upregulation of cyclin D1 and CDK4 (Hrgovic et al., 2012). Benzamide HDACi MS-275 has also been studied for G1 arrest. It has shown to express cyclin D, E and A. The western blot study has shown to downregulate cyclin D1 with 5 μM MS-275. MS-275 also causes

antiproliferative effects marked by $p21^{CIP1/WAF1}$ induction, cyclin D1 downregulation and underphosphorylation of pRb (Rosato et al., 2003a).

On the other hand, many cytotoxic agents and microtubule targeting agents have shown to inhibit tumour cell proliferation by G2/M phase arrest. Reports by (Wang et al., 2016) have shown G2/M phase arrest by eranin in human osteosarcoma. It was seen that the drug caused apoptosis and autophagy via the upregulation of ROS/JNK signalling pathway but significantly reduced the tumour growth. There also have been reports of aloperine an anti-inflammatory drug causing G2/M phase arrest in colon cancer cells by upregulation of p21 and p53 and concomitant decrease in cyclin D1 (Zhang et al., 2014).

However, there seems to be a vast variability for G2 cell cycle arrest in terms of the cell cyclins and cell cyclin inhibitors involved and their expression.

1.7 Background of the project

This project aims to identify small molecules which cause differentiation of leukemic blasts in several AML subtypes. For this reason a panel of genetically distinct (Papaemmanuil et al., 2016) AML cell lines were chosen (Table 1.4). We wanted to target as many commonly occurring co mutations as possible which are not addressed by existing therapies and can be addressed with novel small molecules, for which having a broad cell line panel was necessary. Most common genetic abnormalities across the six cell lines are *NRAS, FLT3* and *TP53*, which play important role in the regulatory processes that govern proliferation, differentiation, and apoptosis, and abnormalities in these three genes have been implicated in the pathogenesis of younger adult patients with AML (Welch et al., 2012). The most common mutation across the samples is *NPM1* which accounts for 27% of cohort. Point mutations in *RAS* oncogenes occur in approximately 20% of AML patients, *TP*53 in 13% patients and *FLT3 ITD* mutations in 20% of AML cases (Quentmeier et al., 2003; Papaemmanuil et al., 2016).

Cell Line	**Mutation**	**AML Subtype (% affected population)**
THP1	*t (9;11); NRAS, TP53, ASXL1*	M5 (10%)
OCI-AML3	Mutation at exon 12 of NPM gene, aberrant cytoplasmic expression of NPM protein	M4 (20%)
HL-60	*NRAS, BCOR*	M2 (25%)
Kasumi 1	*t(8;21), TP53, NPM1, SRSF2, SMCIA*	M2
KG-1	*TP53*	M6 (5%)
ME-1	Has characteristic chromosome abnormality of *M4E0, inv (16); NRAS, FLT3, TP53*	M4 (5%)

Table 1.4: Most common genetic abnormalities across the six cell lines (Ru, 2006).

As part of a previous phenotypic screen, several HDAC inhibitors and structurally related compounds were hits. These compounds carried the zinc ion active site binding motif which inhibited the HDACs. In this project we try to understand if the inhibition of the HDACs is necessary to induce differentiation of AML cells.

This thesis is therefore concerned with:

1. Verifying the activity of screening hits (putative or known HDACi) through resynthesis and their effects on differentiation in various genetically distinct AML cell lines to assess whether the effect is independent of genotype.
2. Verifying whether the action of these compounds is through histone acetylation. For this purpose, we synthesised *meta* analogues for each of the active *ortho* analogues.
3. Access histone acetylation. It is important to monitor the target engagement in the cells and identify the pharmacological effect on perturbation of the HDACs or any other target.

In an attempt to deconvolute the downstream signalling pathway leading to differentiation we used cell cycle regulation to draw comparison in the target identification and the potential mechanism of action between the *ortho* and the *meta* analogues.

Chapter 2: Materials and Methods

2.1 Biological Materials and Methods

Compounds

10 mM stock solutions were prepared in DMSO and stored at -20 ºC. Serial dilutions of the stock solutions were carried out just prior to use in each experiment and final concentration of DMSO was maintained at 0.1%.

Cell Culture

Human leukaemia cell lines THP1, HL-60, Kasumi 1, ME-1, KG-1 and OCI-AML3 were supplied by ATCC. All cell culture reagents were purchased from Invitrogen Life Technologies and cells were maintained in a humidified incubator set to 37 ºC, 5% CO_2. All the cell lines were grown in RPMI containing 10% FBS and 1% L-Glutamine.

Reagents

PE mouse anti human CD 11b and IgG antibody were purchased from BD Biosciences. Antirabbit acetylated H3 was purchased from Millipore. BCA assay kit was purchased from Merck Biosciences. Antirabbit H3 and anti-rabbit IgG was purchased from Abcam Plc. Mouse monoclonal CDK1 (ab32147), rabbit monoclonal Cdk2 (ab16663), rabbit monoclonal cyclin D1, mouse monoclonal to p27 KIP1, rabbit monoclonal JNK1 ab203126, rabbit monoclonal Hsp90, rabbit monoclonal DR5 (ab199357) and beta tubulin were all purchased from Abcam plc. Mouse monoclonal p21 antibody was purchased from Santa Cruz Biotechnology Inc. For the western blot 4-12% bis tris gels and 20X MOPS (SDS) running buffer were used from Thermo Fisher Scientific. RIPA lysis buffer, protease and phosphatase inhibitor cocktail and NP40 detergent were all purchased from Thermo Fisher Scientific. Annexin V- DY-634 PI

apoptosis staining / detection kit (ab214484) from Abcam. Ph3 antibody Alexa-Fluor 488 anti-histone H3 phospho (Ser10) clone 11D8, Cat: 650804 was purchased from Cell Signalling Technology.

HDAC1-GFP plasmid (8.0 kbp) was purchased from Origene and pmax GFP (3469 bp) was purchased from Lonzo. HDAC1 Flag Plasmid was a gift from Eric Verdin (Addgene plasmid # 13820; http://n2t.net/addgene:13820; RRID: Addgene 13820). HDAC inhibition recombinant assay enzyme kit was purchased from Enzolifesciences. HDAC expression kit was purchased from Epigentek and HDAC activity assay kit for pan HDAC inhibition was supplied by Active Motif. RNeasy maxi prep kit was from Qiagen. Tape station test tape and ladder were from Agilent.

Antibodies	**Dilution**
beta tubulin	1:1000
P21	1:200
P27	1:200
CDK1, JNK1, CDK2	1:1000
Hsp90	1:10,000
DR5	1:1000
Total histone 3	1:1000
Acetylated histone 3	1:1000

Table 2.1: Antibodies and their dilution used.

Flow Cytometry

Exponentially growing THP1, OCI-AML3, KG-1 cells were seeded in the 96 well plate at a density of $2x10^5$ cells/mL in the presence of the respective compounds in a final volume of 100 μL. The plates were incubated for 4 days. Cells were pelleted by centrifugation at 1000 rpm and pellets were resuspended in 40 μL of blocking buffer (10 % FBS in DMEM) buffer containing either a mouse anti-CD 11b labelled with FITC (25% CD 11b) or mouse IgG isotype control FITC-labelled (25% IgG). The cells were stored in ice for 20 min. Cell suspension was then centrifuged, washed thrice and resuspended in 200 μL of staining buffer with 1 μg/mL DAPI. The cells were then analysed through Attune NxT flow cytometer (Thermo Fisher Scientific). Data was analysed using Invitrogen Attune NxT software (Thermo Fisher Scientific) and Flow Jo (v9). Compensation was performed on the Attune NxT flow cytometer.

Cell Proliferation and Viability assay

For assessment of cell proliferation and viability in AML cell lines, exponentially growing cells were plated in a 96 well plate at a density of $2x10^5$ cells/mL in a final volume of 100 μL. Cells were incubated in the presence of 10 μM and 1 μM of the respective compounds for 4 days. Viable cell number was determined using the Nucleo Counter (NC-3000) system (Chemo Metec USA Inc) according to manufacturer's protocol. Cells were stained with Solution 13. Solution 13 contains acridine orange which is used as a counterstain staining all living and dead cells thus providing a total count. DAPI stains the dead cells. With the total number of cells and the number of dead cells NucleoView™ software provides the user with the viability, total count, the concentration of nonviable and viable cells.

For each cell line, and each concentration results were plotted using Graphpad Prism Software.

Staining Protocol

The cells were loaded in the cytofunnel with slides, white filter cards and 200 µL of FACS buffer. The cells were then cytospinned at 1000 rpm for 10 min. The samples were then put in the Hema-tek 2000 machine. It is an automated process that allows for the staining of the slides for in vitro use. The Hema-tek pack is used for the staining purposes. The slides were then covered with a glass cover slip and viewed under Olympus BX-30 and analysed with the Infinity software.

Flow Cytometric Analysis of Cell Cycle

Exponentially growing cells were plated in a 96 well plate at a density of $2x10^5$ cells/mL. Cells were incubated the respective compounds and their respective concentrations in a final volume of 100 µL for 24 h, 48 h and 72 h. Cells treated for cell cycle analysis were pelleted by centrifugation at 600 x g for 6 min at room temperature. Pellets were washed once with PBS and stained with propidium iodide solution (0.1 % v/v Triton X 100, 50 µg/mL Propidium Idodide, 200 µg/mL RNAase in PBS) for 2 h at 4 ºC. Samples were analysed by Attune NxT flow cytometer and analysed under Invitrogen Attune NxT software.

Flow Cytometric Analysis for cells stained by Ph3 antibody

Cells were plated and incubated with the respective concentration of the compound as described above. Culture plates were removed from incubator and centrifuged at 1200 rpm for 5 min at room temperature to pellet the cells. During spin PI stock was diluted (1mg/ml in water) into 0.1% sodium citrate, 0.1% triton x100 solution. After spin supernatant of plates was removed by flicking plate out over sink in a firm flick, ensuring not to dislodge the cell pellets. The cells were then resuspended in 100 µL of PI working solution and incubated in the dark at 4 ºC for 2 h (this time might need further optimisation i.e. the longer this incubation the more

stable out histograms should be). The plate was centrifuged at 1200 rpm for 5 mins and the Ph3 antibody was diluted. Cells were resuspended in 50 μL of blocking buffer containing 2.5 μL of PH3 antibody. The plates were incubated on ice for 20 min in the dark.

The plates were then centrifuged at 1200 rpm for 5 mins and washed twice in 200 μL of PBS before analysing on Attune Nxt software.

Western Blot Analysis

For western blot analysis in AML cell lines, exponentially growing cells were plated in a 6-well plate at $2x10^5$ cells/mL in a final volume of 3 mL. Cells were incubated in the presence of 1 μM of compound. Cells ($1x10^6$) were harvested and after 24 h histones were extracted by acid extraction. Cells were pelleted at 560 g for 5 min and then washed with 200 μL PBS. Cells were lysed in 50 μL of BC300/0.5% NP40 and incubated on ice for 30 min followed by centrifugation at 13,000 rpm at 4 ºC for 10 min. To this pellet (containing chromatin and insoluble nuclear factors), 50 μL of 0.4 M HCl was added and then again incubated for 30-60 min, followed by centrifugation at 13,000 rpm (4 ºC, 10 min). The supernatant was isolated and 1 mL of ice-cold acetone was added. The protein was precipitated at 13,000 rpm (4 ºC, 20 min) and the supernatant was then discarded. The pellet was washed twice with ice cold acetone and then resuspended in 4 M urea, 1x SDS loading buffer and 0.5 % mercaptoethanol.

Histones were separated on 16% tris-glycine gels (Invitrogen) transferred to 0.2 μM nitrocellulose membrane and probed with anti-acetyl H3 (1:1000) (Table 2.1) in 5% skimmed milk in PBS. Following primary antibody incubation, membranes were probed with 1:10,000 rabbit-anti-IgG (Table 2.1). Signal was detected using the ECL mix following the proportion of solution A and B provided by the manufacturer.

Nuclear extraction using RIPA buffer

Cells were plated and incubated with the respective concentration of the compound as described above. For the purpose of nuclear extraction, medium was removed from the cells and they were then washed with PBS. They were spin down for 5 min at 1000 rpm and 100 µL of RIPA was added along with the protease inhibitor. The cells were then left on ice for 40 min and then pelleted for 10 min at 13000 rpm at 4 ^{o}C. The protein concentration was calculated using the BCA assay as described below. The purity of the samples was calculated using Nanodrop (A260/A280 ratio). Pure samples had values less than 1.

BCA assay

The standard for the BCA assay was prepared in clean vials with deionised water being the sample buffer. First, the standard was prepared with bovine serum albumin (2 mg/mL stock) according to the following dilutions:

Tube	Volume of BSA	Volume of diluent	Final BSA concentration
1	250 µL from stock	250 µL	1,000 µg/mL
2	250 µL from tube 1	250 µL	500 µg/mL
3	250 µL from tube 2	250 µL	250 µg/mL
4	300 µL from tube 3	300 µL	125 µg/mL
5	100 µL from tube 4	400 µL	25 µg/mL
6	0	400 µL	0 µg/mL

Table 2.2: BSA standard concentrations

Following the preparation of the standard (Table 2.2) the following reaction was carried out in a cuvette. 50 μL of the standard or the sample and 1.0 mL of the BCA working reagent were added. The two were mixed gently and then incubated at 37 ^{o} C for 30 min. The solution was transferred to a clean cuvette and read within 10 min at an absorbance of 562 nm.

Apoptosis Assay

Exponentially growing HL60 cells were seeded in a 96 well plate at the density of $2x10^5$ cells/mL. They were then treated with the respective concentration of the compounds (D6 2.5 μM, mocetinostat 100 nM and 2.5 μM) for a period of 96 h. The cells were then pelleted at 1000 rpm for 5 min followed by a wash with PBS. The cells were resuspended in 1X annexin V binding buffer. Then, 5 μL of the Annexin V-DY634 and 5 μL of PI were added to each 100 μL of cell suspension. The cells were incubated in dark for 15 min, followed by a final suspension in 400 μL of 1X annexin V binding buffer.

Recombinant enzyme assay for HDAC 1,2,6 and 11.

The compounds were prepared from a stock solution of 10 mM. The serial dilutions prepared of the compound were in a 2-fold dilution ranging from 20 μM to 78 nM. For the following reaction trichostatin was used at 500 nM final concentration and the Fluor De- Lys SIRT1 substrate was used at 20 μM.

1. The compounds were prepared in a serial dilution from a stock solution of 10 mM. Four reactions were designated as: 30 min reaction; 30 min reaction plus trichostatin A; 0 min reaction and a standard well.
2. 20 μl of HDAC assay buffer II was added to the 30 min reaction well and the 0 min reaction well. To the third well (30 min. plus trichostatin) 2.5 μl of 10 μM trichostatin

A plus 17.5 µl of HDAC assay buffer II was added. The assay was allowed to equilibrate at a temperature of (37 °C) (standard well left empty until step 7). 25 µl of the 2x substrates (37°C) was added to both 30 min reaction wells. Reactions were allowed to run for 30 min at 37 °C.

3. 50 µl of 1x Developer II plus trichostatin A was added to both 30 min reaction wells.
4. To the 0 min reaction well, 50 µl of 1x Developer II plus trichostatin A was added, immediately followed by 25 µl of 2x substrate.
5. For the standard, 50 µl of 1 µM standard was mixed with 50 µl of 1x Developer II plus trichostatin A in the fourth well.
6. The reactions were allowed to develop for 45 min at 37 °C and the plate was then read in a microplate-reading fluorimeter capable of excitation at a wavelength in the range of 350-380 and detection of emitted light in the range of 440-460 nm.
7. Data analysis: ΔAFU (Arbitrary Fluorescence Units) for the two 30 min reactions (AFU of 30 min reaction (with or without trichostatin) minus AFU of the 0 min reaction) was determined. Then, AFU/pmol was calculated by dividing the deacetylated standard reading (AFU) by 50 pmol of substrate deacetylated in 30 min (divide ΔAFU by AFU/pmol.

Pan HDACi assay

The samples for the following assay were prepared according to Table 2.3.

The plate was incubated at 37 °C for 30-60 min. Then HDAC assay developing solution was prepared by adding TSA into it. 10 µL of 0.2 mM TSA was added into 0.995 mL developer solution to make 2 µM concentration. 50 µL of this HDAC developer solution was added and the plate was incubated for 10-15 min (Table 2.3). The fluorescence was read at 360 nm excitation wavelength and 460 nM emission wavelength.

Reagent	Blank wells	Sample (no inhibitor)	Sample (with inhibitor)	Positive control nuclear extract
HDAC assay buffer	40 μL	10 μL	-	10 μL
TSA (5 μM)	-	-	10 μL	-
HDAC substrate (5 mM)	10 μL	10 μL	10 μL	10 μL
Test sample	-	30 μL	30 μL	-
HeLa	-	-	-	30 μL

Table 2.3: HDAC assay preparation

HDAC expression

Exponentially growing cells were plated in a 6-well plate at $2x10^5$ cells/mL in a final volume of 3 mL. Cells were incubated in the presence of 2.5 μM of D6 and mocetinostat and 30 μM of PK040 and PK026. Cells ($1x10^6$) were harvested after 24 h and pelleted at 560 g for 5 min and then washed with 200 μL PBS. Cells were lysed in 50 μL of BC300/0.5% NP40 and incubated on ice for 30 min followed by centrifugation at 13,000 rpm at 4 ºC for 10 min.

HA1 (10X wash buffer) was diluted with distilled water at a 1:10 ratio (1 ml of HA1 + 9 ml distilled water) in order to create, 1X HA1. The kit contains HA1 (10X wash buffer), HA2 (HDAC assay buffer), HA3 blocking buffer), HA4 (capture antibody, 200 μg/ml), HA5 (detection antibody, 200 μg/ml), HA6 (developing solution), HA7 (stop solution) and HDAC1 control (100 ng/μl).

Protein concentration was adjusted to 1 µg/µl with HA2 and 5 µl (5 µg) of the protein solution was added into the central area of each well. Solution was spread out over the bottom of the strip well by pipetting the solution up and down several times. The strip wells were incubated at 37 °C (with no humidity) for 60-90 minutes to evaporate the solution and completely dry the wells. For the blank, 5 µl of HA2 was added to the wells. For the positive control, HDAC1 control was diluted to 30 ng/µl with HA2 and 5 µl (150 ng) of diluted HDAC1 control solution was added to the wells. 150 µl of HA3 was added to the dried wells and incubated at 37 °C for 30-45 minutes. Each well was aspirated and washed with 150 µl of 1X HA1 three times.

HA4 (at a 1:200 ratio) was diluted to 1 µg/ml with 1X HA1. 50 µl of diluted HA4 was added to each assay strip well and 2 control strip wells. The samples were incubated at 25 ^{o}C for 60 minutes on an orbital shaker (50-100 rpm). Each well was aspirated and washed with 150 µl of 1X HA1 four times. HA5 was diluted (at 1:1000 ratio) to 0.2 µg/ml with 1X HA1. 50 µl of diluted HA5 was added to each strip well and incubated at room temperature for 30 minutes. Each well was washed and aspirated with 150 µl of 1X HA1 four times. 100 µl of HA6 was added to each well and incubated at room temperature for 2-10 minutes away from light. The colour development was monitored in the sample and standard wells (blue). 50 µl of HA7 was added to each well absorbance was read on microplate reader at 450 nm.

HDAC1 level was calculated: HDAC1 level (OD/ml) = (sample OD – blank OD) × sample dilution.

High Efficiency Transformation:

The *E.coli* cells were thawed on ice for 10 min. Then 1µL containing 100 ng of plasmid was added into 50 µL of this cell mixture. The tube was carefully flicked for 4-5 times to mix the cells and DNA. The mixture was placed on ice for 30 min but not mixed. The mixture was then put in the water bath at 42 ^{o}C for 45 seconds. This is called heat shock. Then 950 µL of

the room temperature (25 ^{o}C) SOC was added to the mixture. The mixture was then placed at 30 ^{o}C for 60 min and vigorously shaken at 250 rpm. The selection plates were then warmed to

30 ^{o}C and the DNA+ cells mixture was added. The cells were thoroughly mixed by flicking the tube and inverting and performing 10-fold dilution in SOC. The 100 μL of each dilution was added onto the selection plate and incubated overnight at 30 ^{o}C.

After this the 200 mL of SOC flasks were taken and 200 μL of ampicillin was added in each. Then a colony or two was added in each of them and was allowed to grow at 37 ^{o}C in the incubator followed by the maxiprep.

The DNA was extracted from HiPure plasmid filter DNA purification kits from Invitrogen. The final concentration was prepared in nuclease free water and measured using nanodrop. Nanodrop instruments are used for measuring the DNA and RNA quality and concentration. These instruments can give appropriate measurements for the same with a sample volume of only 1-2 μL. They utilise a spectrometer where the ratio of absorbance at 260 nm and 280 nm is used to assess the purity of DNA and RNA. A ratio of ~1.8 is generally accepted as "pure" for DNA; a ratio of ~2.0 is generally accepted as "pure" for RNA.

For the purpose of transfecting THP1 cells with the plasmid of interest electroporation was used. A million cells were seeded per well in a 24 well plate. 100 μL of the cells (1 million cells) were added in the cuvette and then 10 μL meaning 10 μg of the plasmid was added followed by the passage of current through the cuvette kept in the electroporation machine. The electroporation machine was kindly supplied by Dr. L Fisher, Heidelberg.

RNA extraction

For the RNA extraction experiment 0.5 million cells/mL were used with a total of 5 million cells per sample. The compounds were added with the concentrations of 30 μM for the *meta* analogues and 2.5 μM for D6 and 600 nM for mocetinostat. Following 24 h incubation the RNA was extracted from the cells using RNeasy plus micro kit's manufacture protocol.

RNA quality test

The concentration of RNA was determined by using a Nanodrop (using 1 OD260= 40μg RNA). A 260 /A 280 ratios were also calculated for each sample. Samples with ratios smaller than 1.7 were discarded. The concentration and the absorbance ratio for each of the samples is given in Table 2.4.

Sample	Concentration (ng/μL)	A260/280	A260/230
NT1	253.43	2.06	1.89
NT2	312.4	2.05	1.91
NT3	109.53	2.01	1.8
PK038.1	133.1	2.03	1.78
PK038.2	161	2.06	1.32
PK038.3	148.4	2.03	1.8
Mocetinostat.1	360.2	2.01	1.98
Mocetinostat.2	338.6	2.02	1.85
Mocetinostat.3	132	2.01	1.4
026.1	142.07	1.96	1.1
026.2	59	2.04	1.58
026.3	69	1.95	1.01
040.1	289.2	2.08	2.01
040.2	201.5	2.05	1.65
040.3	607.3	2.07	1.04

Table 2.4: The concentration and the absorbance ratio for each of the samples

Tape Station Test

To test the purity of the sample and to understand how much of the RNA has degraded in the process the tape station test was done on Agilent 4200 tape station system. The samples were diluted as 1:100 in RNAse water. Then in PCR tubes 2 μL of the diluted sample was added with 2 μL of the buffer. The ladder was prepared in the similar manner. The samples were vortexed for 1 min followed by heating on BIORAD machine for 5 min. The samples were

then run for 30 min and the RIN values were determined. RNA is a thermodynamically stable molecule, which is, however, rapidly digested in the presence of the nearly ubiquitous RNase enzymes. In order to evaluate the degree of degradation, electrophoretic methods have been applied that separate the samples according to the size of the comprised molecules.

RNA integrity is evaluated using agarose gel electrophoresis stained with ethidium bromide, which produces a certain banding pattern. Gel images show two bands comprising the 28S and 18S ribosomal RNA (rRNA) species and other bands where smaller RNA species are located. RNA is considered of high quality when the ratio of 28S:18S bands is about 2.0 and higher (Schroeder et al., 2006).

The samples were scored out of 10 meaning more the score less is the degradation of the RNA (Table 2.5).

Sample	RIN value (8 or above)
NT 1	9.7
NT 2	9.6
NT 3	9.7
038 1	9.4
038 2	9.7
038 3	9.6
022 1	9.5
022 2	9.1
022 3	9.2
026 1	9.1
026 2	9.0
026 3	9.5
040 1	9.7
040 2	9.8
040 3	9.4

Table 2.5: RIN values for the samples

Statistical Methods

All data represent at least three independent experiments and were expressed as mean ± standard error of the mean (SEM). Statistical analyses were performed using Student's *t*-test for comparison between two groups, and analysis of variance (ANOVA) and Dunnett's post hoc test for multiple comparisons among groups. A probability value of $p < 0.05$ was considered significant. GraphPad Prism 5 software version 5.01 was used for data analyses.

2.2 Chemistry Experimental Procedure

2.2.1 General Experimental Section

All reactions involving moisture-sensitive reagents were carried out under nitrogen atmosphere using standard vacuum line techniques and glassware was dried and cooled before use. Solvents were dried according to the procedure outlined by Grubbs and co-workers. Water was purified by Elix UV-10 system. All other reagents were used as supplied (analytical or HPLC grade) without prior purification.

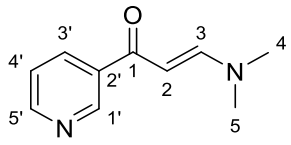
Plates were visualised using UV light (254 nm) and thermal development after dipping in, 1% aq $KMnO_4$. Flash column chromatography was performed either on Kieselgel 60 silica on a glass column. Melting points were recorded on a Gallenkamp Hot stage apparatus and are uncorrected.

IR spectra were recorded on a Bruker Tensor 27 FT-IR spectrometer as thin film samples. Selected characteristic peaks were reported in cm^{-1}. NMR spectra were recorded on Bruker Avance 400 spectrometers in the deuterated solvent stated. The field was locked by external referencing to the relevant deuteron resonance. Spectra were recorded at 25 ^oC. Chemical shifts (δ) are reported in parts per million (ppm). The multiplicity of each signal is indicated by: s (singlet); br. s (broad singlet); d (doublet); t (triplet); q (quartet); m (multiplet). Coupling

constants (*J*) are quoted in Hz and are reported to the nearest 0.1 Hz. The field was locked by external referencing to the relevant deuteron resonance.

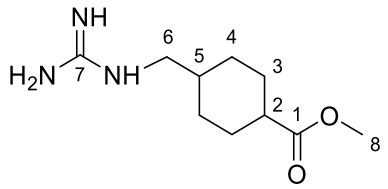
Low resolution mass spectra were recorded on VG Mass Lab 20-250. Accurate mass measurements were run on Bruker Micro TOF internally calibrated with polyalanine. m/z values are reported in Daltons and followed by their percentage abundance in parentheses.

(*E*)-3-(Dimethylamino)-1-(pyridin-3-yl)prop-2-en-1-one



N.N-Dimethylformadamide diacetal (10 mL, 89 mmol) was added dropwise to a mixture of 3-acetylpyridine (6.0 mL, 49 mmol) and acetic acid (600 μL, 9.9 mmol) under nitrogen. The reaction was heated to 95 ºC for 3 h then cooled to 25 ºC and poured onto H_2O (20 mL). The aqueous phase was extracted with DCM and the combined organics were washed once with brine- dried over anhydrous Na_2SO_4 and concentrated to give (*E*)-3-(Dimethylamino)-1-(pyridin-3-yl)prop-2-en-1-one as a brown solid (6.133 g , 34.66 mmol, 70 %); m.p. 72 °C (lit m.p. 90-91 ºC (Kinigopoulou et al., 2016)) ν_{max}/cm^{-1} 1724 (C=O), 1637 (C=C), 1250 (C-N); ^{1}H NMR (400 MHz, $CDCl_3$) 9.08 (1H, dd, *J* 2.2, 0.9, H1'), 8.67 (1H, dd, *J* 4.8, 1.7,H5'), 8.19 (1H, ddd, *J* 7.9, 2.3, 1.8,H3'), 7.85 (1H,d, *J* 12.3,H3), 7.35 (1H, ddd, *J* 7.9, 4.8, 0.9, H4') 5.68 (1H,d, *J* 12.3, H2), 3.19 (3H,s, H5), 3.12 (3H, s, H4); ^{13}C NMR (126 MHz, $CDCl_3$) δ 186.2 (C1), 154.6 (C3), 151.4 (C5'), 148.8 (C1'), 135.0 (C3'), 133.1 (C2'), 123.2 (C4') , 91.7 (C2) , 45.2 (C5), 37.3 (C4) ; m/z (ESI$^+$) 177.1 (MH^+,100%); HRMS (ESI$^+$) $C_{10}H_{14}ON_2$ (MH^+) found 177.1022 requires 177.1022.

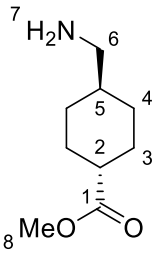
Methyl 4-(guanidinomethyl)cyclohexane-1-carboxylate



1H pyrazole-1-carboxamide hydrochloride (1.8 g, 12.8 mmol) was added to a solution of methyl (1R,4R)-4-(aminomethyl) cyclohexane-1 carboxylate (2.0 g, 11.6 mmol) in DMF (13 mL) followed by addition of DIPEA (4.5 mL, 0.7 mmol) and the mixture was refluxed for 3 h , DMF was then removed under vacuum.

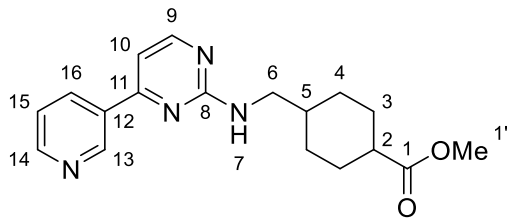
To the remaining viscous oil, saturated aqueous $NaHCO_3$ (50 mL) was slowly added under vigorous stirring followed by addition of water. A white solid was formed, and the stirring was continued for 1 h. This material was filtered off and washed with water to give the compound as a white powder (1.9 g, 8.9 mmol, 65 %); m.p. 155 ºC; ν_{max}/cm^{-1} 1712 (C=O), 3380 (N-H); ^{1}H NMR (400 MHz, DMSO-*d6*) δ 3.59 (3H,s, H8), 2.91 (2H, d, *J* 6.5,H6), 2.33 (4H, d, *J* 2.2,H3), 2.24 (1H, ddt, *J* 12.2, 7.2, 3.6, H2), 1.91 (4H, dd, *J* 13.5, 3.5, H4), 1.42 (1H, s, H5); ^{13}C NMR (126 MHz, DMSO-d_6) δ 175.8 (C1), 160.4 (C7), 51.7 (C8), 46.8 (C2), 42.7 (C5), 36.8 (C6), 28.5 (C4), 29.3 (C3); m/z (ESI^+) 214.2 (MH^+, 100%); HRMS (ESI^+) found 214.1549, $C_{10}H_{20}O_2N_3$ (MH^+) requires 214.1550.

Methyl (1R,4R)-4-(aminomethyl) cyclohexane -1- carboxylate



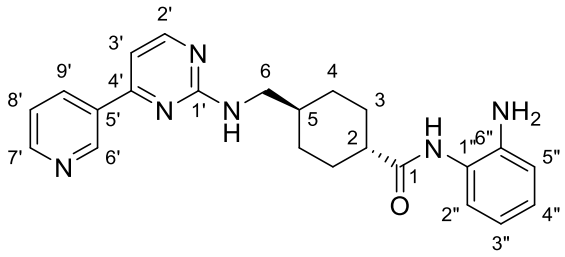
The suspension of the aminomethylcyclohexane carboxylic acid (6.0 g, 38.0 mmol) in MeOH (95 mL) was cooled to 0 ºC before addition of $SOCl_2$ (3.8 mL). The mixture was stirred at and 25 ºC for 16 h then concentrated in vacuum to give the compound as a light green powder (6.43 g, 37.60 mmol, 98 %); m.p. 179 ºC ; ν_{max}/cm^{-1} 1723 (C=O), 1173 (C-O), 2938 (N-H); ^{1}H NMR (400 MHz, DMSO-d_6) δ 3.59 (3H, s, H8), 2.62 (1H, t, *J* 6.2, H2), 2.51 (2H, q, *J* 2.1 , H6), 1.94-1.88 (2H, m, H3), 1.82 (2H, m, H4), 1.56 (1H, m, H5), 1.29 (2H, qd, *J* 12.9, 3.3, H7) ; ^{13}C NMR (100 MHz, DMSO-d_6) δ 175.74 (C1), 51.81 (C8), 44.56 (C6), 42.37 (C2), 35.27 (C5), 29.14 (C3), 28.31 (C4) ; m/z (ESI^+) 172.1 (MH^+, 100%); HRMS (ESI^+) found 172.1330, $C_9H_{18}O_2N$ (MH^+) requires 172.1332.

Methyl 4-(((4-pyridin-3-yl)pyrimidin-2-yl)amino)methyl)cyclohexane-1-1carboxylate



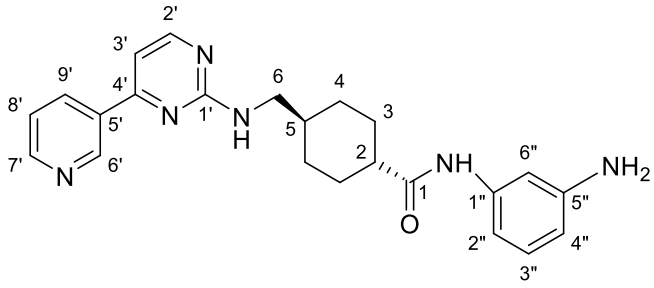
Methyl 4-(guanidinomethyl)cyclohexane-1-carboxylate (1.0 g, 7.0 mmol) and (*E*)-3-(Dimethylamino)-1-(pyridin-3-yl)prop-2-en-1-one (0.9 g, 8.4 mmol) were added subsequently in isopropyl alcohol (7.9 mL) and molecular sieves (4 A°). The mixture was heated to reflux for 16 h, then filtered through a pad of Celite. The filtrate was concentrated in vacuum to obtain the product as a pale yellow solid (450 mg, 1.4 mmol, 20%); m.p. 220 ºC; ν_{max}/cm^{-1} 1726 (C=O), 3247 (N-H), 951 (C-O); ^{1}H NMR (400 MHz, MeOD-d_4) δ 9.09 (1H, s, H13), 8.55 (1H, d, *J* 1.6 , H14), 8.40 (1H, d, *J* 8.1, H16), 8.23 (1 H, d, *J* 5.2 , H9), 7.47 (1H, ddd, *J* 8.0, 4.9, 0.9, H15), 7.04 (1H, d, *J* 5.2, H10), 4.79 (1H, s, H7), 3.21 (3H , s, H1'), 2.50 (1H, s, H2), 2.20 (1 H, tt, *J* 12.3, 3.5, H6), 1.93-1.81 (2H, m, H3), 1.40-1.24 (2H, m, H4); ^{13}C NMR (100 MHz, MeOD-d_4) δ 177.0 (C1), 158.5 (C13), 156.0 (C8), 150.6 (C9), 147.6 (C14), 135.4 (C16), 133.5 (C12), 123.8 (C15), 105.6 (C10), 63.5 (C6), 51.1 (C1'), 37.0 (C5), 29.7 (C3), 28.4 (C4); m/z (ESI$^+$) 327.1 (MH^+, 100%); HRMS (ESI$^+$) found 327.1810, $C_{18}H_{22}O_2N_4$ (MH^+) requires 327.1815.

(1R,4R)-N-(2-aminophenyl)-4-(((4-(pyridine-3-yl)pyrimidin-2-yl)amino)methyl)cyclohexane-1-carboxamide



Methyl 4-(((4-pyridin-3-yl)pyrimidin-2-yl)amino)methyl)cyclohexane-1-1carboxylic acid (200 mg, 0.6 mmol) was dissolved in DMF (6 mL) before sequential addition of DIPEA (428 µL, 3.3 mmol) 1,2-Phenylenediamine (78.0 mg, 0.7 mmol) and HATU (319 mmol, 0.8 mmol). The reaction was stirred for 16 hr. The organic layer was washed with water/brine (1:1) and EtOAc, dried with Na_2SO_4 and concentrated in vacuum to give the crude material as a yellow oil. The product was then columned with (5% MeOH/CH_2Cl_2) to give the product as a white solid (75.0 mg, 0.186 mmol, 30%); m.p. 179 ºC; ν_{max}/cm^{-1} 1720 (C=O), 3300 (N-H); ^{1}H NMR (500 MHz, MeOD-*d*$_4$) δ 9.28 (1H, s, H6'), 8.76-8.61 (1H, m, H7'), 8.53 (1H, t, H9'), 8.37 (1H, d, *J* 5.2, H2'), 7.59 (1H, dd, *J* 8.0, 4.9, H2"), 7.39 (1H, dd, *J* 5.9, 3.2, H3'), 7.30 (1H, m, H4"), 7.09 (1H, dd, *J* 7.9, 1.5, H5"), 6.86 (1H, m, H3"), 6.74 (1H, d, *J* 7.6, 1.4, H8'), 2.52-2.29 (2H, m, H6), 2.08-1.95 (1H, s, H2), 1.76 (1H, s, H5), 1.69-1.57 (2H, m, H4), 1.24-1.12 (2H, m, H3); ^{13}C NMR (100 MHz, MeOD-*d*$_4$) δ 176.5 (C1), 162.7 (C4'), 158.6, (C1'), 150.2 (C7'), 147.4 (C6'), 141.7 (C6"), 135.1 (C2'), 133.5 (C4"), 127.8 (C9'), 126.7 (C5'), 125.6 (C2"), 123.9 (C1"), 118.2 (C5"), 117.2 (C3"), 110.8 (C8'), 105.3 (C3'), 56.1 (C6), 45.2 (C5), 38.8 (C4), 29.8 (C2), 17.3 (C3); m/z (ESI$^+$) 403.2 (MH^+, 100%); HRMS (ESI$^+$) found 403.2239, $C_{23}H_{27}ON_6$ (MH^+) requires 403.2240.

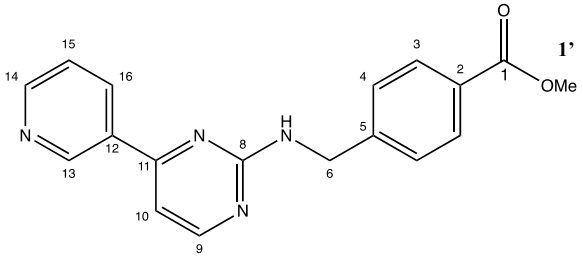
(1R,4R)-N-(2-aminophenyl)-4-(((4-(pyridine-3-yl) pyrimidin-2-yl)amino)methyl)cyclohexane-1-carboxamide



Methyl 4-(((4-pyridin-3-yl) pyrimidin-2-yl)amino)methyl)cyclohexane-1-1carboxylic acid (200 mg, 0.6 mmol) was dissolved in DMF (6 mL) before sequential addition of DIPEA (428 µL, 3.3 mmol) 1,3-Phenylenediamine (78.0 mg, 0.7 mmol) and HATU (319 mg, 0.8 mmol). The reaction was stirred for 16 hr. The organic layer was washed with water/brine (1:1) and EtOAc, dried with Na_2SO_4 and concentrated in vacuum to give the crude material as a yellow oil. The product was then columned with (5% MeOH/CH_2Cl_2) to give the product as a white solid (153.0 mg, 0.380 mmol, 80%); m.p. 180 ºC; ν_{max}/cm^{-1} 1621 (C=O), 3255 (N-H); ^{1}H NMR (500 MHz, MeOH-d_4) δ 9.14 (1H, s, H6'), 8.54 (1H, dd, *J* 4.9, 1.6, H7'), 8.39 (1H, m, H9'), 8.23 (1H, d, *J* 5.2, H2'), 7.46 (1H, dd, *J* 8.0, 4.9, H2"), 7.03 (2H, d, *J* 5.2, H3'), 6.95-6.86 (1H, m, H8'), 6.70 (1H, d, *J* 8.0, 2.0, H4"), 6.35 (1H, m, H3"), 2.22 (2H, m, H6), 2.19 (1H, s, H2), 1.93-1.77 (2H, m, H4), 1.61 (1H, s, H5), 1.46 (2, m, H3); ^{13}C NMR (101 MHz, MeOD-d_4) δ 176.0 (C1), 162.7 (C4'), 158.6 (C1'), 150.2 (C7'), 148.3 (C5"), 147.8 (C6'), 147.4 (C6"), 139.2 (C2'), 138.1 (C1"), 135.0 (C4"), 133.5 (C9'), 128.8 (C5'), 123.9 (C2"), 111.1 (C8'), 105.3 (C3'), 48.2 (C6), 45.8 (C5), 37.3 (C4), 29.8 (C2), 28.9 (C3).

m/z (ESI$^+$) 403.3 (MH^+, 100%); HRMS (ESI$^+$) found 403.22396, $C_{23}H_{27}ON_6$ (MH^+) requires 403.2240.

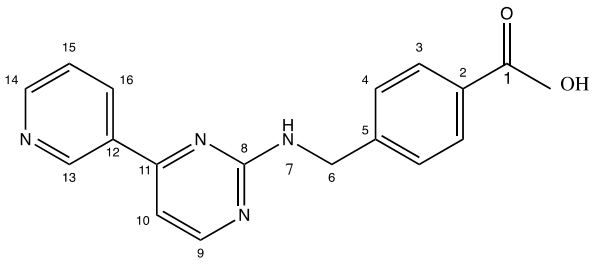
Methyl 4-(((4-pyridin-3-yl) pyrimidin-2-yl) amino) methyl) benzoate



Methyl 4-({[4-(pyridin-3-yl)pyrimidin-2-yl]amino}methyl)benzoate was synthesized from Methyl 4-formyl benzoate (1.0 g, 4.82 mmol) and (*E*)-3-(Dimethylamino)-1-(pyridin-3-yl)prop-2-en-1-one (0.9 g, 5.56 mmol) were added subsequently in isopropyl alcohol (9.4 mL) and molecular sieves (4 A^{o}). The mixture was heated to reflux for 16 h, then filtered through a pad of Celite. The filtrate was concentrated in vacuum to obtain the product as a pale white solid (340 mg, 22.53%) m.p. 175 ºC; ν_{max}/cm^{-1} 1687 (C=O)

^{1}H NMR (DMSO-d_6, 500 MHz) δ: 9.22 (1H, s, H13), 8.58 (1H, d, *J* 1.6 , H14), 8.41 (1H, d, *J* 8.1, H16), 7.98 (1 H, d, *J* 5.2 , H9), 7.89 (1H, ddd, *J* 8.0, 4.9, 0.9, H15), 7.26 (1H, d, *J* 5.2, H10), 4.67 (2H, d, J 5.8, H6, 3.84 (3H,s,H1'); ^{13}C-NMR (DMSO-d_6, 125 MHz) δ: 166.6 (C1), 162.9 (C13), 151.7 (C8), 148.5 (C9), 146.9 (C14), 134.7 (C16), 132.8 (C12), 129.7 (C15) , 127.6 (C3), 122.7 (C4); HRMS (ESI^{+}) *m*/*z* calculated for $C_{18}H_{17}N_4O_2$ $[M + H]^{+}$ 321.1346, found 321.1347.

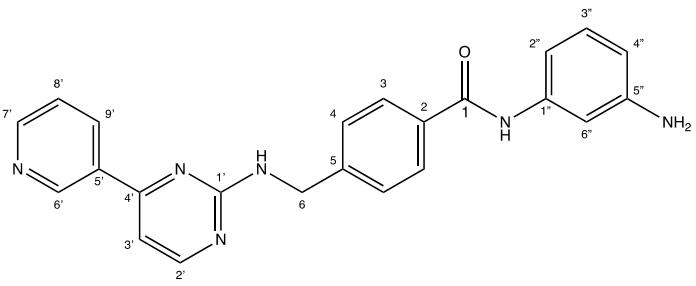
Methyl 4-(((4-pyridin-3-yl)pyrimidin-2-yl)amino)methyl)benzoic acid



Methyl 4-({[4-(pyridin-3-yl)pyrimidin-2-yl]amino}methyl)benzoate (0.3 g, 0.9 mmol) was stirred in a mixture of THF (1.9 mL) and MeOH (1.9 mL) which was then added to a solution of $LiOH.H_2O$ (88.3 mg, 2.09 mmol) in water (0.95 mL) at 25 ^oC. The reaction was stirred at 40^oC overnight, cooled to 25 ^oC followed by an addition of aqueous layer of HCl (pH- 4.5). The mixture was concentrated to dryness, the formed solid was triturated with water, filtered off and dried off to afford the title compound (246 mg, 25.7%) m.p. 223^0C; ν_{max}/cm^{-1} 1654 (C=O)

^{1}H-NMR (DMSO-d6, 500 MHz) δ: 11.72 - 13.85 (1H, m, H1), 9.13 (1H, s, H13), 8.62 (1H, d, H14), 8.33 (1H, d, J 6.1, H16), 8.21 (1H, d, H9), 8.20 (1H, d, H14), 7.94 (2H, d, J 8.0, H9), 7.43 - 7.56 (4H, m, H15), 4.69 (2H, br.s., H4); 13C-NMR (DMSO-d6, 126 MHz) δ: 167.7 (C1) 159.6 (C13), 148.9 (C12), 146.0 (C9), 145.8 (C14), 137.9 (C16), 129.8 (C15), 129.6 (C3), 127.6 (C5), 125.6 (C9), 44.5 (C6. HRMS(ESI+) m/z calculated for $C_{17}H_{14}N_4O_2$ [M + H] + 307.1117, found 307.1190.

N-(3-aminophenyl)-4-(((4-(pyridine-3-yl)pyrimidin-2-yl)amino)methyl)benzamide



Methyl 4-(((4-pyridin-3-yl)pyrimidin-2-yl)amino)methyl)benzoic acid (100 mg, 0.32 mmol) was dissolved in DMF (3.2 mL) before sequential addition of DIPEA (428 µL, 3.3 mmol) 1,3-Phenylenediamine (68.2 mg, 0.6 mmol) and HATU (0.14 g, 0.37 mmol). The reaction was stirred for 16 hr. The organic layer was washed with water/brine (1:1) and EtOAc, dried with Na_2SO_4 and concentrated in vacuum to give the crude material as a yellow oil. The product was then columned with (5% MeOH/CH_2Cl_2) to give the product as a white solid (80%) m.p. 191 ºC; ν_{max}/cm^{-1} 1619 (C=O), 3016 (N-H); ^{1}H NMR (500 MHz, DMSO-d6) 9.87 (1H,s, H6'), 9.25 (1H, s, H7'), 8.69 (1H, d, J 3.7, H9'), 8.42 (2H, d, J 5.2 , H2'), 8.01 (1H, t, J 6.2, H2"), 7.93 (2H, d, J 8.0, H3'), 7.52 (3H, in, H8'), 7.27 (1H, d, J 5.1 , H4"), 7.15 (1H, d, J 7.6, H3"), 6.84 (1H, t, J 7.5, H4), 6.69 (1H, d, J 7.8, H3), 2.90 (2H, m, H6), ^{13}C NMR (101 MHz, MeOD-d_4) δ 177.0 (C1), 175.5 (C4'), 174.6 (C1'), 150.6 (C7'), 149.6 (C5"), 147.5 (C6'), 147.5 (C6"), 139.2 (C2'), 137.1 (C1"), 134.0 (C4"), 133.2 (C9'), 128.7 (C5'), 122.9 (C2"), 111.1 (C8'), 105.3 (C3'), 101.2 (C6), 100.5 (C5), 100.2 (C4). HRMS(ESI+) m/z calculated for $C_{23}H_{20}N_6O$ [M + H] + 397.1717, found 397.1790.

Chapter 3: Screening

Aim

This chapter describes novel compounds that cause the differentiation in THP1, HL60, OCI-AML3 and KG-1 cells. The active hits were defined as the compounds that upregulated CD11b expression to 10% or more, as measured by flow cytometry (a prior optimisation of the assay had been done before by Dr Thomas Jackson and Dr Laia Jose Cullere, where positive controls were tested and an increase of 10% was over the error of the non-treated samples and high enough to pick up the active compounds). CD11b is a common marker for differentiated haematopoietic lineages such as macrophages, neutrophils, natural killer cells. These hits were further validated by a change in morphology and proliferation. The datasets in this chapter show upregulation of CD11b marker in the four cell lines followed by images indicating morphological changes and a block in proliferation. The compounds initiating differentiation also cause a G1 arrest in the cell cycle. The active hits from the screening are listed below (Table 3.1) and comprise of reported HDACi such as mocetinostat (B12), MS-275 (B3), C10 and its analogue B6 with changes in the amine group of the aromatic ring alongside novel analogues D6 and H2.

In addition, one of the novel analogues obtained as a hit from the screening assay was chosen to further study the pathways leading to differentiation. In particular, the Zn^{2+} active site binding motif of the compounds was altered in the design of probes to understand whether HDAC inhibition is responsible for inducing differentiation. The aim of this chapter, thus, is to find a novel analogue that commonly induces differentiation across different cell lines. It also gives a preliminary understanding of whether or not HDACs are involved in the differentiation process.

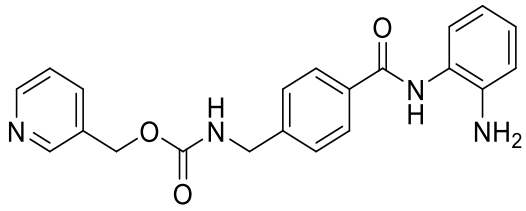
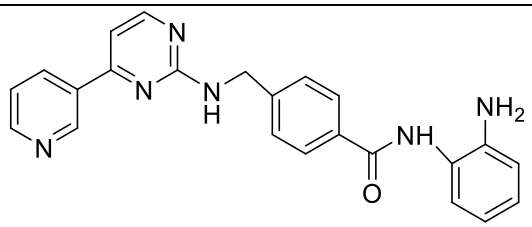
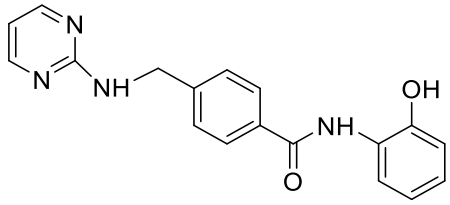
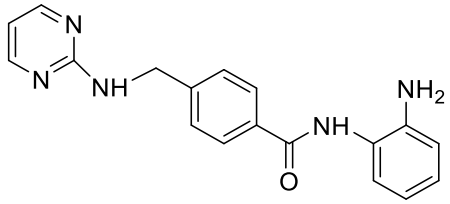
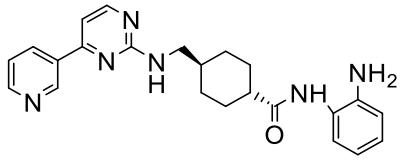
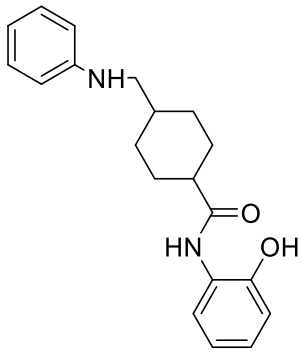
Compound	Well	Name (A.K.A)	Structure
OX01971	B3	MS-275 Class 1, 3	
OX01976	B12	Mocetinostat Class 1, 4	
OX02002	B6	unknown	
OX02004	C10	unknown	
OX02128	D6	unknown	
cjrb743	H2	unknown	

Table 3.1: The active compounds which induce CD11b expression in five cell lines.

3.1 CD11b upregulation in OCI- AML3, HL60, THP1 and KG-1

In the assay- 90 compounds previously prepared in the group for a different project, which included HDAC inhibitors or structurally related novel analogues with unknown HDAC inhibitory activity, were tested at four different concentrations (10 μM, 1 μM, 100 nM and 10 nM). However, for the majority of these compounds, activity was only observed at either 10 μM or 1 μM. Hence, the active compounds were retested only at 10 μM and 1 μM.

As shown in Figure 3.1, the various HDACi and their analogues showed CD11b expression; DAPI was used for calculating the total live cell population. The percentage of cells that expressed CD11b (Figure 3.2 A – R4 pink) were calculated based on the total live cells excluding the debris at the bottom and selecting only the single cell population expressing the marker of interest in pink. DAPI (Figure 3.2 B- R3 red) used for staining the dead cells was used to calculate the viability percentage. The DAPI-stained cells (red) were 0% viable and therefore gated out of the live cells selected in R3, giving the actual viability percentage.

3.1.1 Hits across different cell lines

The active hits were tested in the OCI-AML3 cell line and the novel analogues were found to be more active at 10 μM than 1 μM. GS87 is a highly specific GSK3 kinase inhibitor induces differentiation in OCI-AML3 cells (Hu et al., 2016). GS87 at 30 μM was used as a positive control.

The active hits were also tested in HL60 cell line and the novel analogues were again shown to be more active at 10 μM than 1 μM. Phorbol 12-myristate 13-acetate (PMA) has shown to induce differentiation in HL60 cell line, and hence PMA was used as the positive control for the cell line HL60 (Zhao et al., 2004).

CD11b is not highly expressed in KG-1 cells but a decrease in cell viability upon compound treatment is indicative of a compound effect. Novel analogue D6 was observed to have some

activity in KG-1 cells and morphology analysis and proliferation arrest were necessary to confirm these effects. PMA was used here as the positive control.

D6 and the commercial HDACi mocetinostat or B12 both upregulated CD11b expression of 10% or more in THP1 cells at a concentration of 10 μM. Some of the compounds which expressed CD11b expression also showed a loss in viability as compared to the controls.

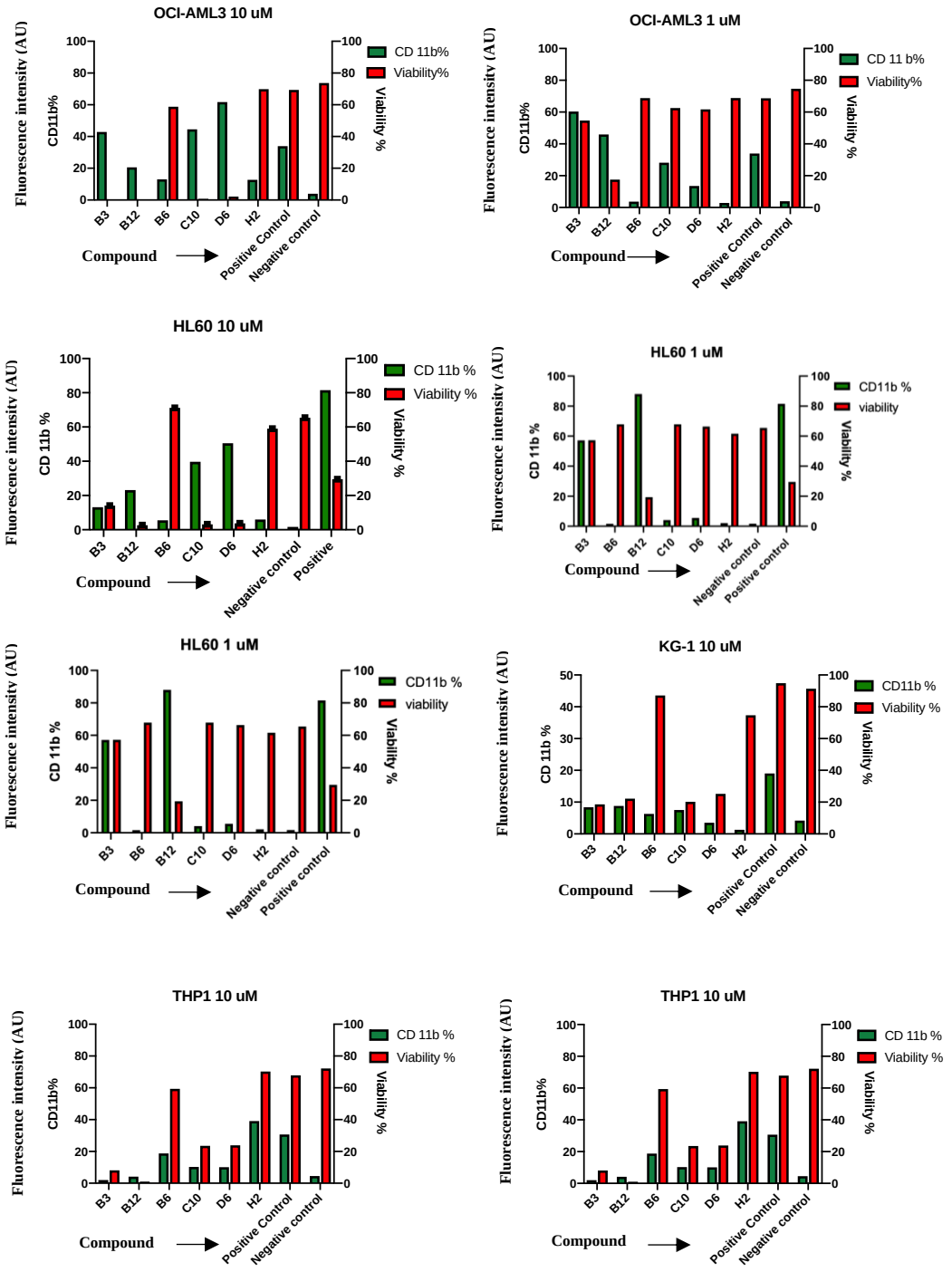
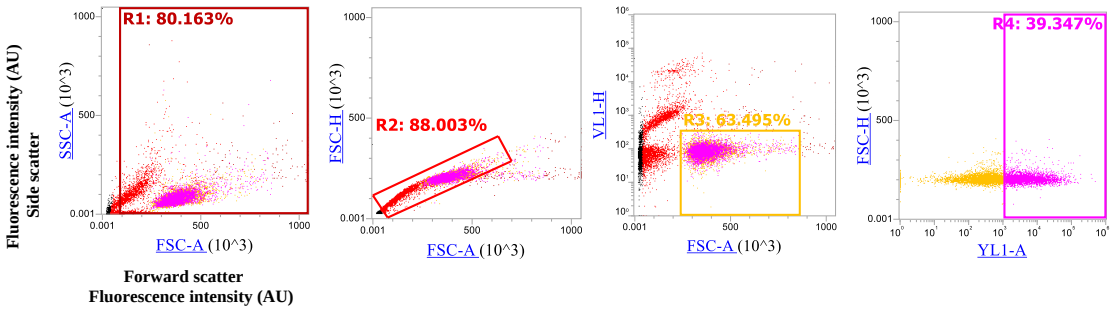


Figure 3.1: Effect of compounds on differentiation. OCI-AML3, HL60, KG-1 and THP1 cells were treated with 10 μM and 1 μM of the following compounds for four days. The negative control for all cells was DMSO vehicle and the positive controls were PMA for HL60 and KG-1 cells, GS87 for OCI-AMl3 and TCP for THP1 cells. The percentage of cells expressing CD11b surface differentiation marker was determined by flow cytometry as described in the Materials and Methods.

THP1 cells treated with TCP (10 µM)

A **TCP (10 µM)**



B **NT**

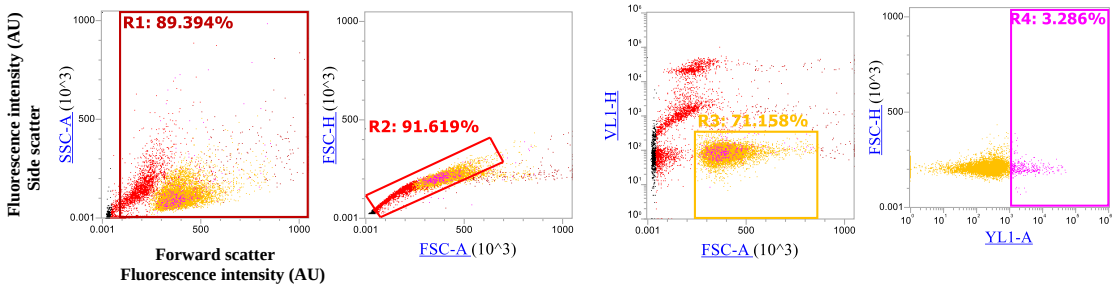


Figure 3.2: (A) Representative FACS plots for positive control (TCP) and (B) non-treated cells. In the plots, R1 denotes forward scatter (FSC) vs. side scatter (SSC) with the gate selecting the population of the total cells excluding the debris at the bottom, R2 denotes single cell population, R3 denotes live cells, R4 denotes the live cells expressing the marker of interest in pink.

3.2 Isotype Control

Verification was required to ensure that the compounds inducing CD11b were not false positives due to nonspecific binding from the antibody, cell auto fluorescence, or compound fluorescence. Cells were initially treated with the compounds in a time point study and were checked for differentiation every 24 hr. At the end of four days cells treated with positive control showed complete differentiation without affecting the cell viability and the DMSO control had no effect on the differentiation of the cells. Thus, four days was chosen as the time point for further studies.

THP1 cells were treated for four days with the respective compounds at both 10 µM and 1 µM. Cells were then stained using either anti-CD11b or with mouse IgG isotype control antibody which has the same fluorophore as CD11b (FITC with excitation wavelength being 495 nm and emission being 516 nm). The data shows that for the novel compound D6 the signal from isotype control binding is not much more than CD11b expression suggesting that the signal does not arise due to non-specific binding (Figure 3.3). This data was common across HL60, OCI-AML3 and KG-1 cells, indicating the specificity of the compound D6 to the target of interest. The isotype control test was done with all the six compounds that came as hits across different cell lines, however, D6 was of particular interest as it had less cytotoxic effects across different cell lines and also due to the difference in the linker group as compared to the commercial HDACi mocetinostat.

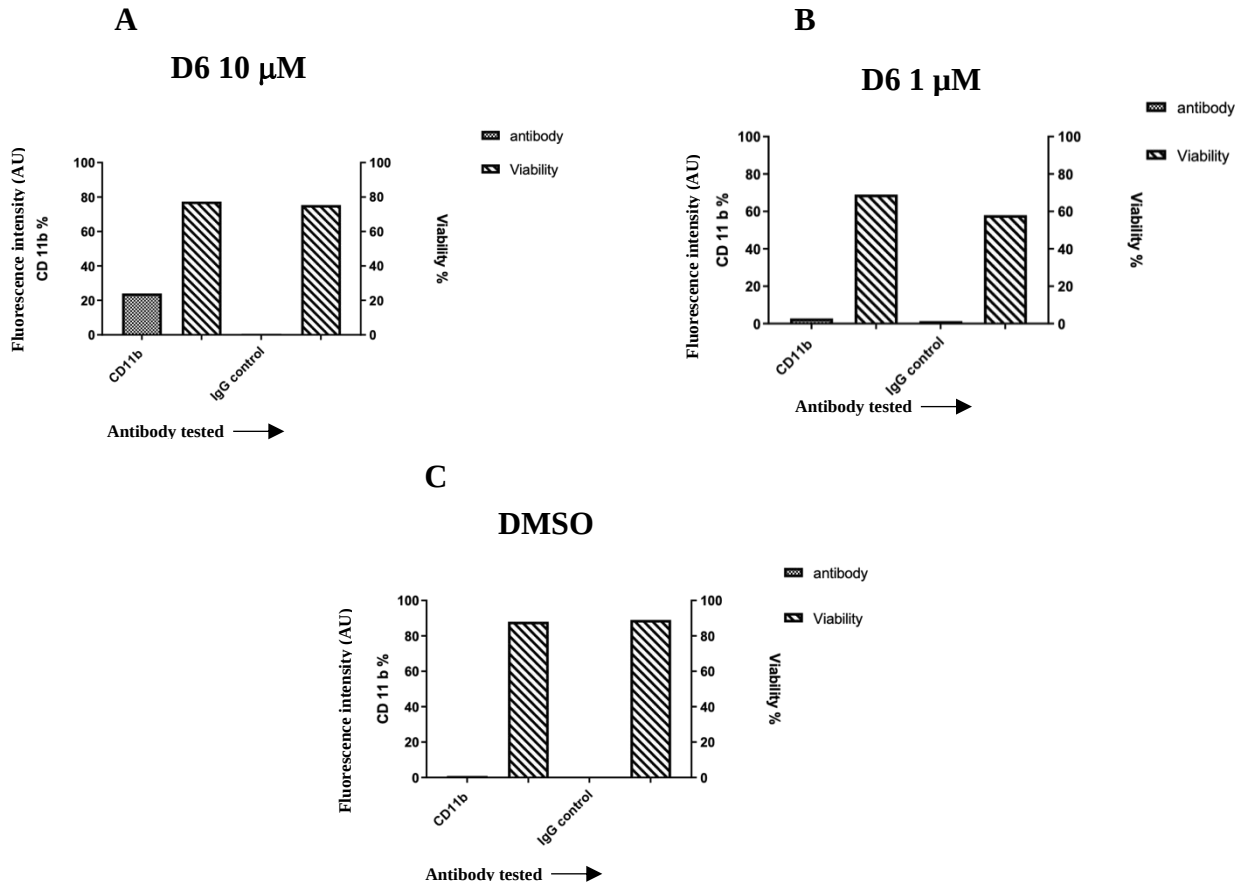


Figure 3.3: D6 specifically increases CD11b expression. THP1 cells were treated with the compound D6 at (A) 10 µM (B) 1 µM and (C) Negative control for four days and were then incubated with either the primary antibody CD11b or the isotype control as described in Materials and Methods.

3.3 Morphology analysis and block in proliferation

As discussed previously, due to the dysregulation of the proliferative factors in leukaemia there is an uncontrolled proliferation of the abnormal cells. However, on inducing differentiation-a block in proliferation is observed. This could be measured by seeding 20,000 cells/mL in a 96-well plate and treating them with the respective concentration of the compounds for 96 h. Following incubation, total cell number was calculated using an automated NC 3000 cell counter machine, with acridine orange staining all cells and DAPI staining the dead cells. The automated software calculates the viability and the total cell number. D6 induced a block in proliferation across the four AML cell lines with a visible reduction in the cell number as

compared to the negative control. There was a reduction in the viability upon compound treatment as a result of the compound-related toxic effects at that particular concentration (Figure 3.4).

The morphological changes that could be observed included an increased proportion of granulocytes, segmented nuclei, presence of vacuoles, macrophage like morphology or expanded cytoplasm (Bruserud, 2000).

To assess the change in the morphology of the cells showing an upregulation of CD11b expression, cells were treated with 10 µM and 1 µM of the compound for four days (Figure 3.5). The cells were then stained using Wright Giemsa stain, with oxidised methylene blue for staining the nucleus blue to purple and eosin Y dye for staining the cytoplasm pink. Images were taken using Olympus BX 30. The cells treated with the compound D6 at both 10 µM and 1 µM showed clear changes in morphology such as the presence of vacuoles, multiple nucleoli and an extended cytoplasm, consistent with myeloid differentiation as compared to the non-treated cells (Figure 3.5 B).

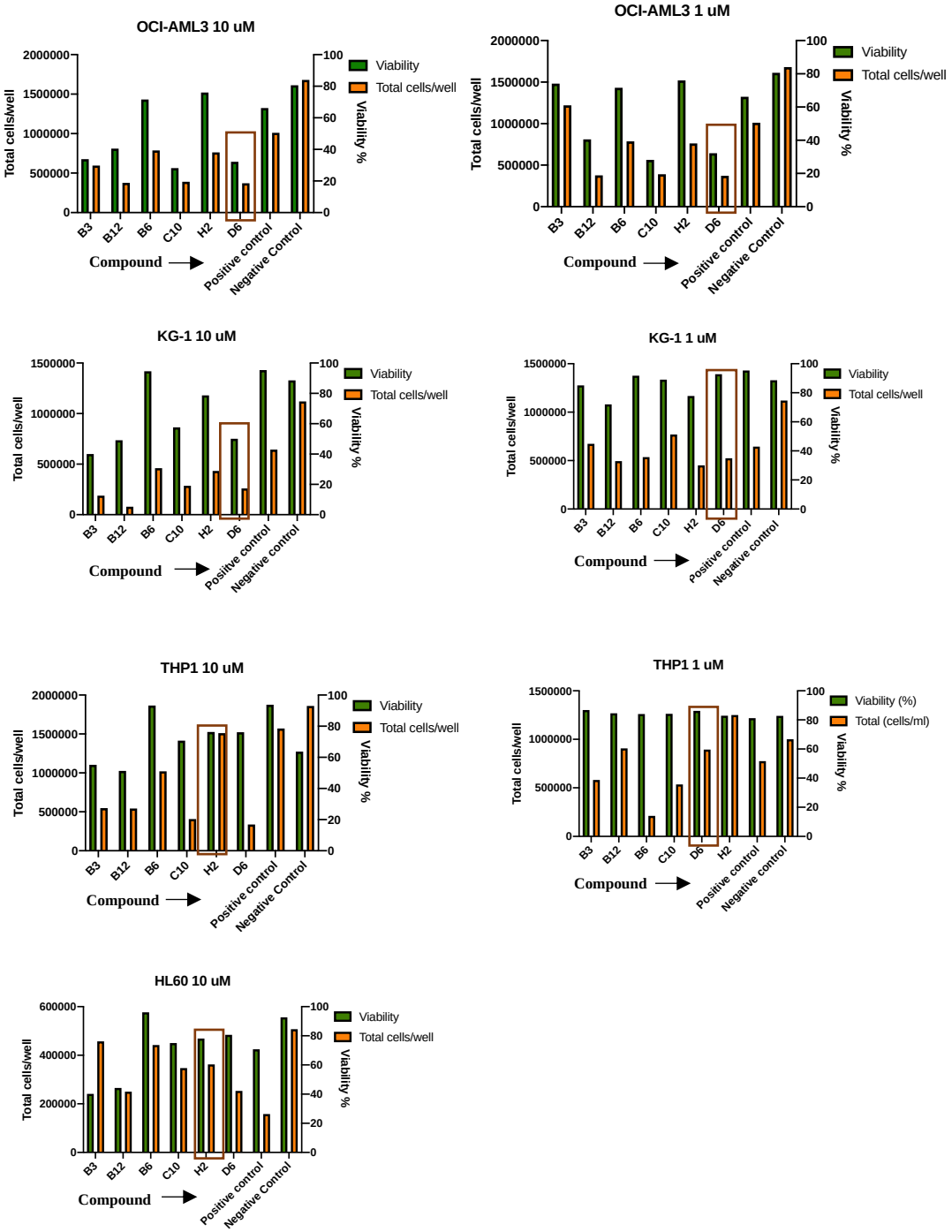


Figure 3.4: Representative data for when D6 inhibits cell proliferation. Equal numbers of OCI-AML3, KG-1, THP1 and HL60 cells were treated with the compounds (10 μM) and (1 μM) for four days and the cell viability (right hand axis) and total cells/well (left hand axis) were counted using Nucleo Counter (NC-3000) system.

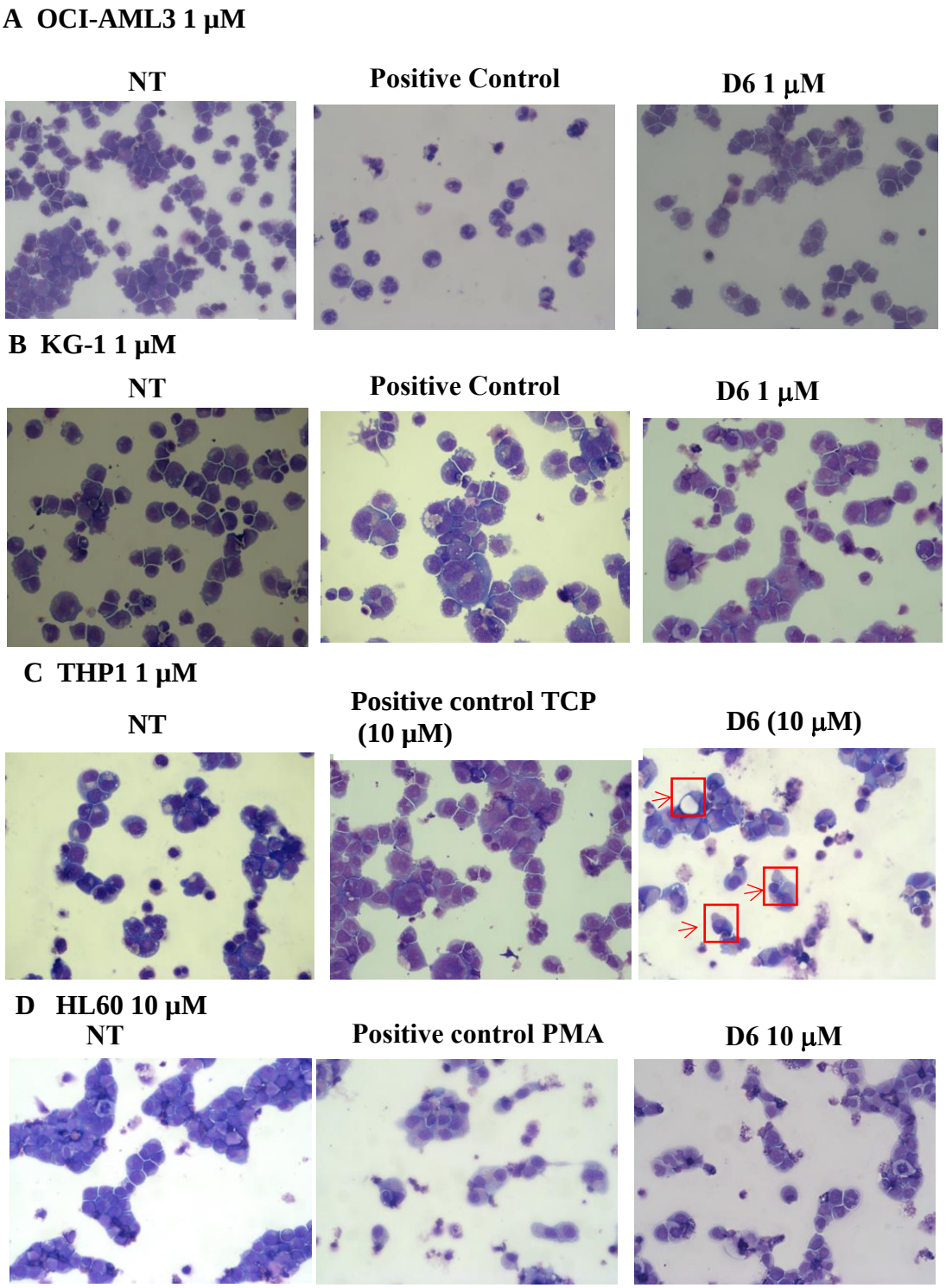


Figure 3.5: A, B, C, D: Compound D6 promotes differentiation of OCI-AML3, KG-1, THP1 and HL60 cells as indicated by red arrows showing the morphologic changes compared with non-treated cells. Cells were stained using Wright-Giemsa Stain. Images were taken using the Olympus BX 30 camera and acquisition software Infinity at magnification X40 and scale bar 20 µm. The arrows indicate representative cells with vacuoles, large cytoplasm and multiple nucleoli.

3.4 Cell Cycle analysis

Leukemic transformations often result in an excess of immature cells that do not differentiate. During differentiation, checkpoint activation leads to cell cycle arrest in G0/G1 phase (Schnerch et al., 2012b). After treatment of THP1 cells with D6 at both 10 µM and 1 µM, they were permeabilised as described in Materials and Methods and stained with DNA binding dye propidium iodide (PI). Propidium iodide binds to the DNA content of the cells and as such, higher intensity corresponds to more DNA per cell. In (Figure 3.6 A), PI histogram showed cells in the three phases of the cell cycle, quantified by the amount of PI. Treatment of the cells with D6 caused a significant increase in the number of cells in G1 phase and subsequent decrease in the cell number for both G2 and S phase as compared to the negative control (Figure 3.6 B). This shows cell cycle arrest in G1 phase as a result of treatment.

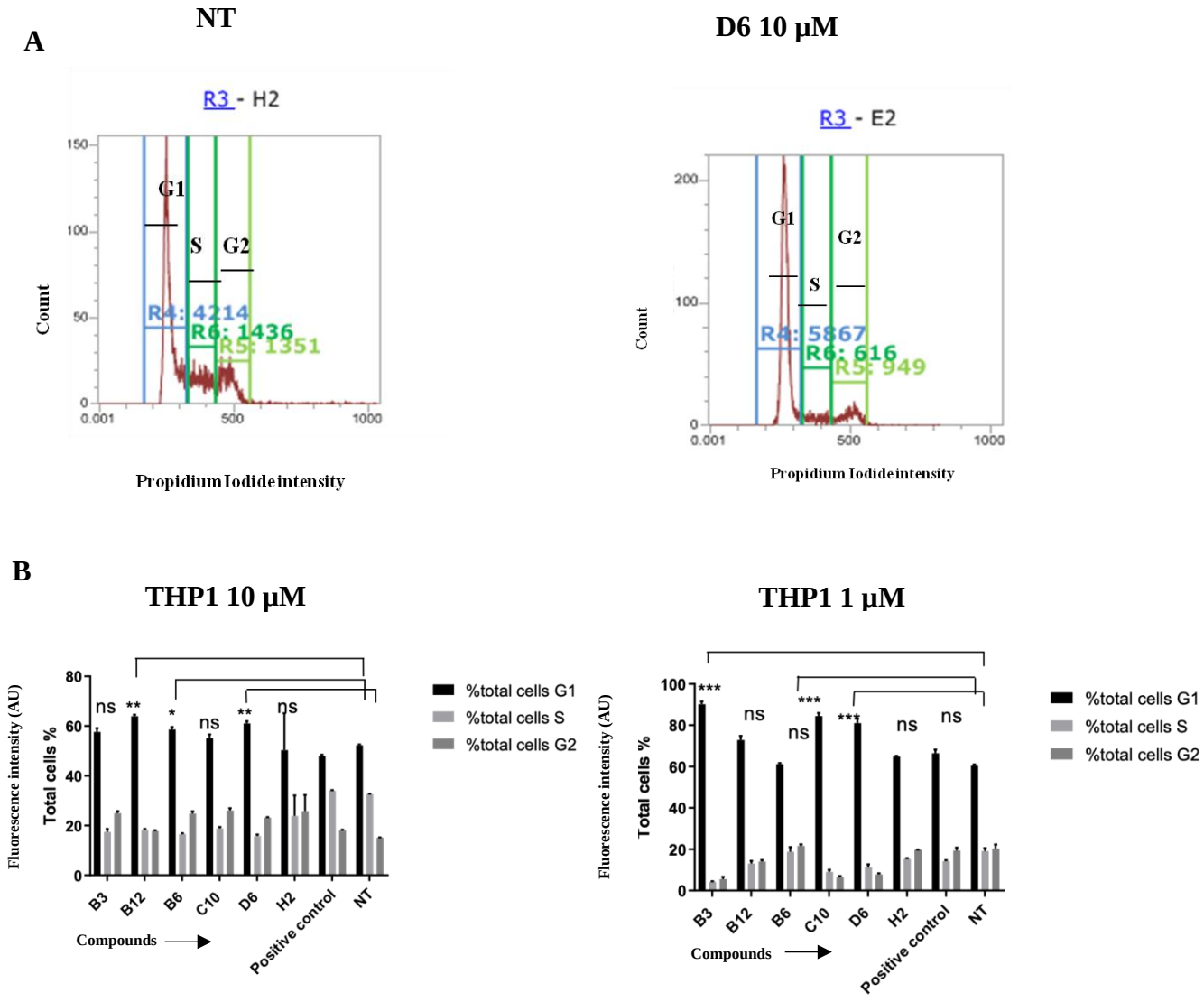


Figure 3.6: (A) Representative FACS plots of cell cycle analysis for THP1 cells after treatment with the compounds at 10 µM and 1 µM for four days. The y- axis denotes the percentage of cells undergoing the respective G1, S and G2 phases of the cell cycle and the x- axis denotes the compounds treated with the cells. NT serves as the negative control. (B) Quantification of cell cycle distribution using propidium iodide which stains the DNA in the cell. Total n=3 for each of the samples. P values were calculated using Two-way ANOVA. *P<0.05, ** P<0.01, ***P< 0.001.

3.5 Synthesis

Previous studies have shown that the anilide aryl ring with a chelating group (NH_2 or OH) at the *ortho* position binds potently to the active zinc ion *via* bidentate coordination at the catalytic site and exerts HDAC inhibitory effects. It was decided to make an inactive or potentially inactive counterpart with the chelating group being shifted from the *ortho* to the *meta* position thereby precluding the possibility of chelation to the active site zinc ion. It was postulated that if the compounds acted only via HDAC inhibition, the *meta* analogues would be unable to induce differentiation.

The novel compound D6 showed differentiation effects on three genetically different cell lines. However, it was important to study if the working mechanism of D6 was through the acetylation of the histones. For this purpose, D6 was prepared along with its analogue with the amine at the *meta* position to help determine whether the active compounds alter histone acetylation. Mocetinostat (referred to as B12 in the previous experiments) and its *meta* analogue were also prepared to serve as controls in these experiments (Table 3.2).

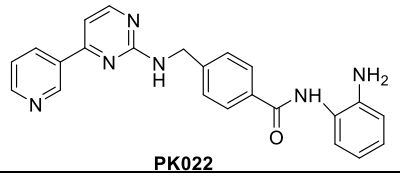
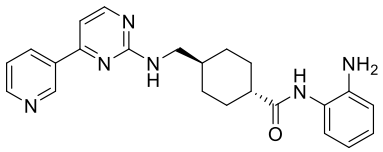
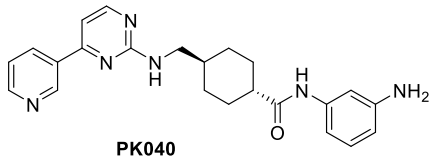
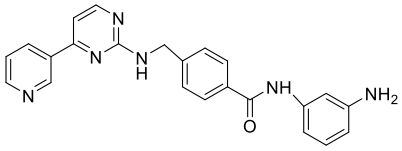
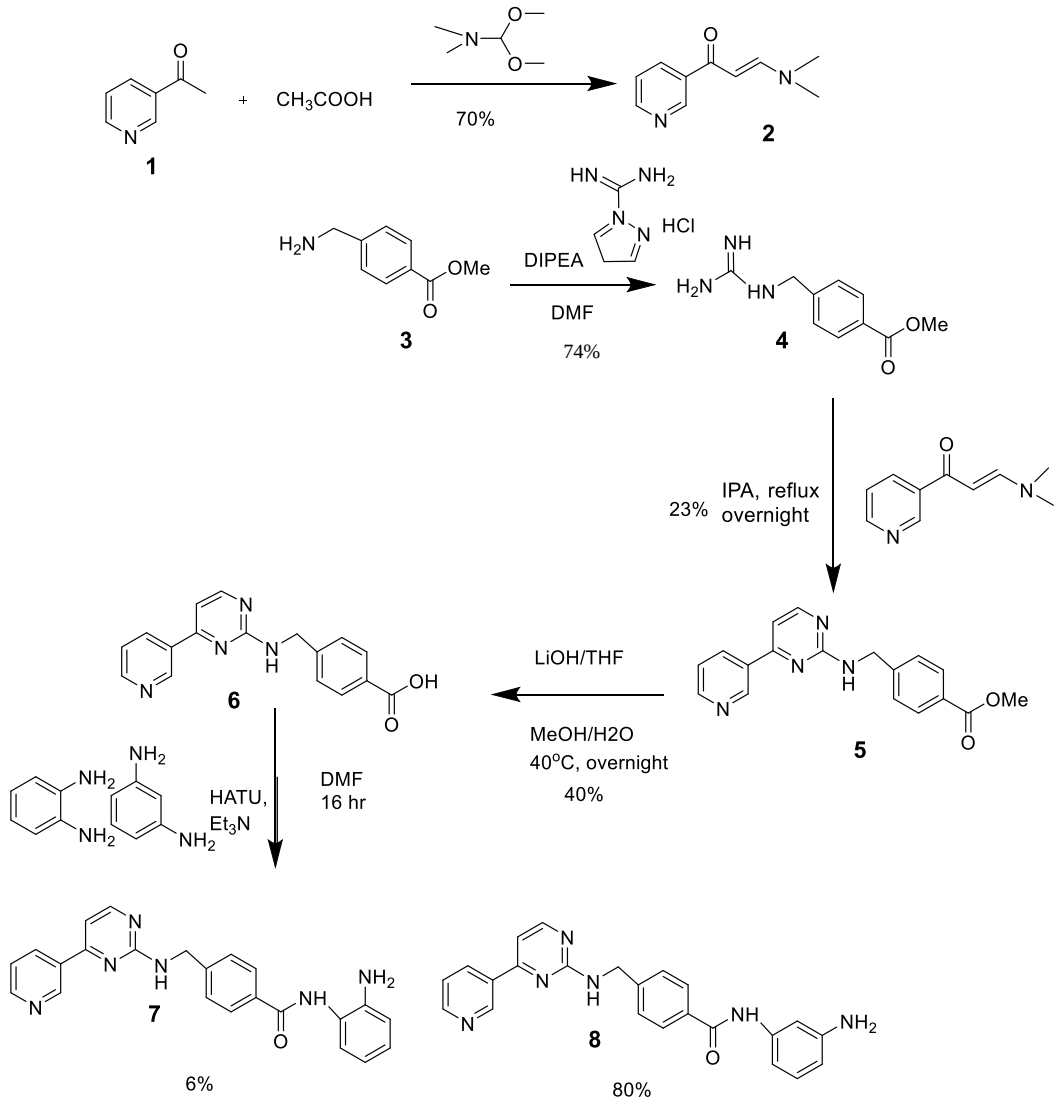
Analogue	Structure
PK022 aka Mocetinostat	 PK022
D6	 PK038
PK040	 PK040
PK026	 PK026

Table 3.2: The novel compound D6, HDACi mocetinostat and its *meta* analogue PK040 and PK026 respectively.

3.5.1 Synthesis of mocetinostat (PK022) and its *meta* analogue (PK026)

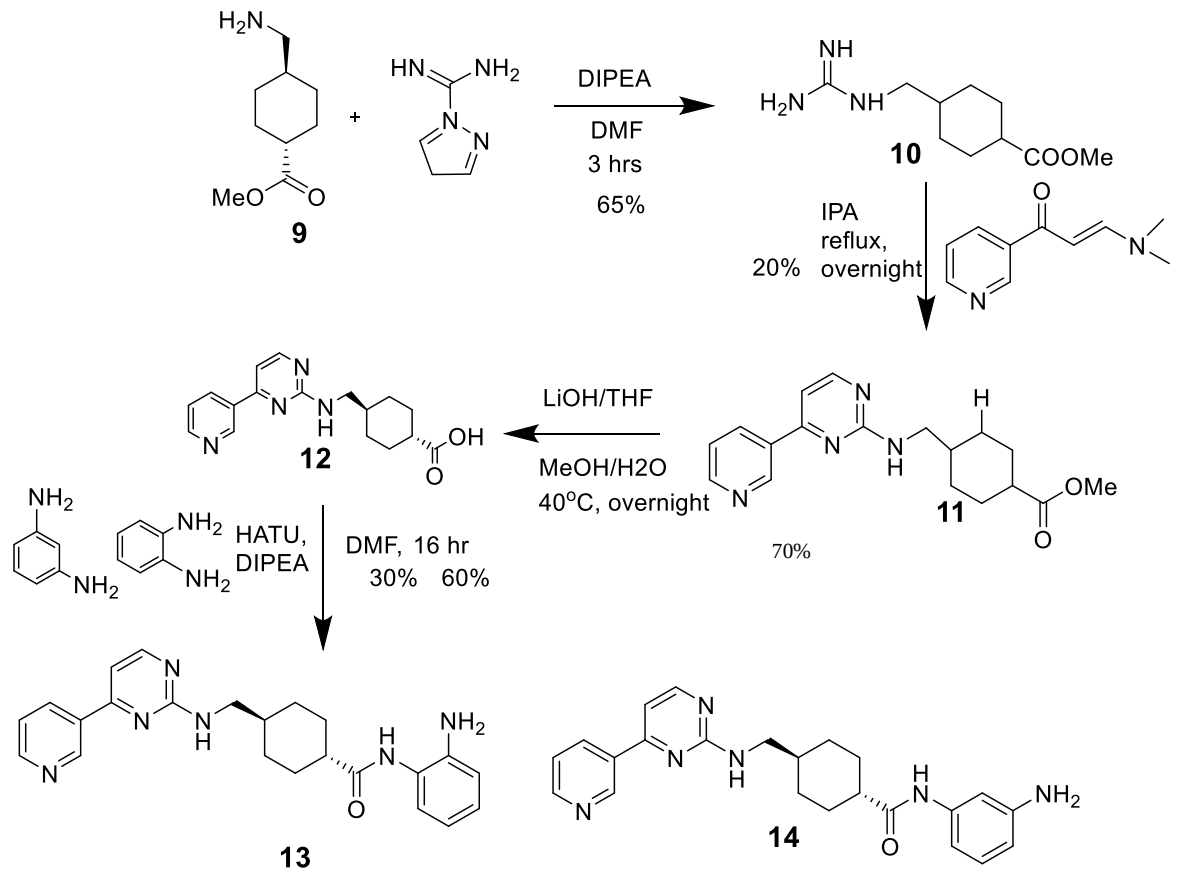
The product was obtained starting from commercially available 3-acetylpyridine **1** (Scheme 1.1). The reaction of **1** with *N*,*N*-dimethylformamide dimethyl acetal gave **2**. Treatment of the amine **3** with pyrazole-1-carboxamidine hydrochloride in a basic medium gave guanidine **4**, which was reacted with **2** to form **5**. The methyl ester was hydrolysed to provide acid **6**, which underwent amide coupling with 1,2-phenylenediamine to provide mocetinostat **7**, and with 1,3-phenylenediamine to give its analogue **8** with the amine at the *meta* position to serve as a potential inactive control. **7** and **8** were obtained in overall yields of 6% and 80% respectively.



Scheme 1.1: Synthesis of mocetinostat or PK022 (**7**) and its *meta* analogue or PK026 (**8**).

3.5.2 Synthesis of the novel compound D6 and its *meta* analogue (PK040)

The novel compound D6 was obtained following similar synthetic conditions as for mocetinostat. As shown in Scheme 1.2, in this case methyl (1*R*,4*R*)-4-(aminomethyl) cyclohexane-1-carboxylate **9** was used as the starting material. **9** was then treated with 1-H-pyrazole-1-carboxamide hydrochloride to give guanidine **10,** which was then reacted with **2** to give pyrimidine **11**. Compound **11** was hydrolysed at similar conditions and the acid form **12** was subjected to amide coupling with 1,2-phenylenediamine to give OX02128 (D6). The treatment of **12** with 1,3-phenylenediamine gave the *meta*-amine analogue **14**.



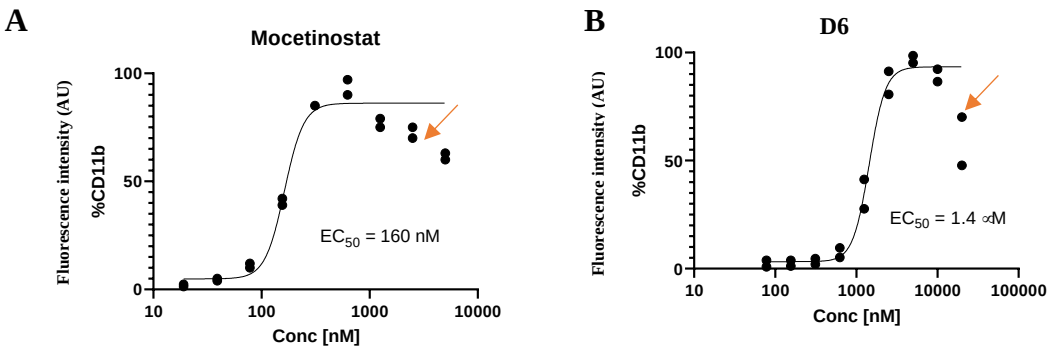
Scheme 1.2: Schematic for the synthesis of the novel compound OX02128 or D6 (**13**) and its *meta* analogue PK040 (**14**).

Compound PK038 will be referred as D6 and compound PK022 as mocetinostat throughout the following chapters.

3.6 Dose response curves in HL60 cell line

In order to determine the potency of our selected compound D6, its activity was tested at various concentrations. HL60 cells were treated with D6 and its analogue for four days with concentrations ranging from 40 μM to 78 nM. CD11b expression rate and viability for each compound are shown in Figure 3.7 A. Treatment of HL60 cells with D6 gave an EC_{50} value of 1.4 μM, while HDACi mocetinostat gave an EC_{50} of 160 nM. However, it was interesting to see that the analogues containing amine groups at the *meta* position which were designed to be inactive analogues were active at higher concentrations. These compounds are less potent, with EC_{50} values of 7.4 μM for PK026 and 14.4 μM for PK040.

In the dose response curves of mocetinostat and D6 some drop in the effect of CD11b was observed at higher concentrations (shown by the arrow in Fig 3.7 A and B). The higher concentrations were giving a relatively lower CD11b expression. This could be result of reduced antibody antibody interaction at higher concentration or it could also be due to the decrease in the cell numbers as a result of toxicity caused by compounds at such high concentrations.



C

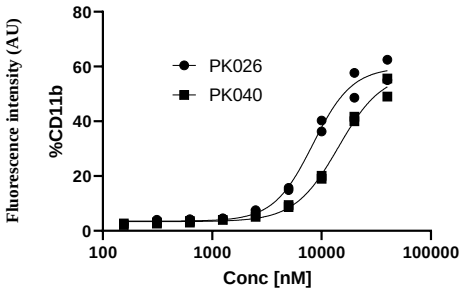


Figure 3.7: Representative flow cytometric analyses for HL60 cells treated with different compounds. (A) mocetinostat gave an EC_{50} of 160 nM (B) D6 gave an EC_{50} of 1.4 μM and orange arrows indicating drop in the effect of CD11b. (C) The *meta* analogues of mocetinostat had an EC_{50} of 7.4 μM and PK040 an EC_{50} of 14.4 μM. The compounds were tested in technical triplicates for each of the concentrations and the experiments performed in biological triplicates.

3.6.1 Dose response curve in OCI-AML3 and THP1

Similar dose response experiments were performed for the other two cell lines, OCI-AML3 and THP1. The OCI-AML3 cells were treated with the respective compounds for four days in a concentration range of 40 μM to 78 nM. Novel analogue D6 induced some activity with an EC_{50} value of 6 μM and the *meta* analogues PK026 and PK040 were shown to be only active at the much higher concentration of 51 μM and 53 μM. However, on treatment of THP1 cells with the four compounds, only the *ortho* analogues D6 and mocetinostat induced a response and the *meta* analogues were shown to be inactive. These results were further validated by a proliferation assay and morphological analysis. However, for THP1 morphological changes and a block in proliferation were only observed with D6 and not with the *meta* analogues. As for OCI-AML3, clear morphological changes could be seen on treatment with D6, PK026 and PK040, followed by a block in proliferation confirming differentiation. The data for the two cell lines is attached in the appendices (Figure 9-14).

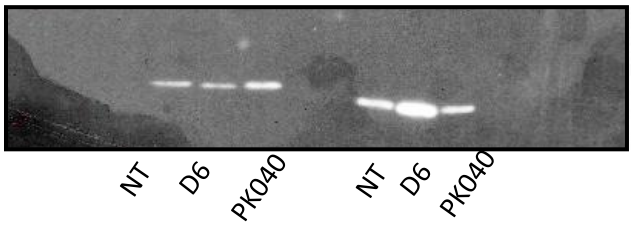
3.7 Western blot

Histones have *N*-terminal lysine residues and may undergo a variety of posttranslational modifications including acetylation and deacetylation.

It is well established that a HDACi inhibits HDACs and thereby promotes acetylation of lysine residues. This can be measured using a western blot technique. Since histone 3 is the most abundant histone, it was selected as the substrate for the acetylation assay. An anti-histone 3 (acetyl K9) antibody, specific to H3 and acetylated at lysine position 9 was used.

To begin with, the expression of total histone and acetylated histone on treatment with HDACi was investigated. HL60 cells were treated for 24 h with 2.5 μM of D6 or 30 μM of its *meta* analogue PK040. In Figure 3.8, NT samples serving as the negative control did not show an increase in the acetylated levels of histone 3. Histone acetylation of H3 with D6 was confirmed, however, the *meta* analogue did not show upregulation of the acetylated histone 3. Since HL60 had shown the CD11b expression of 90% or more for its positive control and a concomitant change in morphology with the active hits found from the FACS analysis, we decided to use HL60 as the main cell line for exploring the mechanism in depth.

A



B

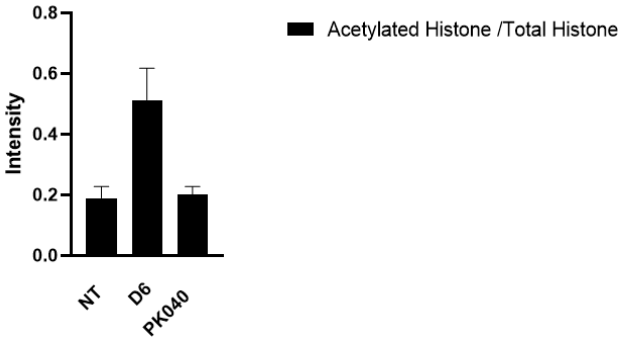


Figure 3.8: (A) Western blot analysis of the effect of D6 and its analogue PK040 (with amine at the *meta* position) on histone H3 acetylation after 24 h treatment in HL60 cells. (B) Quantification of acetylated histone 3 level normalised to total histone 3 with treatment of D6 and PK040. Error bars shown as SEM for total n=3 (biological triplicates) for each of the samples.

3.8 CD11b Time point study- HL60 cell line

Compound dosage for the following experiments were selected based on the EC_{80} concentration to obtain a large compound response while limiting cell death. Also because of biological variability and quite sharp slopes the EC_{80} values were of more significance. The concentrations chosen were 30 μM for the *meta* analogues, 2.5 μM for D6 and 600 nM for mocetinostat.

To reconfirm the upregulation of CD11b expression, a timepoint study was performed where the cells were treated with the respective compounds for 4 h, 12 h, 24 h, 48 h, 72 h and 96 h.

In Figure 3.9 (C) and (D) upregulation of Cd11b marker from as early as 24 h was confirmed for both the *ortho* (mocetinostat and D6) and the *meta* (PK026 and PK040) analogues.

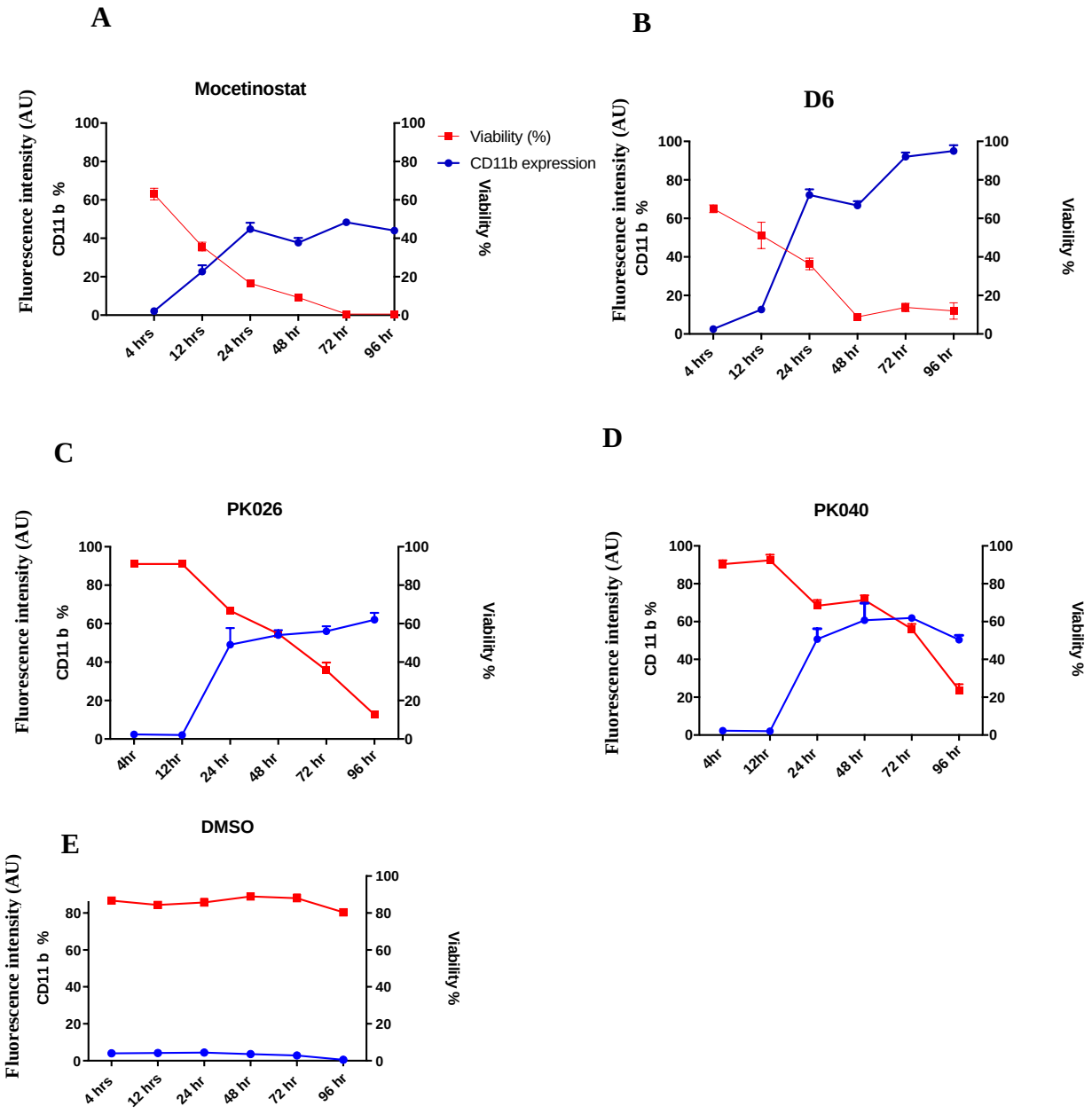


Figure 3.9: HL60 cells were treated with the respective compounds for a timepoint of 4 h, 12 h, and every 24 h until 96 h. FACS analysis shows the increase in CD11b expression for (A) 600 nM mocetinostat (B) 2.5 μM D6 (C) 30 μM PK026 and (D) PK040. Error bars shown as SEM of the three biological and three technical triplicates.

3.8.1 Western blot timepoint study

The novel analogues were hypothesised to induce CD11b expression and initiate differentiation through HDAC inhibition. Since in the previous time point study CD11b upregulation was observed as early as 24 h, it was decided to determine whether the increase in acetylated level of histone 3 was concomitant with Cd11b upregulation.

The results in Figure 3.9 show cell viability and cell number after treatment with the compounds for 4, 12 and 24 h. Viability remained close to 90% for both the *ortho* and the *meta* analogues, indicating no toxicity caused by the compounds at these time points and concentrations.

On probing the membrane with the control antibody histone 3 and acetylated histone 3 for the three different time points, D6 increased the acetylated levels of histone 3 from as early as 12 h (Figure 3.10). The band intensity for all the samples was measured for both total histone 3 and acetylated histone 3 antibody. The data for this was normalised and then expressed as band intensity of total histone 3 over acetylated histone 3.

A

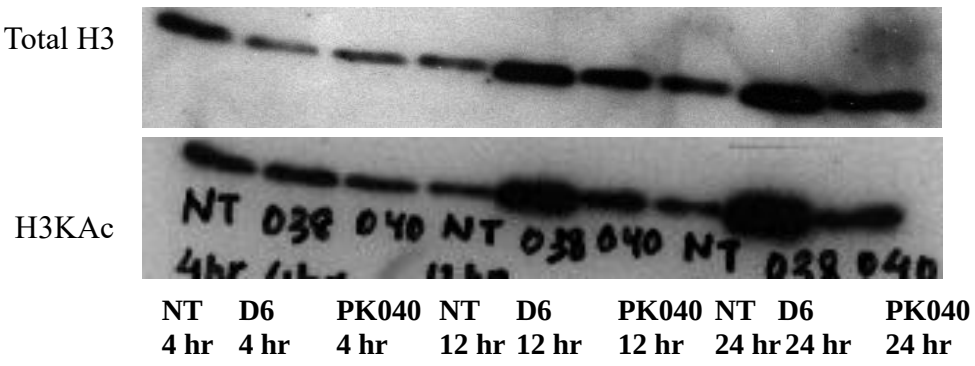


Figure 3.10: (A) The western blot shows total histone 3 levels and the acetylated level of histone for cell lysates treated with the compounds D6 and PK040. Only D6 increased histone acetylation.

The western blot data revealed that, in the case of D6, the increase in the acetylated level of histone is concomitant with the increase in CD11b expression. However, with *meta* analogue PK040, there is no increase in the acetylated level of histone 3 at 12 h and no increase in the CD11b expression too at that period of time (Figure 3.10). Also, PK040 does not increase the acetylated level of histone at 24 h but causes a significant increase in the expression of CD11b. This signifies an alternative mechanism of action directing the differentiation in HL60 cell line with the *meta* analogues.

3.9 Discussion

This chapter uses a phenotypic screen to identify compounds which cause differentiation of at least four genetically distinct AML cell lines. The variability in the potencies for these compounds across different cell lines is due to the vast genetic variability across different AML cell lines.

All the compounds were tested against these AML cell lines in two different concentrations of 10 μM and 1 μM. Ideally, hits were identified as compounds with 10 % or more upregulation of CD11b marker (a marker for differentiated lineages such as macrophages and neutrophils) with a good viability percentage. Viability was measured with the help of DAPI. Compound D6 was identified as a hit across different cell lines and caused less cell death. However, it wasn't known whether HDAC inhibition was responsible for the differentiation effects observed with this compound. Therefore, it was decided to investigate this compound further to understand its molecular mechanism of action. It was also decided to choose mocetinostat to serve as a control HDAC inhibitor throughout the study.

Since HDAC inhibitors are known for binding to the zinc active site binding motif, *meta* analogues were prepared for the above chosen *ortho* compounds in order to preclude the binding to the zinc ion active binding site. The *meta* analogues PK026 and PK040 were

initially prepared for the purpose of serving as the mechanistic probe without HDAC inhibitory activity however a dose response curve of these compounds were shown to be active, inducing differentiation but with a much lower potency. Western blots with the prepared compounds show increase in the acetylated levels of histone for only mocetinostat and D6, whereas the *meta* analogues fail to increase the acetylation of the histones indicating that they are causing differentiation via an alternative mechanism of action. Next, it was important to determine if D6 falls under pan HDAC inhibitor or could be a more specific one. The *meta* analogues PK026 and PK040 also needed to be studied to gain an insight into their target which leads to their observed differentiation effects in AML cell lines.

Chapter 4: Compound Profiling

Aim

In the literature several HDAC inhibitors (HDACis) explored against acute myeloid leukaemia are at preclinical development stage. Some of these HDACis include vorinostat and panobinostat, which are currently used in combination with other DNA hypomethylating agents (San et al., 2019). Despite the therapeutic efficacy, improvement is observed with these HDACis in combination with conventional chemotherapy or other epigenetic inhibitors, and the results are still modest (San et al., 2019).

The major drawback of these compounds is the high cytotoxic effects and the off target effects setting limits to their clinical utility (Benedetti et al., 2015). These compounds are well known pan HDAC inhibitors and are known to inhibit more than two HDAC enzymes of even different HDAC groups. It has been postulated that the isotype selective HDAC inhibitors can help overcome this hurdle and prove to be of better potential with clinical efficacy and safety (Hsu et al., 2017). For this purpose, it is important to focus on a HDAC inhibitor that could be more specific and less toxic.

As described previously (Chapter 1, Section 1.4.1) HDACs can be divided into 11 different isoforms based on structural homology and functions. The class I proteins (HDAC1, HDAC2, HDAC3, and HDAC8) have sequence similarity to the yeast Rpd3 protein. The class II proteins (HDAC4, HDAC5, HDAC6, HDAC7, HDAC9, and HDAC10) have sequence similarity to the yeast Hda1 protein. It was of particular interest to understand which of these specific isotypes was inhibited by the novel analogue D6. This chapter provides a comparison between the inhibitory profiles of mocetinostat, D6 and *meta* analogues PK026, PK040. This assay helped us to reconfirm the western blot results obtained in the previous chapter regarding their *meta* analogues.

Thus, here the profiles for HDAC inhibition for each of these analogues is compared *via* a recombinant enzyme assay and with *in situ* conditions. The latter part of the chapter focuses on answering whether or not HDAC inhibition is the primary mechanism leading to the differentiation effects observed, or if there is an alternative mechanism. For this purpose, cells were overexpressed with the HDAC1 plasmid and then analysed for the expression of CD11b in response to the inhibitor treatment.

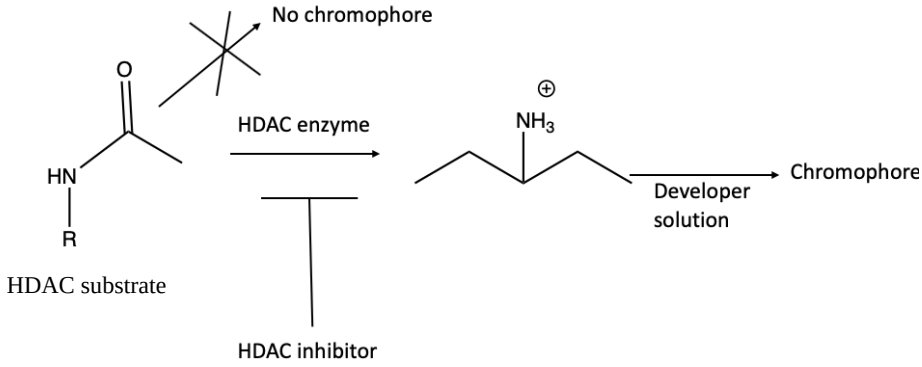
4.1 Pan HDAC inhibitory assays

HDAC inhibitory assays can be divided into pan inhibitory assays and recombinant assays. Both assays primarily help to understand whether or not an unknown compound is behaving as a HDACi. A recombinant assay gives a more specific profile of the compound by calculating the IC_{50} value against each of the recombinant HDAC enzymes. However, most of these proteins are regulated by dynamic and post translational mechanisms in cells. While, the recombinant tools can be more valuable, they are unable to give an insight into the functionality of these proteins in their biological systems. Thus, medicinal chemistry increasingly takes into account cellular assays to get a better understanding of how the protein interacts in this set up (Zhang et al., 2012).

In the previous chapter (Section 3.8.1), an increase was observed in the acetylation levels of histone3 by western blot with both D6 and mocetinostat whereas PK026 and PK040 did not increase the expression level of acetylated histone3. Thus, it became important to validate those results while confirming whether or not the *meta* analogues PK026 and PK040 caused any HDAC inhibition in HL60 cells.

First, a pan HDAC inhibitory assay was used from Active Motif which was sensitive for different HDACs from different classes; covering subtypes HDAC I, II and IV and particularly HDACs 1, 2, 6, 10 and 11. It is noteworthy that class III HDACs were not included as they are

structurally dissimilar from Zn^{2+} dependent enzymes and operate via NAD^{+} dependent mechanism. The assay utilizes a short peptide substrate with an acetylated lysine chain that could be deacetylated by a HDAC enzyme. Once the substrate is deacetylated, a developing solution is then added in order to react with the lysine residue. This leads to the release of a chromophore from the substrate which results in a yellow coloured product that absorbs maximally at 405 nm (Scheme 4.1)



Scheme 4.1: HDAC activity assay

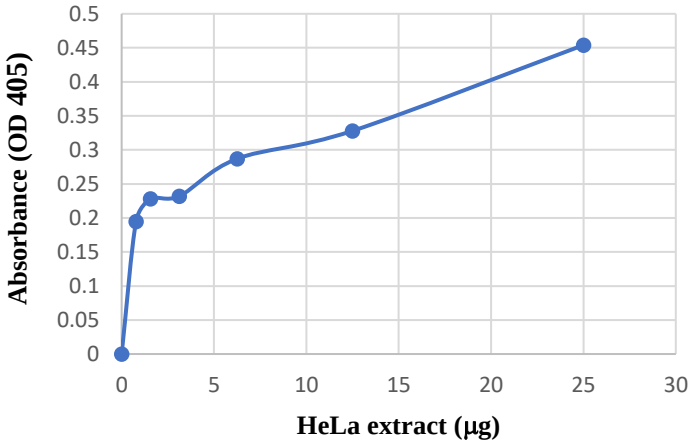
The assay was set up with the establishment of a standard curve where the standard was a non-acetylated version of the substrate peptide BOC-Lys-AMC which allows for the quantification of enzymatic activity (Figure 21 in appendices). Followed by this, the titration of HeLa cell extract (provided in the kit) helped to provide the signal window. The positive control for the assay were HL60 cells treated with TSA (a pan HDACi) with a lower absorbance value of 0.1, negative control of the assay consisted of only HL60 cell lysates with a higher absorbance.

4.1.1 Optimising the protein amount from HL60 cells for the assay

Increasing concentrations of HeLa extract were initially investigated to determine the signal window. However, with HL60 cells it was important to determine the quantity of extract needed that would give similar absorbance value to that of HeLa extracts to be used as the control in the future experiments. In this experiment, 600,000 cells were seeded in 3 mL in a 6 well plate and incubated for a period of 24 h. A BCA assay was used to determine the protein concentration in the HL60 extracts. Increasing amount of protein from HL60 cell extracts were quantified based on the concentration obtained from the BCA assay (explained in Materials and Methods) (Figure 19 Appendices).

In Figure 4.1 A the blue line represents activity from untreated HeLa extracts. 20 μg of HeLa extract was sufficient to produce a high absorbance value. It shows that the OD values at 405 nm were 0.4 for 20 μg of HeLa extract and 0.35 for 400 μg of non- treated HL60 cells (Figure 4.2 B). Thus 400 μg of non-treated HL60 cells were enough to provide a good signal window.

A



B

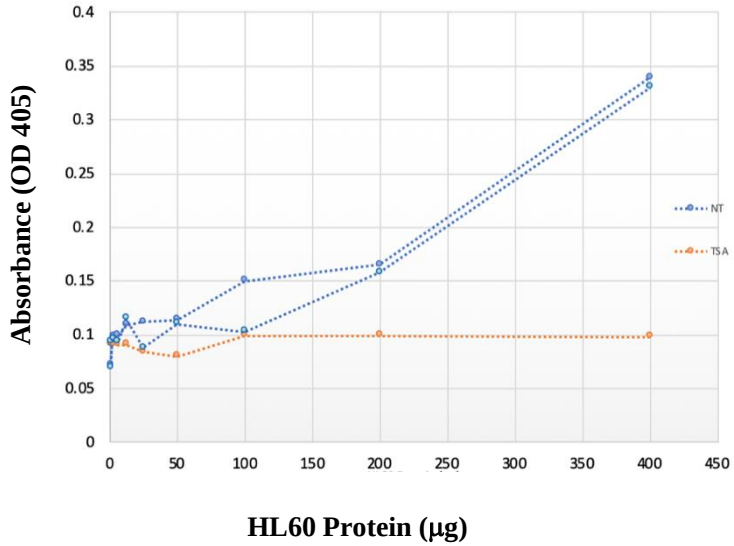


Figure 4.1: (A) HeLa cells were added in different amount (x-axis) ranging from 0 to 30 µg and checked for absorbance value at 405 nm on y-axis. (B) HL60 cells (NT) (in blue line) were loaded in amounts ranging from 0 to 500 µg (x-axis) quantified by BCA assay (reference appendices) and checked for absorbance value on the y-axis at 405 nm. HL60 cells treated with TSA (500 nM) (in orange line) were used as the control for this assay.

After confirming that 400 µg of HL60 extracts gave similar absorbance value to 20 µg of HeLa cell extract so significant signal window, the HL60 cell lysates were treated with compounds at a dose range of 100 µM to 256 pM with sequential five-fold dilutions. These were then tested for the HDAC activity as described in the Materials and Methods section. The negative control

with non-treated samples (NT) show an OD value of 0.6 whereas the positive control of TSA show an OD value of 0.2. The controls for the experiment confirmed that the assay had worked properly. The assay shows that the *ortho* analogues D6 and mocetinostat decreased the OD value in a concentration dependent manner, consistent with inhibition of lysine deacetylation. However, for the *meta* analogues PK026 and PK040 no inhibition of the HDACs is observed (Figure 4.2). The assay shows that *meta* analogues do not decrease the OD indicating that they are not behaving as HDAC inhibitors.

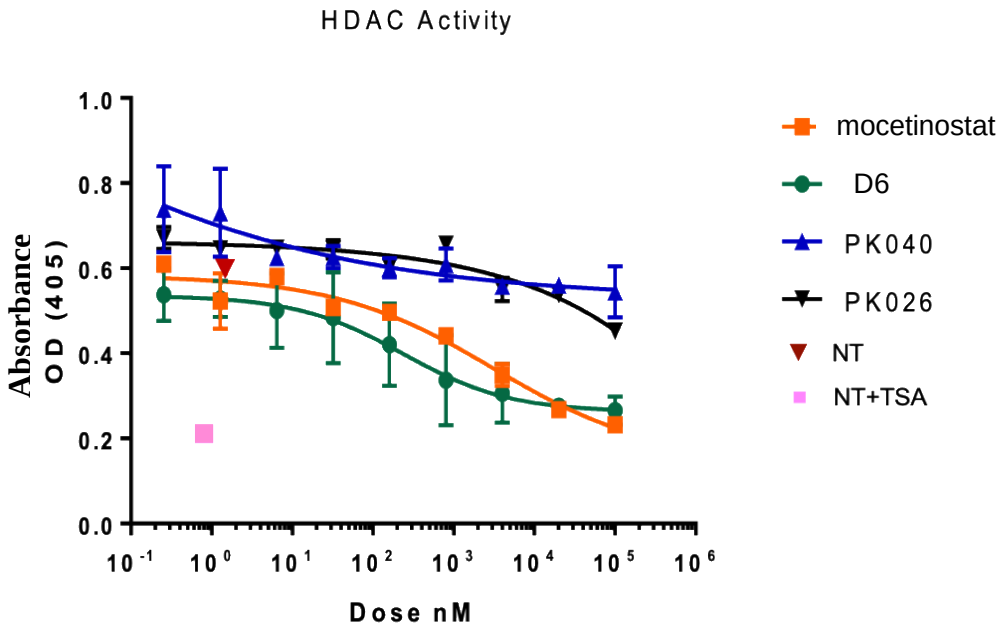


Figure 4.2: Functional HDAC activity assay: HL60 cell extracts (400 µg protein) were treated with various doses of the compounds mocetinostat (PK022), D6, PK026 and PK040. The compound doses are shown on the x-axis and the OD values on the y-axis. TSA (500 nM) was used as positive control and non-treated HL60 cells as negative control. Results are shown as means based on experiments performed in technical and biological triplicate; bars, ±SEM.

4.2.1 *In situ* HDAC activity assessment

In the previous experiment it was determined that both mocetinostat (PK022) and D6 inhibit the function of HDACs extracted from HL60 cells but PK026 and PK040 do not. However, it is possible that longer exposure of these compounds to HL60 cells may impact HDAC activity through other direct or indirect mechanisms. Therefore, to properly understand the effect on HDAC protein function in an *in situ* environment on treatment with the four compounds, it was decided to perform an experiment using the pan HDAC inhibitory assay (Section 4.1) but this time with a different method of sample preparation.

First HL60 cells were treated for 24 h in a 6-well plate with the respective concentration of the compounds - D6 (2.5 μM), mocetinostat (2.5 μM), PK040 and PK026 (30 μM). The following concentrations were chosen as the EC_{80} values from the dose response curve in the HL60 model obtained in Chapter 3 (Section 3.6). EC_{80} values made sure that there was 80% of response as well as a good viability from the chosen concentration and provided a sufficiently large signal window. Following this, the cell lysates were prepared (Figure 4.3 A), and the assay was performed as described above. Again, the non-treated sample shows the highest OD value of around 0.4 whereas the positive control of TSA (500 nM) shows an OD value of 0.1. It could be seen that along with the two HDACi mocetinostat and D6, the *meta* analogues PK040 and PK026 also decrease the OD value as compared to the non-treated sample, indicating a decrease in the deacetylation level of the acetylated substrate (Figure 4.3 B). This is in contrast to the effects seen in the previous section where compounds were added directly to the prepared cell lysates.

To rationalise these effects, the protein levels of HDAC1 and HDAC2 enzymes were analysed with the same set of samples. Since HDAC1 and HDAC2 are the two highly expressed HDACs, it was hypothesized that any change in HDAC activity as a result of

HDAC inhibition could have arisen as a result of a decrease in the amount of HDAC1 and 2 enzyme (Jamaladdin et al., 2014).

The HDAC1 assay kit from Epigentek is a quantitative kit designed for measuring total HDAC1 amount from cells. The assay works on the principle of indirect ELISA where the antigen is primarily immobilized on the surface of the microtiter plate, which blocks the surface with blocking proteins as mentioned above. The primary antibody (in antisera) binding to the immobilized antigen is then allowed to react with the enzyme-labelled secondary antibody, followed by the development of color. In this assay, the nuclear proteins containing HDAC1 are stably coated on the strip wells. This HDAC1 protein is recombinant protein (data provided with the kit manual). The HDAC1 is then recognized with a high-affinity specific antibody. The amount of HDAC1 can be quantified through a HRP conjugated secondary antibody-colour development system and is proportional to the intensity of colour development.

In this assay, the samples prepared for the HDAC activity assay are normalised using BCA assay. The non-treated samples serve as the positive control as these samples expressed the highest levels of HDAC (*i.e.* 8-10 ng/mg). A decrease in the expression of HDAC1 and 2 is observed upon treatment with mocetinostat, D6 and the *meta* analogues PK026 and PK040 when compared to the control (Figure 4.3 C and D).

The results obtained with the *in situ* HDAC inhibitory assay suggest that there might be an indirect effect exerted by the *meta* analogues leading to the differentiation effects, which may involve the reduction in the HDAC expression.

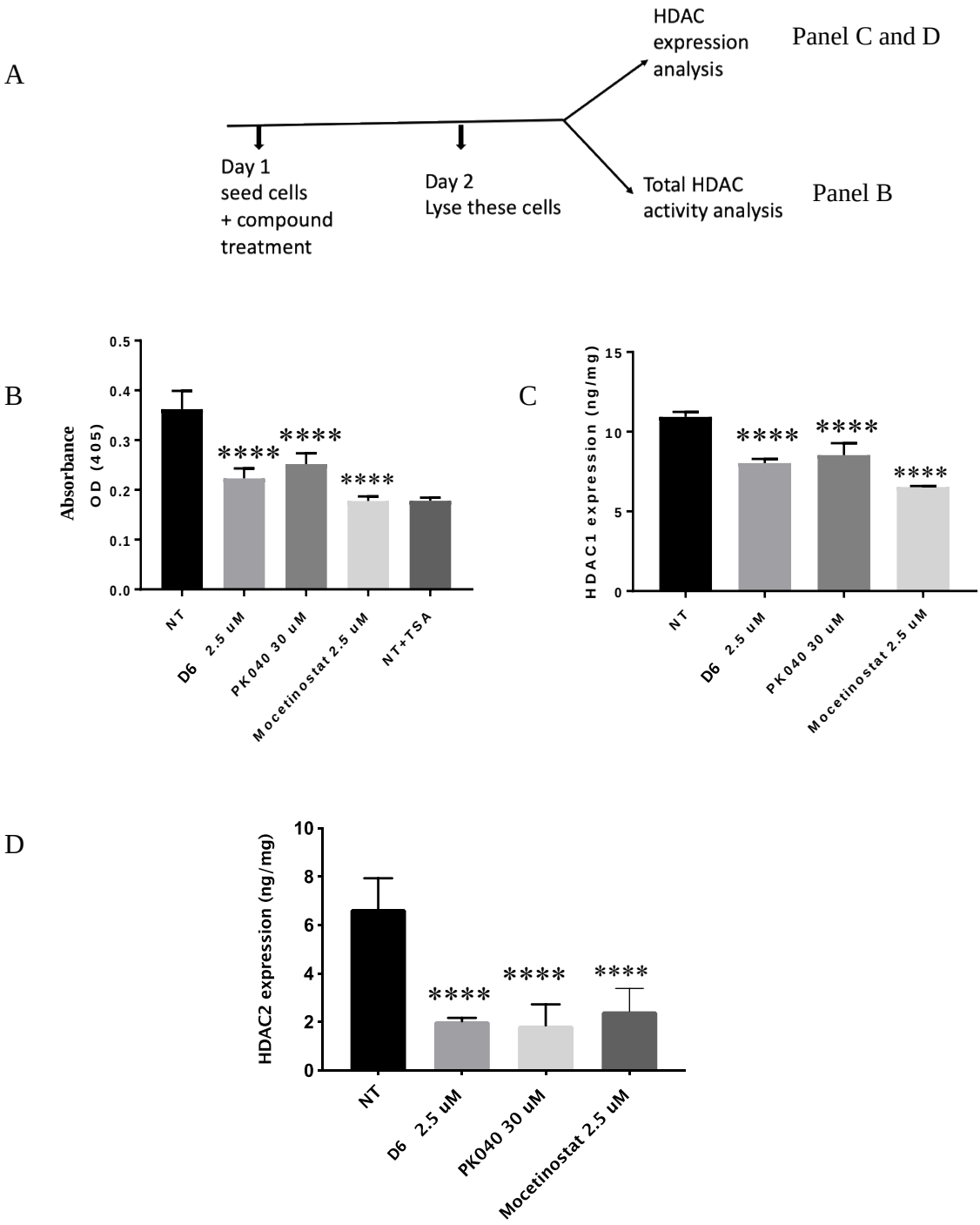


Figure 4.3: (A) Design for the *in situ* HDAC activity assay where the HL60 cells were treated with the respective concentrations of the compounds for 24 h (B) HDAC activity assay where the x-axis indicates the compound and its concentration with NT as the negative control and NT+TSA is the positive control. (C) HDAC1 and (D) HDAC2 expression for the same set of samples using HDAC1 and HDAC2 colorimetric amount quantification kit. In this assay the NT served as the positive control. Results are shown as means based on experiments performed in technical and biological triplicate, bars, ±SEM. Two-way ANOVA. *P<0.05, **P<0.01, ***P<0.001.

4.3 Recombinant Enzyme Assays

The recombinant enzyme assay kit is designed to measure the HDAC activity using the recombinant form of the protein. This assay helps with the compound profiling. The HDACs that were tested included HDAC1 and 2 from group I, HDAC6 from group II and HDAC11 from group IV. Since only Zn^{2+} dependent enzymes were of interest and group III enzymes were NAD^{+} dependent HDACs, these were not included in the assay. With this, both D6 and mocetinostat and *meta* analogues PK026 and PK040 were tested for different groups of HDACs and to understand the specificity of the inhibitory profiles of these compounds. The assay again utilizes a short peptide substrate that had acetylated lysine residues. Once the residue is deacetylated, the lysine residue interacts with the developing solution to produce a fluorescent signal. Increasing quantities of the deacetylated peptide fragments are first incubated with the developing solution to allow for the quantification of substrate turnover (Figure 22 in appendix). Next, the DMSO as vehicle control and TSA as positive control provided the signal window for the experiment.

4.3.1 HDAC1

HDAC1 is a highly expressed protein shown to catalyse the regulatory deacetylation of non-histone proteins, including p53 (Elmallah and Micheau, 2019). HDAC1 inhibition assay was included because overexpression of HDAC1 has been found in various cancer types including AML (Ishihama et al., 2007). This assay was set up as described in Materials and Methods.

The assay works well and showed a higher value of 25,000 AFU for the vehicle control and lower value of 2200 AFU for the positive control with TSA. The compounds were treated from a concentration range of 200 μM to 761 pM in a four- fold dilution. It was observed that the *ortho* analogues D6 (PK038) and mocetinostat (PK022) inhibited HDAC1 and had their IC_{50} values as 2.3 μM and 170 nM respectively calculated in Graph Pad Prism (Figure 4.4).

The literature value reported for HDAC1 inhibition of mocetinostat is 156 nM (Fournel et al., 2008), which is consistent with the value obtained herein. However, the *meta* analogues PK026 and PK040 did not cause any inhibition of HDAC1 enzyme, as anticipated.

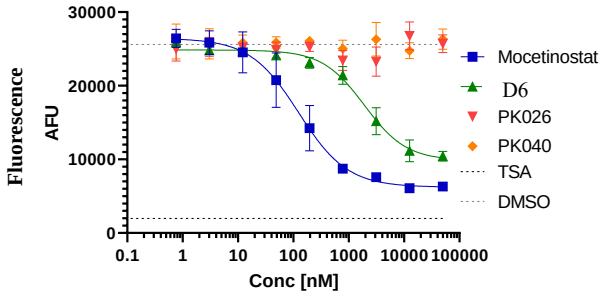


Figure 4.4: The compounds were measured as a dose response curve in the HDAC1 recombinant assay. The controls included the DMSO as vehicle control (no inhibitor) and the positive control included TSA (500 nM). Results are shown as means based on experiments performed in biological triplicate, bars, ±SEM

4.3.1.2 HDAC2

Next, HDAC2 enzyme was chosen for the assay, it is highly homologous of HDAC1 and is the first class I HDAC to be identified to the human homolog of the yeast histone deacetylase Rpd3. HDAC2 found, along with HDAC1, in the Sin3, NuRD and CoREST, also can act independently of these complexes to deacetylate non-histone proteins such as transcription factors (Dovey et al., 2010). HDACi such as SAHA, TSA and MS-275 are known to inhibit both HDAC1 and 2(Yang et al., 2019). It was important to check the profile of the compounds against HDAC2 enzyme and check if there was any difference in this profile from the commercially available HDACi.

Similar to HDAC1 recombinant assay kit, a dose response curve was performed for the compounds by treating them with 0.03 µg/µL of enzyme. The concentration of the substrate used was 10 µM. The reaction was allowed to progress for 2 h before adding the developing

solution. In the assay the control values for the vehicle control (DMSO) and the positive control with TSA were 6000 AFU and 1000 AFU respectively. While only mocetinostat inhibited HDAC2 with an IC_{50} value of 2.2 μM (in line with the literature reported value of 1.5 μM (Fournel et al., 2008), the other compounds had no effect on HDAC2 even upto 100 μM (Figure 4.5). This may suggest that D6 has a distinct profile to mocetinostat as it inhibits HDAC1 and not HDAC2.

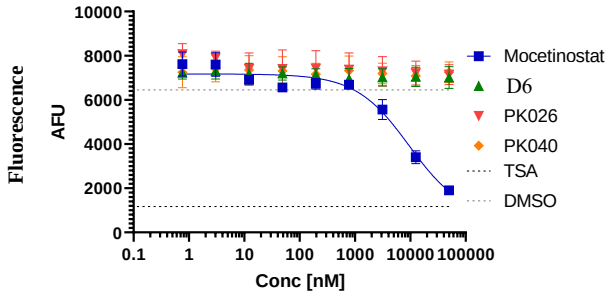


Figure 4.5: The compounds were assayed in a dose response curve for HDAC2 enzyme inhibition against mocetinostat, D6, PK026 and PK040 with their respective IC_{50} values. The controls included the DMSO as vehicle control (no inhibitor) and the positive control included TSA (500 nM). Results are shown as means based on experiments performed in biological triplicate, bars, ±SEM

4.3.1.3 HDAC 6

HDAC6 is a member of the class IIb mammalian histone deacetylases involved in regulating chromatin structure during transcription. HDAC6 also participates in regulating expression of a group of genes involved in the remodelling of chromatin during cell differentiation. The compounds were tested against HDAC6 as inhibition of HDAC6 by histone deacetylase inhibitors causes α-tubulin acetylation, accumulation of ubiquitinated proteins and subsequent apoptosis of malignant cells in AML patients (Krämer et al., 201). The assay was performed in a similar manner to that of the previous HDAC recombinant assays. The same concentrations of substrate and enzyme were used as described previously. The assay worked well with the vehicle control (DMSO) and positive control (TSA at 500 nM) giving absorbance values of

140000 and 3000 AFU respectively. None of the compounds inhibited HDAC6 protein, suggesting that these compounds were not class IIb HDAC inhibitors which is consistent with the literature (Fournel et al., 2008)(Figure 4.6).

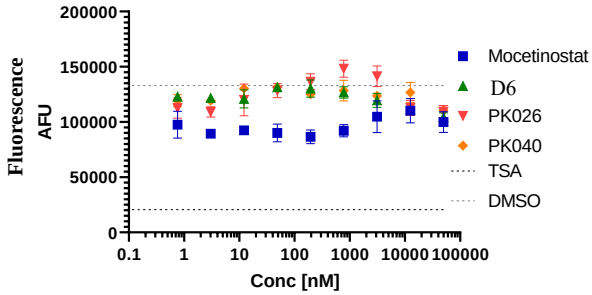


Figure 4.6: The compounds were assayed in a dose response curve for HDAC6 enzyme inhibition against mocetinostat, D6, PK026 and PK040 with their respective IC_{50} values. The controls included the DMSO as vehicle control (no inhibitor) and the positive control TSA (500 nM). Results are shown as means based on experiments performed in biological triplicate, bars, ±SEM

4.3.1.4 HDAC11

HDAC11 is the newest enzyme of the HDAC family. Based on its sequence and cofactor, HDAC11 belongs to class IV set of enzymes. It was important to test the compounds against HDAC11 as overexpression of HDAC11 has been found in AML cell lines such as NB4, U937 and HL60. This enzyme affects the cytokine production hence the neutrophil differentiation in these cells (Sahakian et al., 2013). The assay works in a similar manner to that of the previous assays. A varying range of compounds were treated with 20 μM of HDAC11 substrate and 0.03 μg/μL of enzyme for 2 h followed by treatment with the developing solution for another 1 h. In the assay the values for the vehicle control (DMSO) and the positive control (TSA at 500 nM) were 2000 AFU and 980 AFU respectively.

Both mocetinostat and novel analogue D6 inhibited HDAC11 with similar potency and had an IC_{50} of 800 nM and 1.5 μM respectively which is consistent with the literature (Fournel et al., 2008) (Figure 4.7). However, the *meta* analogues PK026 and PK040 did not inhibit HDAC11 up to 100 μM.

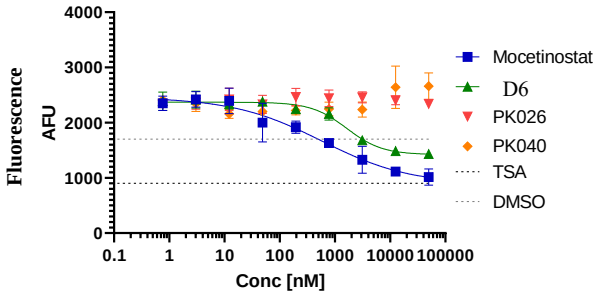


Figure 4.7: The compounds were assayed in a dose response curve for HDAC11 enzyme inhibition against mocetinostat, D6, PK026 and PK040 with their respective IC_{50} values. The controls included the DMSO as vehicle control (no inhibitor) and the positive control TSA (500 nM). Results are shown as means based on experiments performed in biological triplicate, bars, ±SEM

As D6 was confirmed to inhibit HDACs, its profile appeared different to that of mocetinostat. It was of interest to check if at higher concentrations (above EC_{50} value), it also causes upregulation of apoptotic factors leading to apoptosis (Rosato et al., 2003c).

4.4 Apoptosis Assay

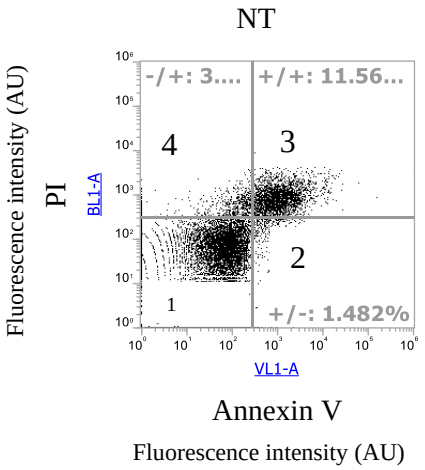
Apoptosis is central to the hematopoietic system. Deregulation of apoptosis disrupts the complex and delicate balance between cell proliferation, cell survival and cell death and has a major role in the development of diseases such as cancer, and particularly leukemia ((Testa and Riccioni, 2007)). HDACis in particular are well known for causing apoptosis in transformed cell lines by both extrinsic and intrinsic pathways. Acetylation of histones by pan HDACis such as TSA or SAHA has shown to cause cell death by apoptosis. These compounds

cause hyperacetylation of histones, a large increase in sub G1 population, and an induction of PARP proteolysis - all indicative of late apoptosis (De los Santos et al., 2007).

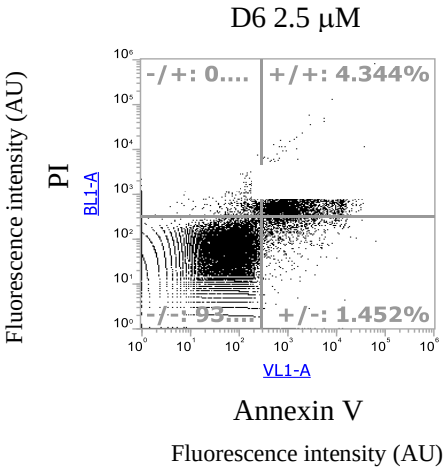
Recent reports on HDACi MS-275 show that at a higher concentration of 5 μM it causes apoptosis in 70% of AML cells from as early as 48 h (Rosato et al., 2003a).

To confirm how much apoptosis is caused by both *ortho* analogues, and in particular to compare the difference between the level of cell death caused by the commercial HDACi mocetinostat and novel analogue D6, HL60 cells were with the compounds for a period of four days. To detect cell death, Annexin V and propidium iodide (PI) staining was analysed by flow cytometry. The Annexin V binds to phosphatidylserine exposed on the cell surface during apoptosis and provides corresponding signal (Schutte et al., 1998) for detecting cellular apoptosis, while PI detects necrotic or late apoptotic cells, characterized by the loss of the integrity of the plasma and nuclear membranes (Fish et al., 2000). The data generated by flow cytometry were plotted in two-dimensional dot plots in which PI was represented versus Annexin V antibody (FITC). These plots were divided into four regions corresponding to: 1) viable cells which were negative to both probes (PI/FITC -/-); 2) apoptotic cells which were PI negative and Annexin positive (PI/FITC -/+); 3) late apoptotic cells which were PI and Annexin positive (PI/FITC +/+); 4) necrotic cells which were PI positive and Annexin negative (PI/FITC +/-) (Figure 4.8 A). D6 caused much less cell death as compared to mocetinostat at the higher concentration of 2.5 μM (EC_{80} for D6). However, for a concentration lower than its EC_{50} value (156 nM) mocetinostat caused much less cell death (Figure 4.8 D). The results suggest that D6 even at a higher concentration of 2.5 μM does not cause a lot of cell death unlike other commercial HDACi such as MS-275 or mocetinostat ((Rosato et al., 2003c).

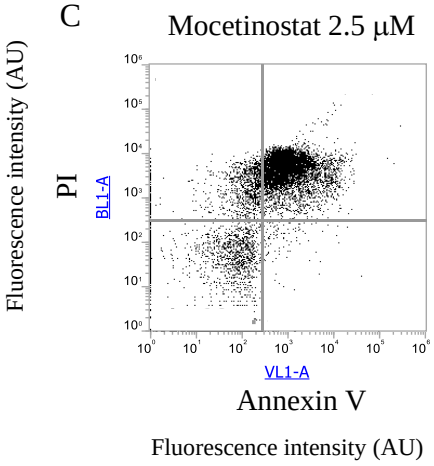
A


NT
-/+: 3....
+/+: 11.56...
4
3
2
1
+/-: 1.482%
PI
BL1-A
Fluorescence intensity (AU)
VL1-A
Annexin V
Fluorescence intensity (AU)

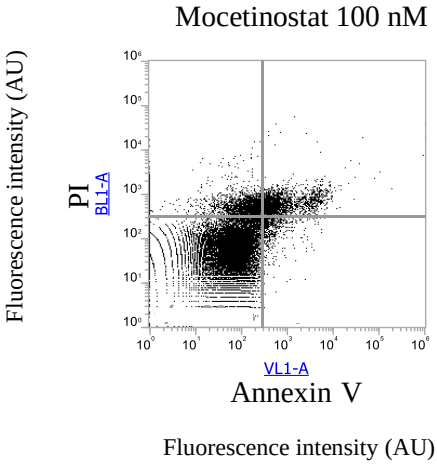
B


D6 2.5 µM
-/+: 0....
+/+: 4.344%
-/-: 93....
+/-: 1.452%
PI
BL1-A
Fluorescence intensity (AU)
VL1-A
Annexin V
Fluorescence intensity (AU)

C


Mocetinostat 2.5 µM
PI
BL1-A
Fluorescence intensity (AU)
VL1-A
Annexin V
Fluorescence intensity (AU)

D


Mocetinostat 100 nM
PI
BL1-A
Fluorescence intensity (AU)
VL1-A
Annexin V
Fluorescence intensity (AU)

E

Compound	Concentration	% cells PI	% cells with Annexin V
Mocetinostat	2.5 μM	85%	87%
Mocetinostat	100 nM	19%	21%
PK038	2.5 μM	37%	34%
Negative control		15%	18%

Figure 4.8: Cells were treated with (B) 2.5 μM of D6 and (C) 2.5 μM and (D) 100 nM of mocetinostat for 96 h. Cells were stained using Annexin V/PI assay reagent and analysed by flow cytometry. (E) Table here represents the percentage of cells expressing % PI and % Annexin V for the samples including the negative control.

4.5 Rescue Experiment

So far, differentiation effects with the four analogues were observed. Recombinant enzyme assay confirmed that the *ortho* analogues mocetinostat and D6 are HDAC inhibitors. However, it was still not clear whether the differentiation effects seen upon treatment with mocetinostat and D6 were a result of a secondary mechanism which was upstream of HDAC inhibition or a direct result of HDAC inhibition. For this purpose, a protocol was designed where THP1 cells were transiently transfected with HDAC1 plasmid as it was shown to be commonly inhibited by both mocetinostat and D6 and is known to have highest relative expression compared to other HDACs (Dovey et al., 2010). It was decided to proceed with THP1 cells as they are more tolerant towards transfection with higher transfection efficiencies (unpublished results from Dr T. Jackson) and generated data similar to that of HL60 cells (Chapter 3 Figure 3.5). Following the overexpression of the protein, it was decided to compare the EC_{50} values with the control groups i.e. non-transfected cells and empty vector (pcDNA3) transfected cells. If with the

overexpression of HDAC1- the potency of the compounds decreases conferring resistance to the compound treatment, then it could be inferred that HDAC1 inhibition is leading to the differentiation in AML cell lines. This section is divided into the following aims:

1. Transiently transfect THP1 cells with HDAC1- GFP plasmid and empty vector (GFP) plasmid
2. FACS sorting for cells expressing GFP
3. Confirm with western blot (HDAC1) overexpression
4. Treat the sorted cell population with increasing doses of D6 and mocetinostat for 48 h and check for expression of CD11b

Similar studies had been done before where a melanoma cell line conferred resistance to a pan HDACi – NaB mediated apoptosis by overexpressing HDAC1. It could be seen down-regulation of HDAC1 by an antisense vector sensitized the cells to NaB-induced apoptosis, whereas its overexpression conferred resistance to this agent (Figure 4.9)(Bandyopadhyay et al., 2004).

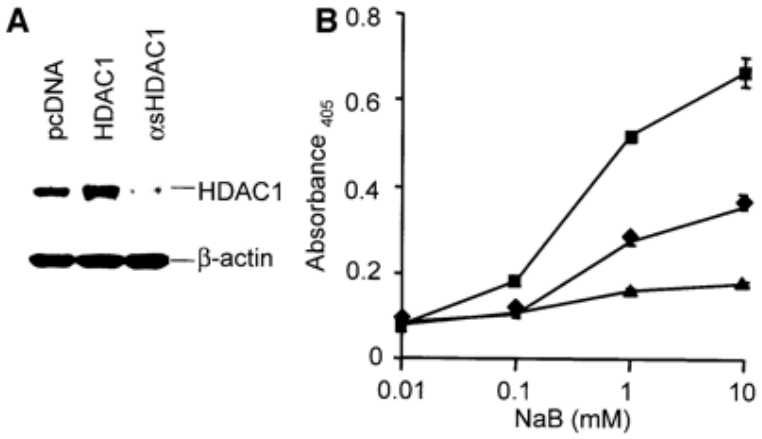


Figure 4.9: Overexpression of HDAC1 conferred resistance to NaB-induced apoptosis. (A) Expression levels of HDAC1 in HDAC1- and antisense HDAC1- (asHDAC1) expressing cells. Fifty micrograms of total protein from the isolated clones were analyzed in SDS-PAGE by immunoblot analysis with anti-HDAC1 antibody. (B) HDAC1- (▲) or asHDAC1- (▪) expressing clones along with empty vector (♦) were treated with increasing concentrations of NaB for 48 hours. The extracts were assayed for apoptosis by cell death ELISA detection kit (Adapted from (Bandyopadhyay et al., 2004)).

4.5.1 Transient Transfection with HDAC1- GFP plasmid

Transfection refers to the delivery of DNA or RNA into eukaryotic cells and is a powerful tool used to study and control gene expression (Kim and Eberwine, 2010).

When cells are transiently transfected with plasmids, the DNA is introduced into the nucleus of the cell but does not integrate into the chromosome. This means that many copies of the gene of interest are present, leading to high levels of expressed protein. Transcription of the transfected gene can be analysed within 24–96 h after introduction of the DNA depending on the construct used. Transient transfection is most efficient when supercoiled plasmid DNA is used (Cherng et al., 1999). Cloned genes can be transfected into cells for biochemical characterization, mutational analysis, investigation of the effects of gene expression on cell growth or regulatory elements (Maurisse et al., 2010). There are several methods used for

transfecting cells; some of the common ones include lipid transfection, RNAi and siRNA transfection, co-transfection or electroporation. For this experiment electroporation was of particular interest. As THP1 cells consist of monocytes and neutrophils, it has been shown that most of the other techniques used for transfection in THP1 affect the viability of these cells or interfere with their behaviour. However, electroporation is one technique which helps to overcome this problem by providing reliable and efficient transfection without compromising the cell viability and the cell behaviour (Maeß et al., 2014). Electroporation is based on a simple process - host cells and selected DNA molecules are suspended in a conductive solution - where an electrical circuit is closed around the mixture. An electrical pulse at an optimized voltage, only lasting a few microseconds to a millisecond, is discharged through the cell suspension. This disturbs the phospholipid bilayer of the membrane and results in the formation of temporary pores. The electric potential across the cell membrane simultaneously rises to allow charged molecules like DNA to be driven across the membrane through the pores in a manner similar to electrophoresis (Shigekawa and Dower, 1988). One of the advantages of this technique is that once it is optimized it is able to transfect a large number of cells in a short period of time (Stroh et al., 2010).

For this experiment HDAC1 (GFP tagged) plasmid from Origene was used with pcDNA3 as the vector (Figure 4.10). Empty vector pmax-GFP tagged plasmid was purchased from Lonzo and was used as the control as it consisted of the same vector bone as HDAC1 (Figure 4.10 B). Electroporation was used for the transfection of the cell line as described in the Materials and methods. Following a 48 h transfection, the cells were analysed in the microscope to look for GFP expressing cells in both the control and HDAC1 groups (Figure 4.10 C).

The same batch of samples were also analysed under flow cytometry to confirm the percentage of GFP expression (Figure 4.11). The control vector pmax GFP had roughly 61% viable cells out of which 16% were GFP positive. The negative control for the experiment included THP1

cells only with no GFP insertion and the results confirmed that the mock cells or only THP1 cells showed 0.5% of GFP expression (Figure 4.11 A). However, the HDAC1-GFP plasmid caused excessive cell death leaving only 16% viable cells out of which only 1.6% expressed GFP (Figure 4.11 B). Due to such large cell death the samples could not be taken further for GFP sorting.

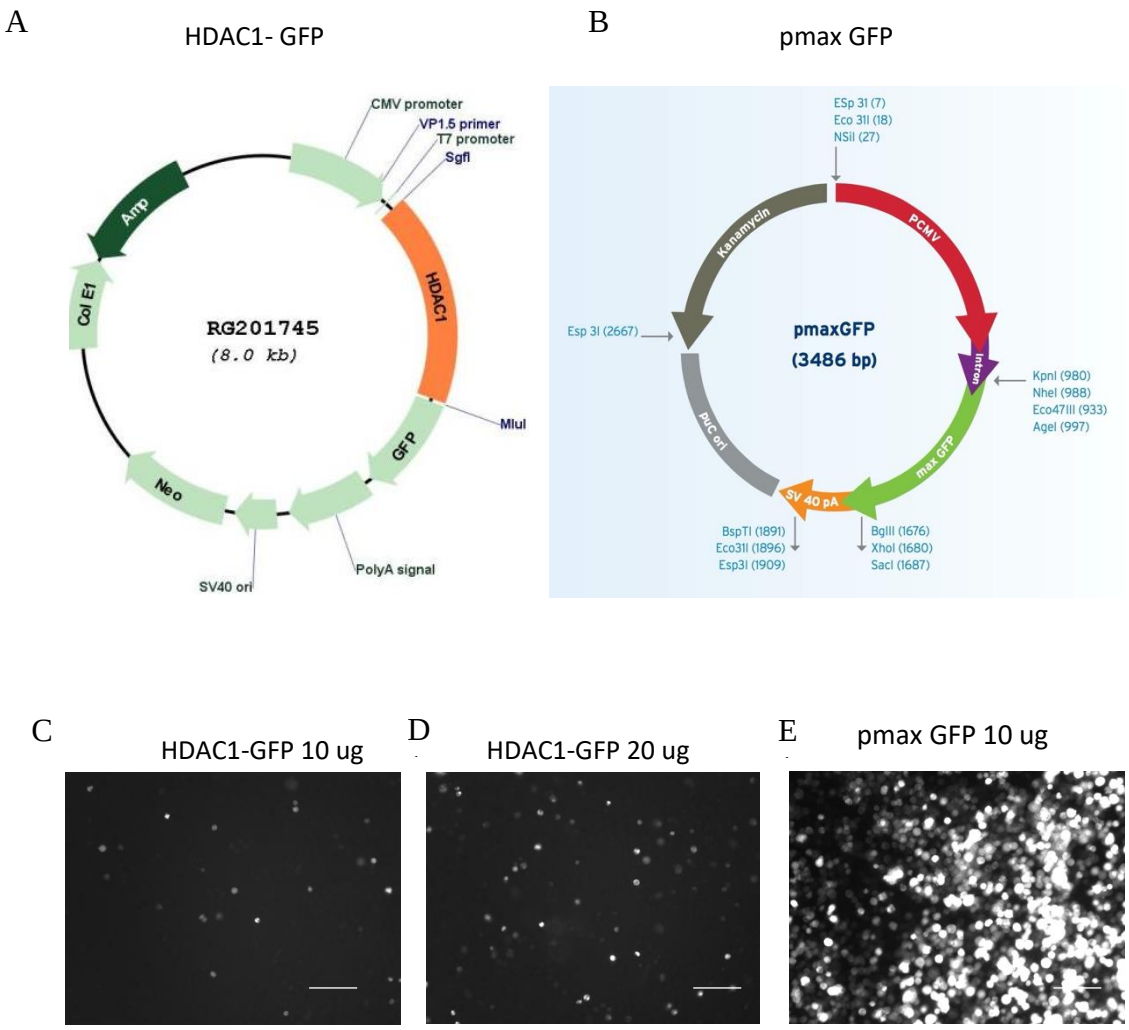


Figure 4.10: (A) HDAC1- GFP map as provided by Origene and (B) pmax-GFP map as provided by Lonza. (C) Transfected cells were incubated for a period of 48 h and then checked under Olympus fluorescence microscope and acquisition software infinity at magnification X20. Scale bar = 10 µm.

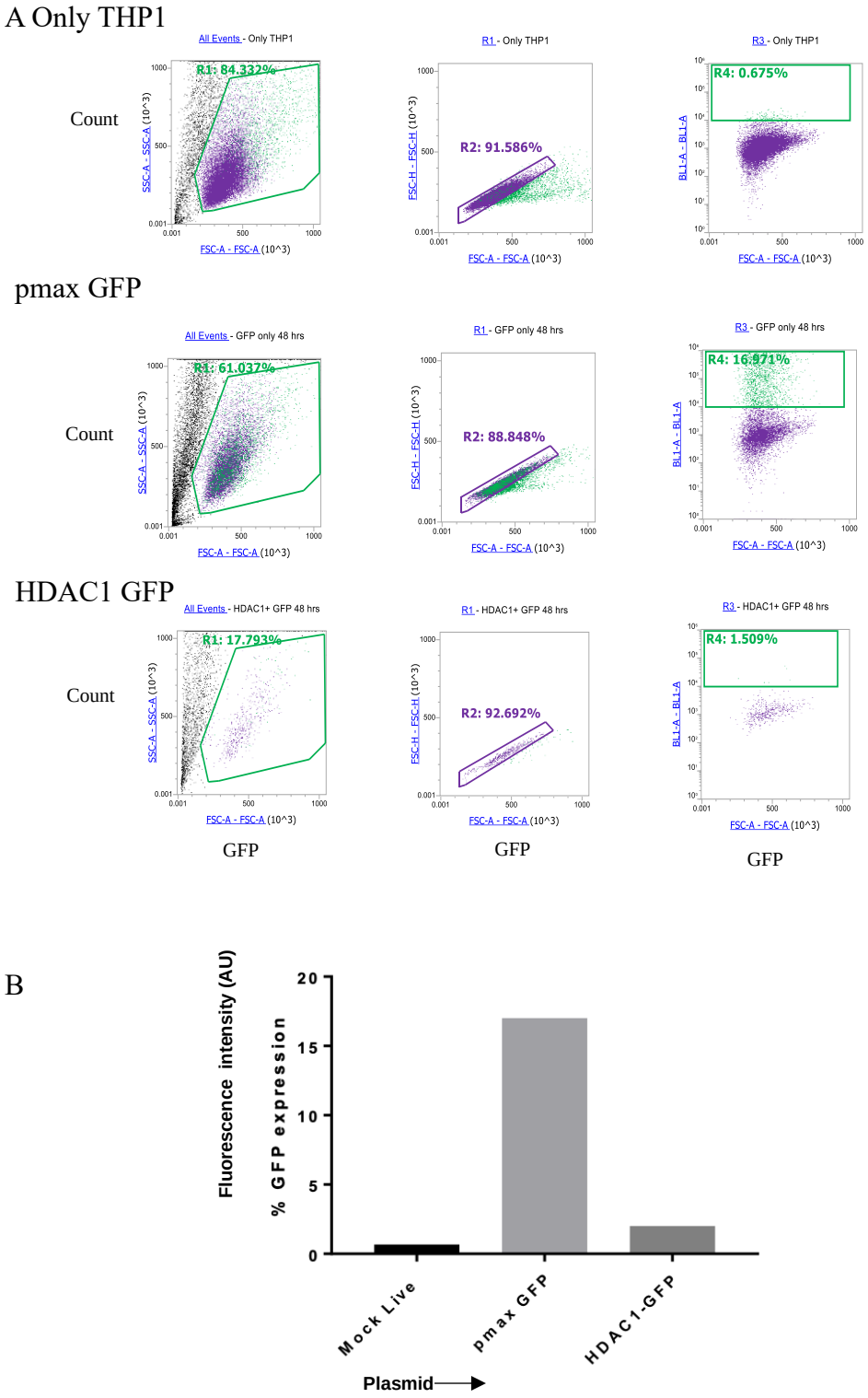


Figure 4.11: (A) THP1 cells transfected with empty vector pmaxGFP and HDAC1-GFP plasmid for a period of 48 h. Representative FACS plots denotes forward scatter (FSC) vs side scatter (SSC) with the gate selecting population of the total cells excluding the debris at the bottom and the dead cells on the left; single cell population is shown followed by the GFP marker (marker of interest) in green. (B) %GFP expression as shown on a bar graph depicting the % GFP expression on the y-axis and the type of transfection on the x-axis.

Transfected cells could show expression anywhere between 24 to 96 h as that is estimated to be the amount of time needed for the gene to be transcribed from transient transfection. However, 48 h from the FACS plots above showed less than 5% transfection for HDAC1- GFP plasmid, so it was decided to prolong the transfection time to 72 h before analysing the transfection efficiency. An exposure of 72 h with the plasmid instead caused a lot of cell death (Figure 4.12). One of the reasons for the cell death could be the relatively bigger size of HDAC1 plasmid (8.0 kbp) compared to pmax GFP plasmid.

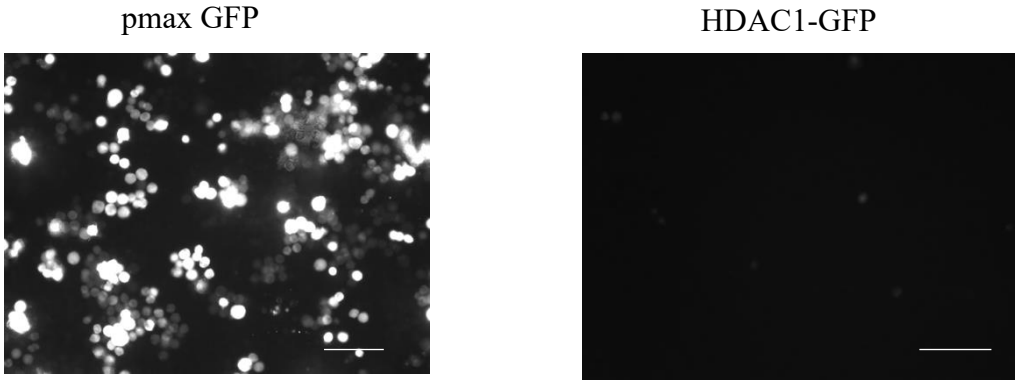


Figure 4.12: Transfected cells were incubated for a period of 72 h and then checked under Olympus fluorescence microscope and acquisition software infinity at magnification X20. Scale bar = 10 μm.

4.5.2 Transfection with only HDAC1 plasmid

The GFP tagged HDAC1 plasmid caused a lot of cell death and affected the cell sorting of GFP expressing cells. The plasmid construct was changed and replaced with a new HDAC1 plasmid without the GFP tag. HDAC1-flag plasmid of 6869 bp (Figure 4.13 A) was purchased from Addgene. Due to the absence of a fluorescent marker tagged to this plasmid, a western blot had to be utilised, instead of FACS or fluorescent microscopy, to confirm the overexpression of HDAC1. Again, pcDNA3 plasmid was used as the control as it had the same vector base as

that of HDAC1-flag. A total of 10 million cells were used for each plasmid and the two plasmids (HDAC1 and pcDNA3) were transfected at 10 μg/million cells for 48 h followed by a viability and cell count check. Both the plasmids caused cell death and a decrease in viability. The cells were counted by Nucleo cell counter using acridine orange (counts total cell number) dye and DAPI (counts dead cells). The cells treated with HDAC1 plasmid and pcDNA3 had viability values of 56% and 67% respectively, which was higher than those obtained with the previous GFP tagged plasmids. The cell counts for both of the transfected cells had decreased from 1.06 million per mL to 130,000 for pcDNA3 and 60,200 for HDAC1. However, these values were sufficient enough to further proceed with the experiment. To confirm a successful transfection, cell lysate of a million cells was extracted and probed with HDAC1 antibody to confirm its overexpression by western blot. With the rest of the cells, a dose response curve was set by treating the cells with increasing doses of mocetinostat and D6. The cells were incubated for a time period of 48, 72 and 96 h. The expression of CD11b was then analysed by FACS.

As shown in Figure 4.13 B, with the western blot an overexpression of the HDAC1 protein was observed as compared to the empty vector pcDNA3 plasmid. This confirmed that the transfection was successful in THP1 cells and that these cells can be treated with the compounds.

A



B



HDAC1 pcDNA3 pcDNA3 HDAC1

β Tubulin **HDAC1**

Figure 4.13: (A) The HDAC-Flag map from Addgene. (B) The cells were transfected and incubated for a period of 48 h. Western blot indicating beta tubulin for loading control, HDAC1 expression for HDAC1 transfected cells and pcDNA3 transfected cells.

However, on comparing the EC_{50} values from the dose response curves for D6 treated, non-transfected cells to that of transfected cells (pcDNA3 and HDAC1), not much difference in the values was obtained (Figure 4.14 A, B and C). Similar results were seen for mocetinostat treated cells (Figure 4.14 D, E and F). The experiments were done in biological triplicates and the results indicated no change in the EC_{50} values with both D6 and mocetinostat. Since the EC_{50} values between the control groups and the HDAC1 treated cells were similar, the experiments were inconclusive. It was hard to determine if there was any change in the potency between the overexpressed HDAC1 cells and the control groups.

As the results did not indicate clearly any change in the EC_{50} value, it was decided to compare the EC_{50} value of transfected cells treated with *ortho* analogues mocetinostat and D6 to that of the commercial pan HDACi sodium butyrate. In the literature, it has been indicated that overexpression of HDAC1 protein conferred resistance to NaB and induced apoptosis in melanoma cell line (Bandyopadhyay et al., 2004). For this purpose, HDAC1 was overexpressed in THP1 cells by electroporation in the similar manner as stated above and then treated with NaB instead of mocetinostat and D6. However, even though the western blots confirmed the upregulation of HDAC1 in that batch of cells (Figure 4.15 A), the EC_{50} values did not change (Figure 4.15 B). For some drugs, resistance cannot result from 'target gene' overexpression because no such single gene exists. A drug's efficacy can depend on binding to multiple targets or a drug can act on non-protein targets. The overexpression mediated resistance is therefore most relevant and well defined for drugs with a single protein target (Palmer and Kishony, 2015).

Hence, this particular experiment could not confirm the hypothesis laid, as no significant change was observed between the EC_{50} values for any of the three compounds. The reason for this remains unclear, however large cell death could be one of the reasons attributed for the same. Another reason could be that differentiation caused by these compounds is not *via*

HDAC1 inhibition but through another HDAC which was not overexpressed in the cell line of interest, thus leaving the possibility of other HDACs to be explored.

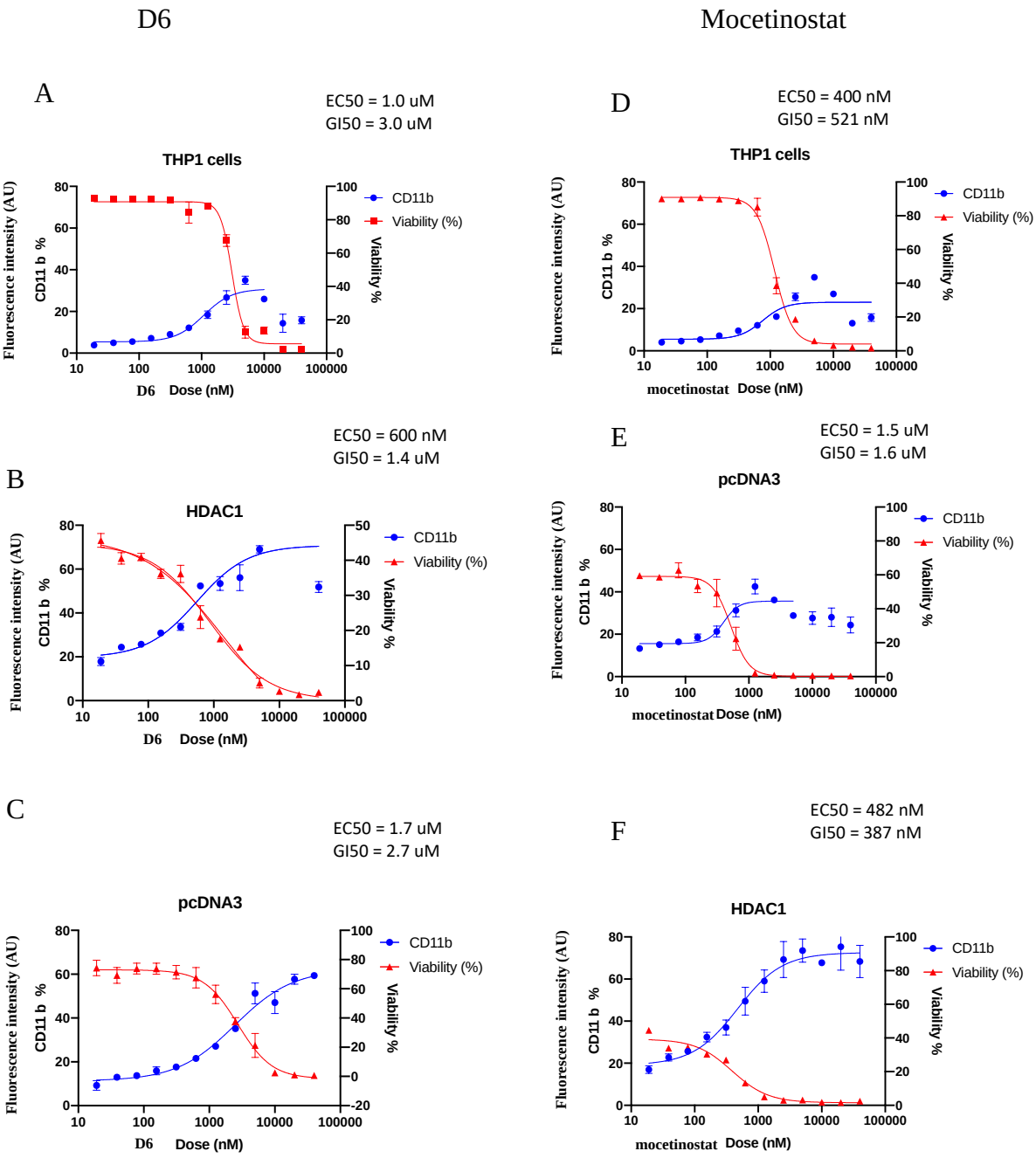
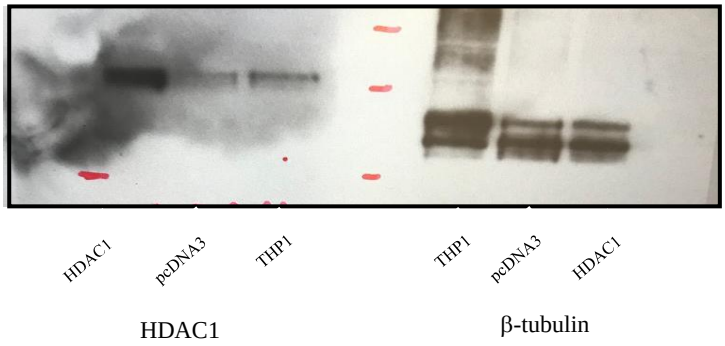


Figure 4.14: Flow cytometric analysis for (A)THP1 cells (B) THP1 cells transfected with HDAC1 plasmid and (C) THP1 cells transfected with pcDNA3 plasmid treated with different concentrations of D6. Similarly (D) THP1 cells (E) THP1 cells transfected with HDAC1 plasmid and (F) THP1 cells

transfected with pcDNA3 plasmid treated with different concentrations of mocetinostat. Results are shown as means based on experiments performed in technical and biological triplicate, bars, ±SEM

A



B

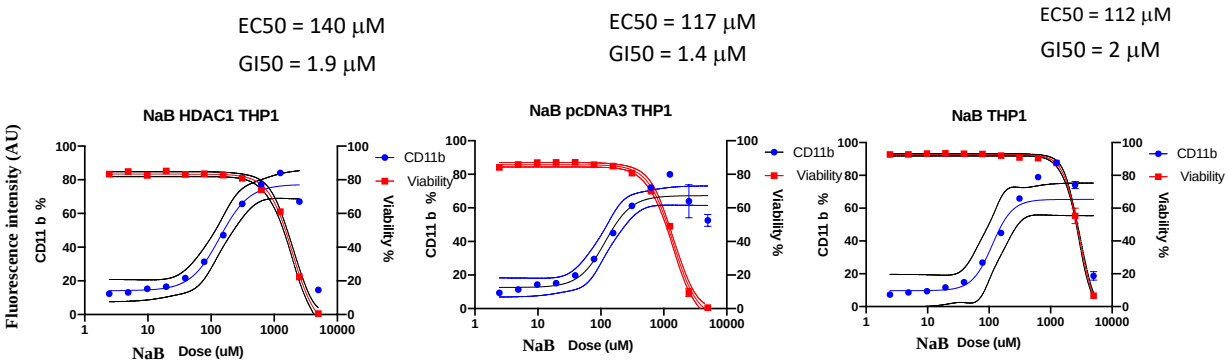


Figure 4.15: (A) Western blot depicting overexpression of HDAC1 for HDAC1 transfected cells as compared to empty vector pcDNA3 and only THP1 cells. Loading control beta tubulin for THP1 only, THP1 transfected with pcDNA3 and THP1 transfected with HDAC1.

(B) Flow cytometric analysis for THP1 cells transfected with HDAC1 plasmid, pcDNA3 plasmid against different concentrations of NaB. The results are represented as means based on experiment performed in technical triplicates and biological duplicate, bars, ±SEM

4.6 Discussion

In this chapter, a successful characterisation of novel analogue D6 and its *meta* analogue PK040, and mocetinostat and its *meta* analogue PK026 confirms that D6 is slightly more specific than the commercial HDACi mocetinostat as it causes inhibition of only HDAC1 and 11 unlike mocetinostat which inhibits HDAC1, 2 and 11 (Table 4.1). This is worth noting as HDAC1 and HDAC2 have been reported to have a similar homology hence an inhibitor affecting only one of the two is unique (Tsai and Seto, 2002). The table below indicates the IC_{50} values of each of the compounds against the HDACs inhibited. Consistent with the data from the western blot of acetylated histones, *meta* analogues PK026 and PK040 do not inhibit any of the HDACs and are hence not working *via* HDAC inhibition to cause differentiation.

	HDAC inhibitors		Non-HDAC inhibitors	
HDAC	**Mocetinostat**	**PK038**	**PK026**	**PK040**
HDAC1	IC50 170 nM	IC50 2.3 μM	IC50 >30 μM	IC50 >30 μM
HDAC2	IC50 2.2 μM	IC50 >30 μM	IC50 >30 μM	IC50 >30 μM
HDAC6	IC50 >30 μM	IC50 >30 μM	IC50 >30 μM	IC50 >30 μM
HDAC11	IC50 800 nM	1.5 μM	IC50 >30 μM	IC50 >30 μM

Table 4.1: HDAC inhibitory profiles for mocetinostat, D6, PK040 and PK026 obtained via recombinant enzyme assay.

In the next part of the chapter, an attempt is made to understand the toxicity of the compounds with the help of an Annexin V/PI assay by flow cytometry. It has been shown in the literature that commercial HDACi MS-275 causes dose- and time-dependent apoptosis in U937 and HL60 cells, however, leads to an increase in ROS species at as early as 2 h (Rosato et al., 2003b). Primary induction of ROS has been linked to the onset of apoptosis (Yang et al., 2018).

However, with D6 at the concentration of the EC_{80} value, very little (<30%) cell death was seen. This indicates that at this concentration D6 causes differentiation.

Next, in an attempt to confirm whether or not HDAC inhibition is the primary mechanism leading to differentiation, HDAC1 was overexpressed in THP1 cells, as it was inhibited by both mocetinostat and D6 in the recombinant enzyme assay- this allows to check whether or not overexpressing HDAC1 in the cells of interest and treating them with increasing dose of the compound allows the cells to confer resistance to the compound. If a decrease is observed in EC_{50} value for overexpressed cells compared to the controls, it would imply that there is a primary mechanism upstream of HDAC inhibition leading to the effects seen. In the data there was no change in the EC_{50} values even when overexpression of HDAC1 was confirmed with western blot. This may imply that HDAC1 is not involved in the mechanism of action of mocetinostat and D6 in inducing differentiation but does not rule out other HDACs. Further experiments are needed to confirm this hypothesis.

Chapter 5: Cell Cycle analysis and Target Validation

Aims

The previous chapter described the profile of both *ortho* and *meta* analogues. It also confirmed that D6 had a distinct profile to that of mocetinostat. On the other hand, *meta* analogues PK040 and PK026 did not show any HDAC inhibition leaving the molecular target and mechanism of action for the two still unknown.

This chapter explores the in-depth pathway analysis for both the *ortho* and *meta* analogues with the help of cell cycle analysis and RNA sequencing data. RNA sequencing provides a greater insight into the transcriptome of the cell and could thus provide insights into novel pathways and suggest novel molecular targets (Haidula, 2016).

5.1 G1 arrest in AML cell lines

The four major phases of cell cycle include G1, S phase, G2 and M phase. In a normal cell cycle, cells can exit from the G1 phase and enter into a state of quiescence (G0) from where they can undergo differentiation or re-enter cell cycle to proliferate (Schnerch et al., 2012a).

In AML, genetic mutations play a role in the regulation of cell division. To explore this in detail, this chapter focuses on G1 arrest and cell cycle exit, a crucial part of terminal differentiation and confirms if the effects are similar with both *ortho* and *meta* analogues.

A variety of AML cells include THP1, Kasumi, OCI-AML3, KG-1 and HL60. These were treated with the EC_{80} of the four compounds for a period of 48 h and then analysed for DNA content using flow cytometry (Figure 5.1).

From the results, it could be seen that at 48 h mocetinostat induced G1 arrest in THP1, OCI-AML3 and HL60 cells. However, in Kasumi, mocetinostat caused a considerable amount of cell death. The novel analogue D6 also caused G1 arrest in THP1, OCI-AML3, Kasumi and HL60 cells (Figure 5.1). This is consistent with the previously reported results of HDACi MS-275 inducing G1 arrest at 48 h in AML cell line U937 (Rosato et al., 2003c).

The *meta* analogues did not cause any change in the cell cycle progression in THP1, OCI-AML3 and KG-1 cells (Figure 5.2).

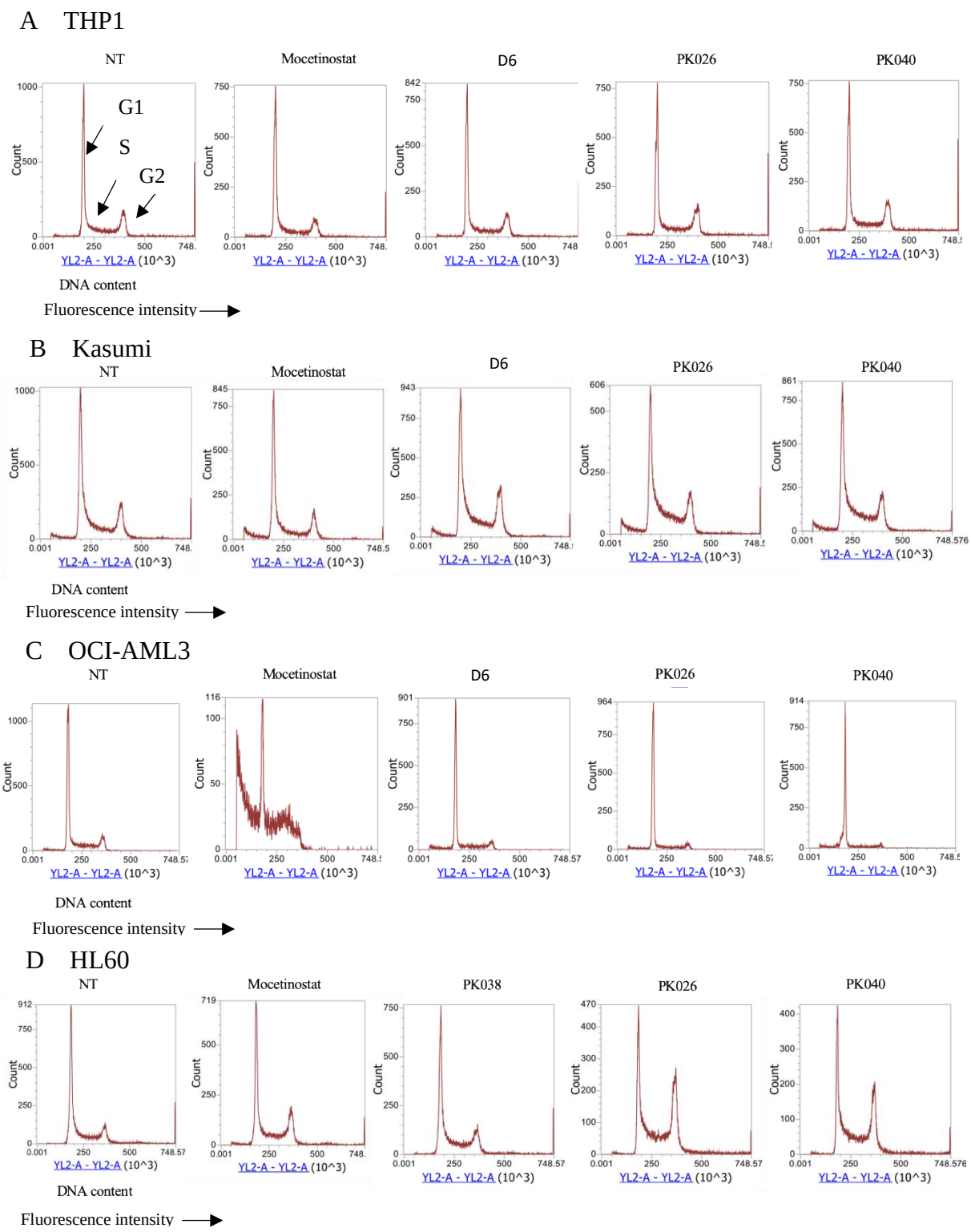


Figure 5.1: Representative FACS plots for (A) THP1(B) Kasumi (C) OCI-AML3 and (D) HL60 cells. The cells were treated with 625 nM of mocetinostat, 2.5 μM of D6 and 30 μM of PK026 and PK040 for 48 h, n=3.

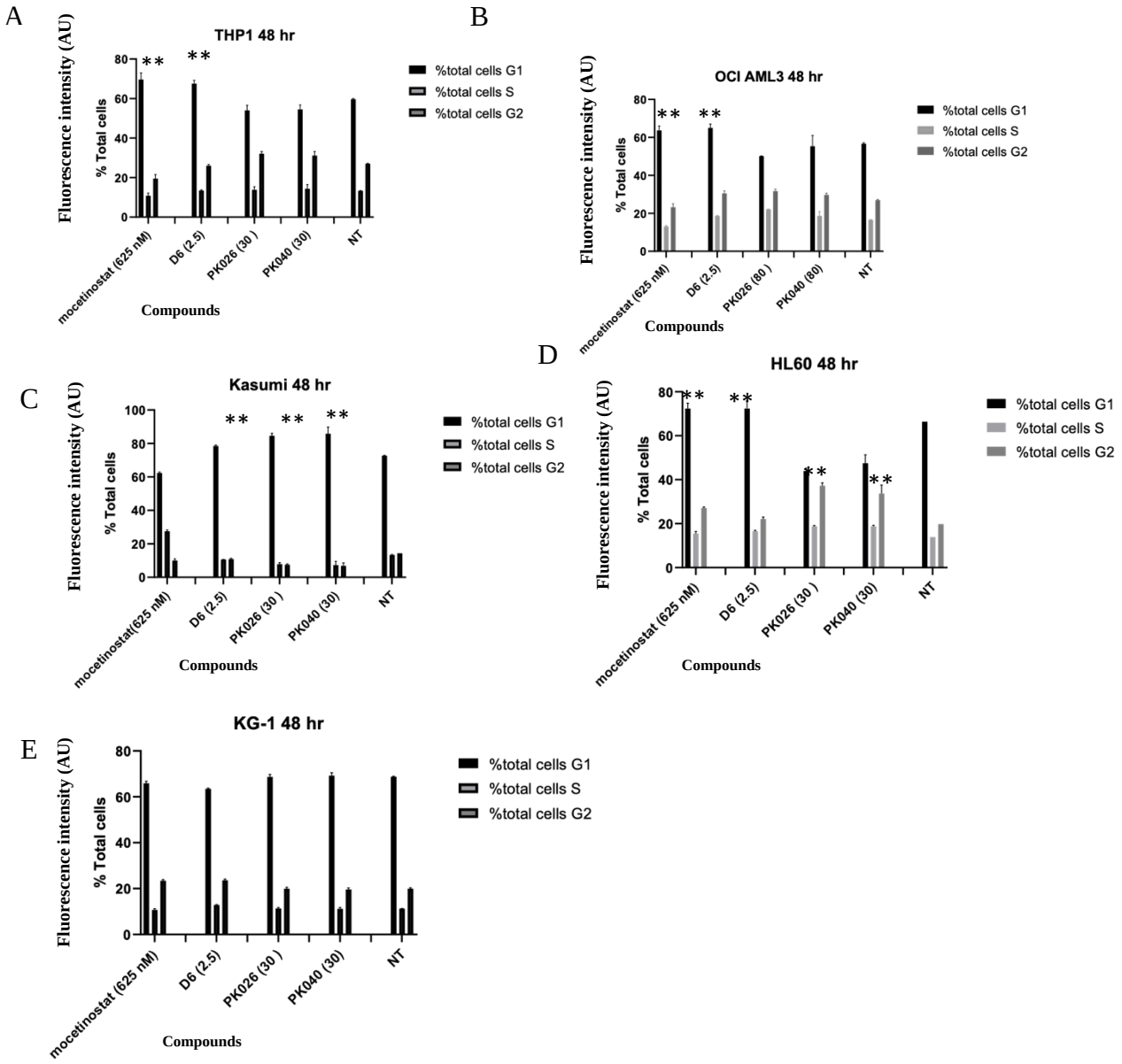


Figure 5.2: Effect of mocetinostat, D6, PK026 and PK040 on cell cycle distribution. (A) THP1 cells (B) OCI-AML3 (C) Kasumi (D) HL60 (E) KG-1 were exposed to the following concentration of compounds for 48 h, after which they were stained with PI, and subjected to cell cycle analysis using flow cytometry. The y- axis denotes the percentage of cells undergoing the respective G1, S and G2 phases of the cell cycle and the x- axis denotes the compounds treated with the cells. Values represent the means ± SEM for three separate experiments performed in triplicate. P values were calculated using Two-way ANOVA. *P<0.05, ** P<0.01, ***P< 0.001.

5.3 G2 arrest and differentiation

In the cell cycle, G2 phase allows the cell to rapidly grow and synthesise protein following which the cell undergoes mitosis. There are several checkpoints which ensure that only the cells with non damaged DNA are able to enter mitosis and divide their genetic material into their daughter cells (Schnerch et al., 2012a). In the literature, compounds such as aloperine and eranin induce G2 arrest in colon cancer cells and bone cancer cells respectively, and the subsequent induction of apoptosis and autophagy pathway as a result of this arrest (Wang et al., 2016)(Zhang et al., 2014). Some results suggest a relation between G2 arrest and cell differentiation in normal cells (Ayeni et al., 2016), however, the relation between G2 phase arrest and the induction of differentiation hasn't been explored in AML cell lines.

The results in section 5.2 were interesting especially for HL60 cells as the cells underwent G1 arrest on treatment with mocetinostat and D6 and G2 arrest on treatment with PK026 and PK040 (Figure 5.1 D).

In order to confirm these results, and to determine the time point leading to clear G1 or G2 arrest with *meta* analogues PK026 and PK040, HL60 cells were treated with the respective concentration of the compounds for a period of 24, 48, and 72 h (Figure 5.4). It was reconfirmed that the *ortho* analogues mocetinostat and D6 induced G1 arrest at all time points until 72 h however the *meta* analogues PK026 and PK040 induced clear G2 arrest only at 48 h (Figure 5.4 A, B). At 72 h the viability of the cells with the *meta* analogues was very low with less than 300 events (single cell entry) recorded and most of them in sub G1 phase (Figure 5.3) which is why this time point was not taken further.

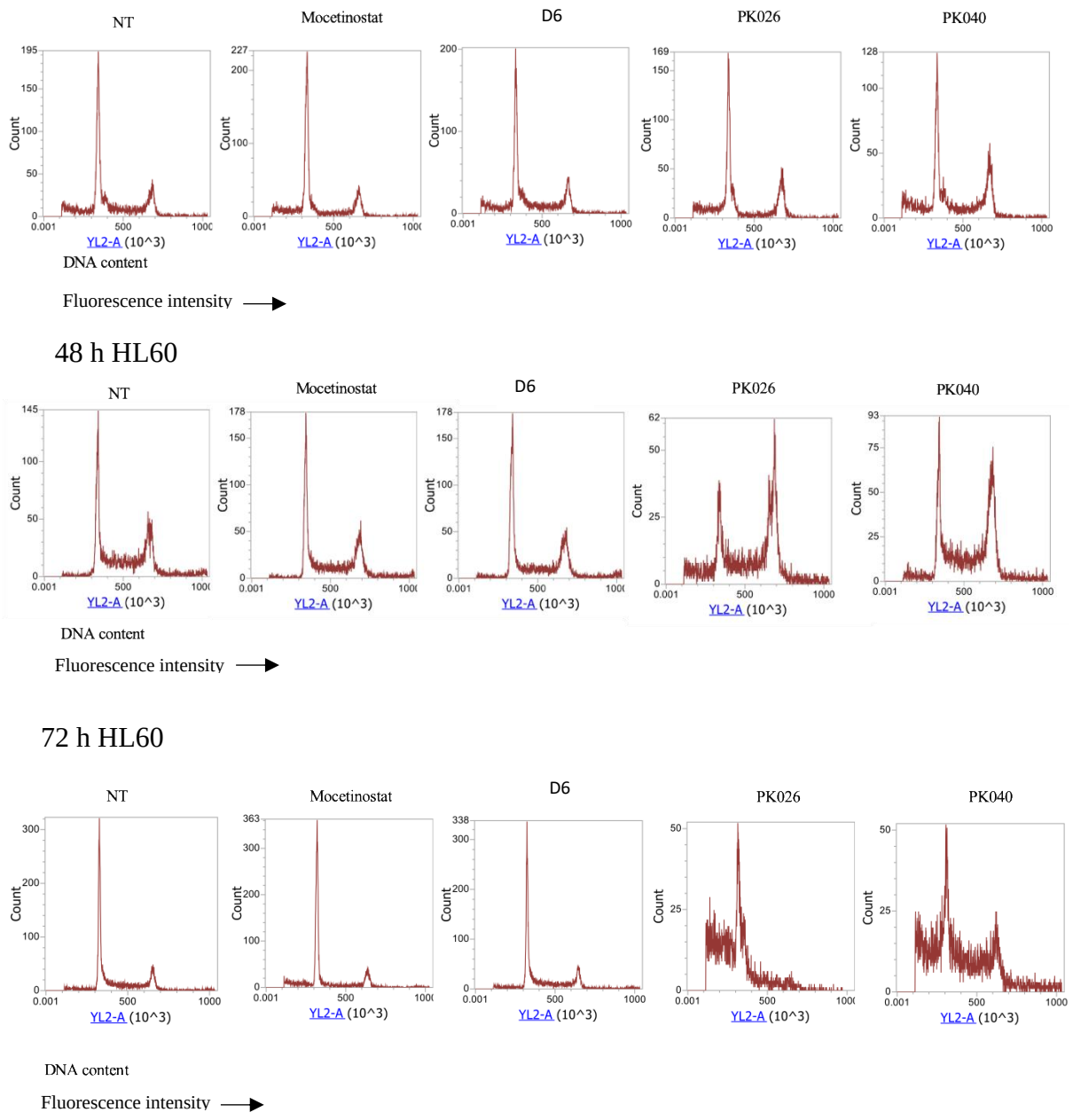


Figure 5.3: Representative FACS plots of cell cycle analysis for HL60 cells after treatment with the compounds at respective concentrations for 24 h, 48 h and 72 h, n=3.

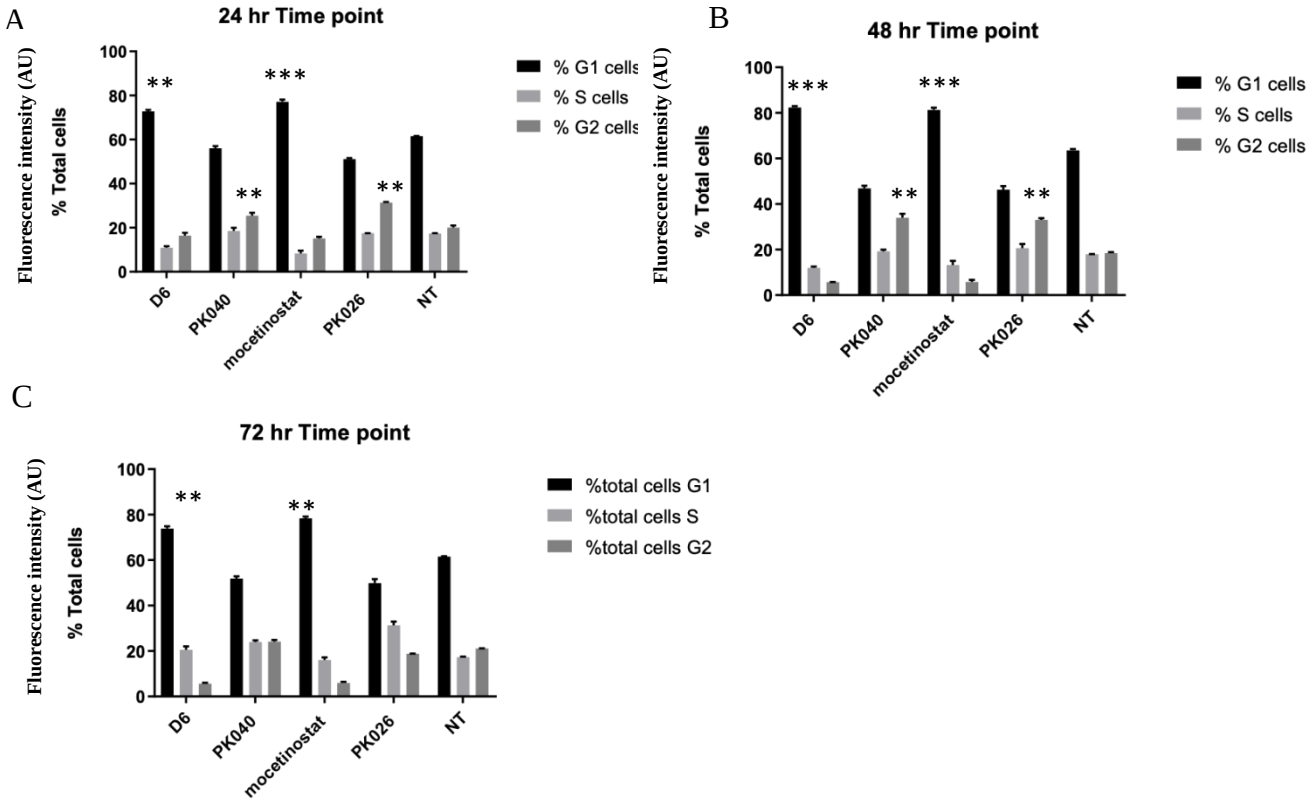


Figure 5.4: Effect of the compound PK026, PK040, mocetinostat (PK022), D6 on cell cycle and distribution. HL60 were exposed to the respective concentration of compounds for (A) 24 h and (B) 48 h and (C) 72 h after which they were treated with PI and subjected to cell cycle analysis using flow cytometry. The y- axis denotes the percentage of cells undergoing the respective G1, S and G2 phases of the cell cycle and the x- axis denotes the compounds treated with the cells. Values represent the means ± SEM for three separate experiments performed in triplicate. P values were calculated using Two-way ANOVA. *P<0.05, ** P<0.01, ***P< 0.001.

The relation between G2 phase arrest in cell cycle and the concomitant differentiation effects have not been explored in AML cells. It is known from the time point studies in Chapter 3 (Section 3.8,figure 3.9) that these *meta* analogues PK026 and PK040 start increasing CD11b expression from as early as 24 h, hence it was important to understand the underlying mechanisms initiating G2 arrest with the *meta* analogues and also causing concomitant increase in CD11b expression or differentiation. In order to further investigate the mechanism leading to G1 arrest and G2 arrest with the compounds it was decided to look for the cell cyclins and their inhibitors known to be involved in cell cycle progression or the process of differentiation.

5.4 Cell cyclins

CDKs, cyclins and CDKIs are not only crucial for cell cycle regulation but also play an indispensable role in the process of transcription, metabolism, epigenetic regulation, stem cell self- renewal and neuronal function (Lim and Kaldis, 2013). CDKs are seen as the engines of the cell cycle progression whereas the CDKIs tightly regulate the kinase activity of these CDK complexes and regulate their progression under unfavourable conditions. In this chapter, a mix of cell cyclins and their inhibitors which have been studied for G1 or G2 arrest in cancer cell lines are examined with the aim to gain an insight about the pathways leading to the known effects with the novel compounds. The most common CDKs and CDKIs involved in the terminal cell differentiation of AML cells include CDK1, CDK2 and p21 respectively (Rosato et al., 2003c) (Nobuyuki Horie et al., 2004). Apart from these, molecular chaperone protein hsp90 has been reported to play a role in modulation of differentiation and apoptosis and is thus included in the analysis (Kovacs et al., 2005).

In leukemic cells the expression profiles of death receptor DR5 is usually associated with the induction of apoptosis (Chen et al., 2015). It was important to confirm if the compounds at the concentrations inducing differentiation also activate this receptor inducing apoptosis.

HL60 cells were seeded in a 6-well plate in a final volume of 3 mL and then treated with 2.5 μM of D6, 625 nM of mocetinostat (PK022) and 30 μM of PK026 and PK040 for a period of 24 h. The cell lysates were then extracted using RIPA buffer and the total protein concentration was calculated using BCA assay (described in Materials and Methods), 30 μg of protein was used for loading the gels. The membranes were then probed with CDK1 and 2, p21, hsp90 and DR5 antibodies. Non treated samples served as the control throughout the experiment.

The membrane confirmed equal loading for the five samples as confirmed by beta tubulin expression. Downregulation of CDK1 and 2 for the cells treated with the HDACi mocetinostat and the novel compound D6 confirmed inhibition of the two CDKs consistent with G1 arrest. However, there was a clear upregulation of CDK1 and CDK2 for the cells treated with the *meta* analogues PK026 and PK040 (Figure 5.5 A).

To check the effect of the compounds on cell cyclin inhibitor p21, HL60 cells were treated with commercial HDACi MS-275 (serving as the positive control), mocetinostat, D6 and PK040. The membrane showed upregulation of p21 with MS275 treated cells and not with the novel analogue D6 or its *meta* analogue PK040 (Figure 5.5 B).

The results indicated that both *ortho* and *meta* analogues did not upregulate the expression of hsp90 and DR5 compared to the non-treated control sample.

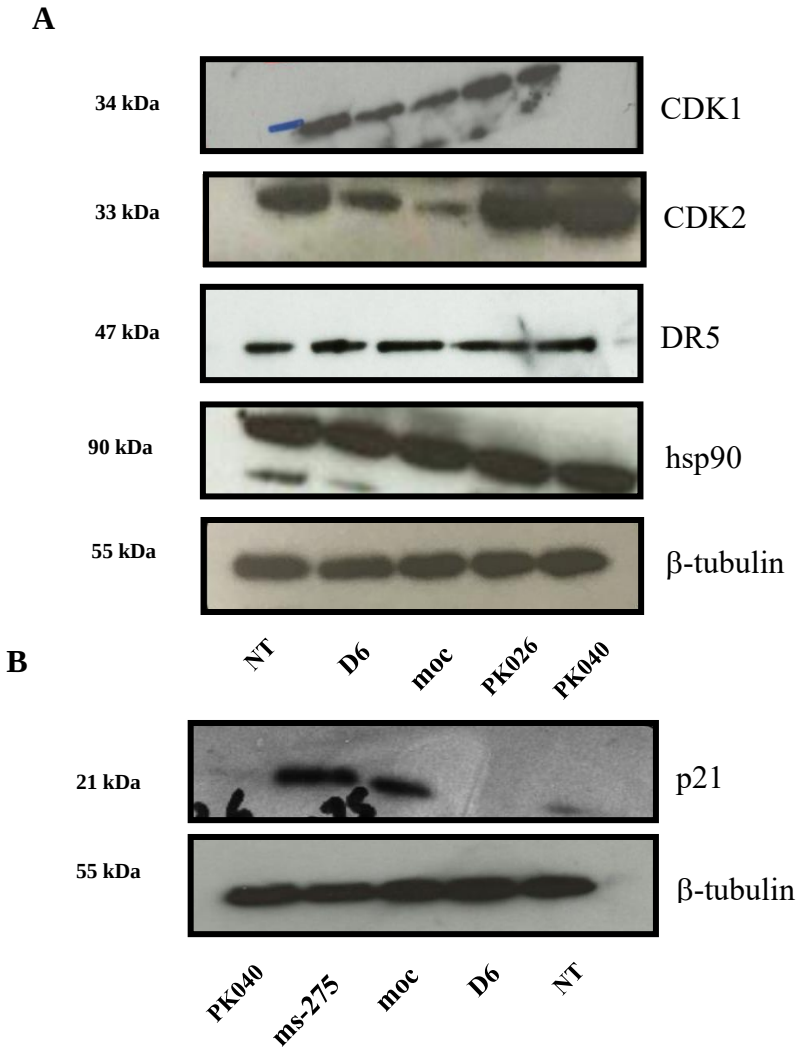


Figure 5.5: Western blot analysis of the time-dependent modification effects of D6, mocetinostat (PK022), PK026 and PK040 on the expression. HL60 Cells were exposed to 2.5 μM D6, 625 nM mocetinostat and 30 μM PK026 and PK040 for 24 h and probed for different cell cycle regulatory proteins where b-tubulin serves as the loading control. (A) Effect on the regulation of cell cycle-regulatory proteins including CDK1, CDK2, DR5 and hsp90 was determined by western blot; (B) effect on the cell cycle inhibitory protein p21. The experiment was performed in biological triplicates.

In this study, *ortho* analogues PK022 (mocetinostat) and D6 show differentiation of AML cells and also a reduction of CDK1 and 2 expression which is in line with the previous reports where inhibition or loss of function of CDK1 and 2 have been reported to induce a switch from proliferation to differentiation in NSCs (Lim and Kaldis, 2012).

Even though there are not many studies confirming the role of CDK1 and 2 during G2-M phase transition especially in an AML cell line, but, in a study by Chung and Bunz at John Hopkins, the upregulation of CDK2 is important for DNA damage checkpoint regulation and to prevent the cells from mitotic entry (Chung and Bunz, 2010). However, the role of these CDKs and the increase in their expression in AML cell line HL60 is clearly identified here (Figure 5.4 A). It was also interesting to observe that *meta* analogues PK026 and PK040 caused upregulation of CDK2 expression and the concomitant increase of the CD11b expression in HL60 cell line. Further studies need to be done to understand this in detail.

It was decided to look at the expression of cell cyclin inhibitor p21 as it is well established that during differentiation in HL60 cells the activity of cell cycle related genes and their inhibitors increases depending upon the expression of genes associated with the terminal cell types of differentiation (Nobuyuki Horie et al., 2004) (Nebbioso et al., 2005b). The results also showed upregulation of p21 expression with commercial HDACi MS-275 and mocetinostat which was in line with the previously reported results of p21 dependent growth arrest at G1 phase and differentiation with MS-275 treated leukemic cells (Rosato et al., 2003c). However, the novel analogue D6 and its *meta* analogue PK040 did not cause an upregulation of p21 expression suggesting that there might be an alternate mechanism of action involving other cyclin inhibitors/ genes leading to differentiation. Further, experiments need to be done to be able to verify this result.

In the literature, HDACi such as MS-275 and SAHA at 1 μM induce differentiation in AML cell lines by activating the tumour selective death signalling pathway (TRAIL) and its receptor DR5 (Nebbioso et al., 2005b),(Rosato et al., 2003a). However, in this study, no change in the expression of DR5 receptor suggested that the four compounds do not initiate the pathway for apoptosis at their respective concentrations. Similarly, there was no change in the expression for hsp90 which is reported to modulate differentiation and cell cycle regulation and is

recognized as the target of HDAC6 (Kovacs et al., 2005)(Burrows et al., 2004). Since the compounds did not inhibit HDAC6 in the recombinant enzyme assay (Chapter 4 Section 4.3.13) it could be inferred that hsp90 is not the target for these compounds to regulate cell cycle progression.

5.5 Microtubule Inhibition assay

Microtubules are the highly dynamic mitotic spindles and the most successful target for anticancer therapy. These structures are fundamental for cell proliferation, cell shape and separation of chromosomes during mitosis. The microtubule inhibitors have been in great success by binding to tubulin subunit, inducing mitotic arrest and subsequent apoptosis (Liu et al., 2019). There have been reports where inhibitors such as PDP induced occurrence of apoptosis in HL60 cell line along with G2/M phase arrest ((Tseng et al., 2002).

Since the *meta* analogues PK026 and PK040 cause G2 arrest in HL60 cells, it is important to confirm if this was a result of microtubule disruption. It was decided to treat the HL60 cells with *meta* analogues (30 μM) for a period of 24 h and then stain the cells using phospho histone 3 or P-H3 antibody which marks the G2/M transition and stains the condensed chromatin just before chromosomal segregation. P-H3 at serine 10 is very specific and has a short half- life of about 30-60 minutes which helps to understand if the compounds are undergoing G2 arrest due to microtubule disruption.

In this experiment the non-treated cells served as negative control and vinblastine (a known microtubule inhibitor) at a concentration of 5 nM served as the positive control. With the flow cytometry data (Figure 5.6) it could be seen that vinblastine had significantly increased the population of cells labelled with Ph3 antibody (to 9.4%) but the *meta* analogue PK026 and PK040 used at a concentration of 30 μM failed to cause an increase of more than 1.5% in Ph3-labelled cells and showed values similar to the negative control (non- treated cells), thereby

ruling out the possibility of these compounds working through microtubule disruption or behaving as microtubule inhibitors.

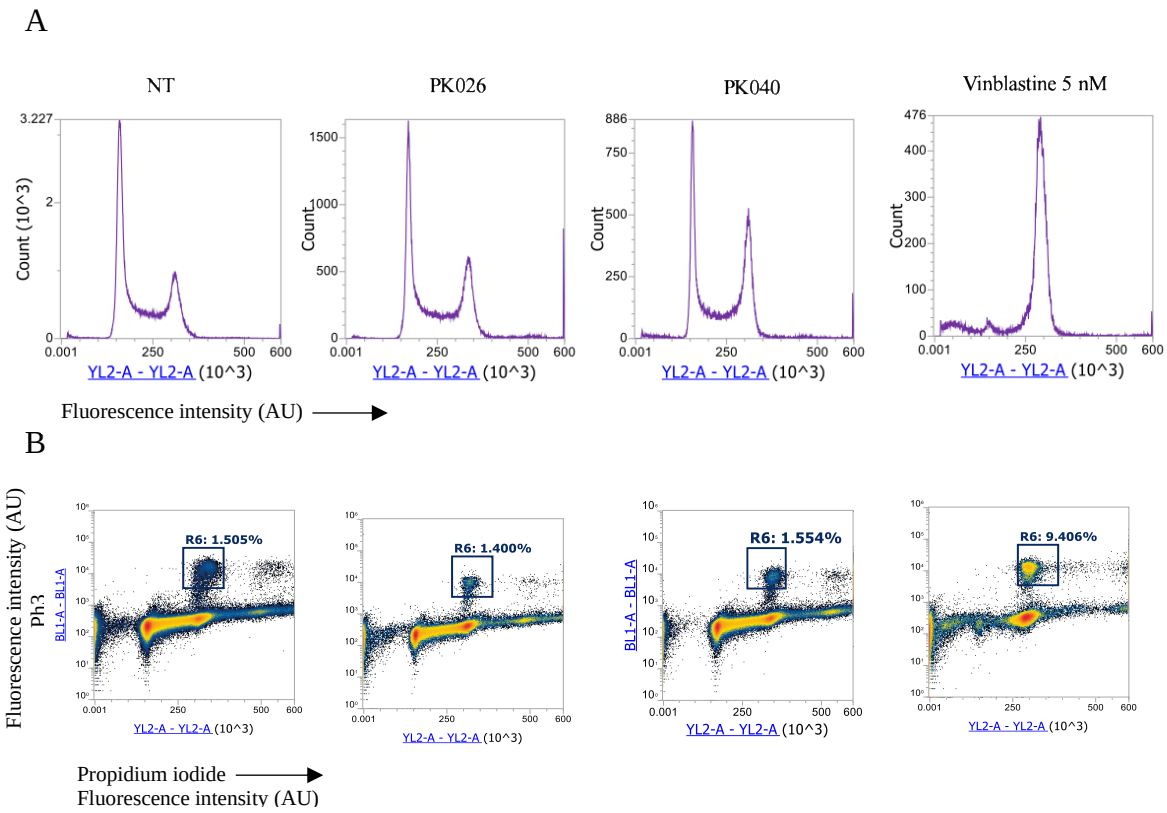


Figure 5.6: Effect of the compound PK026, PK040 on cell cycle and distribution. HL60 were exposed to the following concentration of compounds for 24 h after which they were treated with PI and ph3 and subjected to cell cycle analysis using flow cytometry. (A) the representative FACS plots. (B) Representative FACS plots of cell cycle analysis for HL60 cells and the % of ph3 population denoted by the square boxes. The y axis depicts the value of ph3 antibody and x axis propidium iodide value. Values represent the means for three separate experiments performed in triplicate.

5.6 RNA samples

As discussed above RNA sequencing helps to identify changes in gene expression caused by compound treatment. It not only aids to identify the relevant targets and pathways regulated of the novel compounds from the phenotypic screening, but also provides a broad spectrum of the compound biology. RNA sequencing study was carried out with the help of Oxford Genomics

Centre and Dr Thomas Jackson (Milne group) to identify any significant changes in RNA expression as a result of the compound treatment. The samples were sequenced using poly-A RNA sequencing. The benefit with this approach is that the prepared libraries, and therefore data, predominantly relates to protein coding transcripts. Standard approaches include selection of polyadenylated RNA (polyA) transcripts using oligo (dT) primers, and depletion of highly abundant rRNAs through hybridization capture followed by magnetic bead separation. This is ideal for comparative gene expression analysis and makes good use of the capacity of each sequencing lane by focusing on the full length, mature poly-A transcripts alone (Hunt and Walker).

HL60 cells were treated with the respective concentrations of the compounds for a period of 24 h followed by RNA extraction (as described in Materials and Methods). DMSO samples (0.1%) were treated as the negative control.

For the purpose of confirming the quality of the cells, and to relate the RNA signatures to phenotype, the same batch of HL60 cells were treated with all the four compounds and were analysed for both CD11b expression and cell cycle progression (Figure 5.7). The samples for CD11b assay were incubated for 96 h and then stained with CD11b as mentioned in Materials and Methods and analysed by flow cytometry. The samples for cell cycle progression were incubated for a period of 24, 48 and 72 h. The plate was then treated with PI and analysed by flow cytometry to check the DNA content in each of the phases.

Overall, the results confirmed the effects seen before which was a G1 arrest with mocetinostat (PK022) and D6 and a G2 arrest with PK026 and PK040 at all the three time points. There was also concomitant increase in CD11b expression post 96 h for all the four samples as compared to the negative control (Figure 16 and 17 attached in appendices).

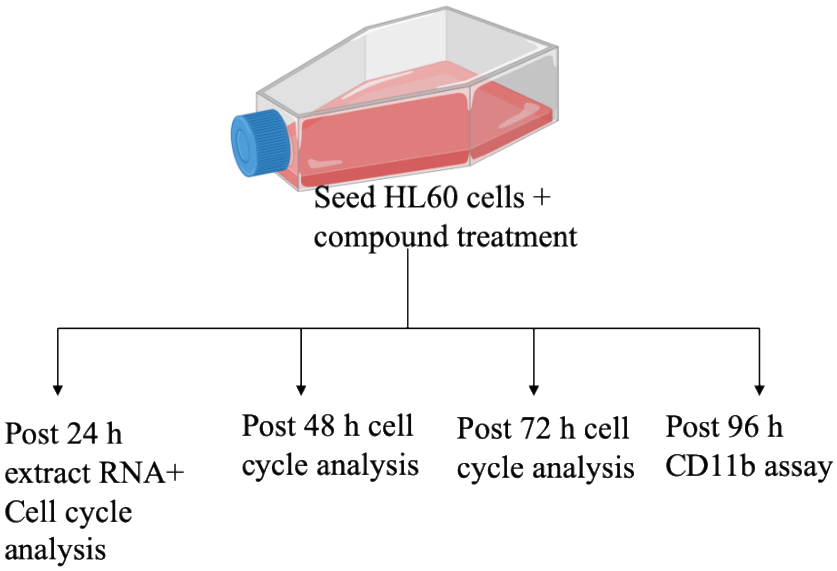


Figure 5.7: Experimental design for HL60 cells treated with 2.5 mM D6, 625 nM mocetinostat and 30 mM PK026 and PK040 undergoing RNA sequencing.

The RNA extracted from samples was safe from any DNA or protein contamination and also had high integrity quality as shown by nanodrop and tapestation test respectively (results attached in appendices).

The Volcano plots of the *ortho* analogues mocetinostat and D6 showed a significant difference (P_{adj}<0.05) in the regulation of gene expression as compared to the non-treated samples (Figure 5.8). However, there were not many differentially regulated genes between the non-treated samples and the *meta* analogues. This could imply that the time point of 24 h, chosen for the treatment of the compounds with the cells might not be enough to cause an upregulation in the expression of target genes. It could also imply that the *meta* analogues do not induce a change or only few changes at the transcriptional level.

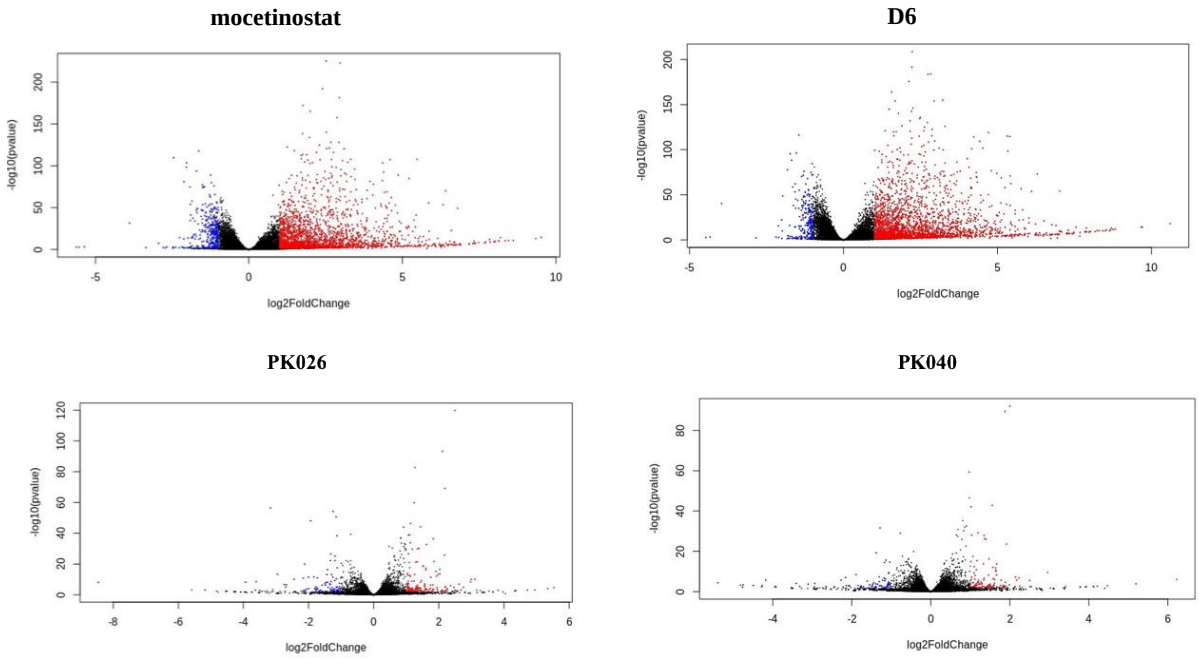


Figure 5.8: Volcano plot of the differentially expressed genes between normal vs compound treated groups. Significantly down-regulated genes are in dark blue (sig=True), significantly up-regulated genes are in red (sig=True), non-significant genes are in black. The x axis represents log2FoldChange and the y axis represents -log10(pvalue).

The next analysis involved hierarchical clustering of the genes from different samples. The results from the heat map below indicated that D6 and mocetinostat were clustered further from the non-treated samples highlighting difference between their upregulated and downregulated genes. However, mocetinostat and D6 looked similar at global gene expression level. The *meta* analogues clustered closely with the non-treated samples, confirming further that there were few differences between them and the non-treated samples (Figure 5.9).

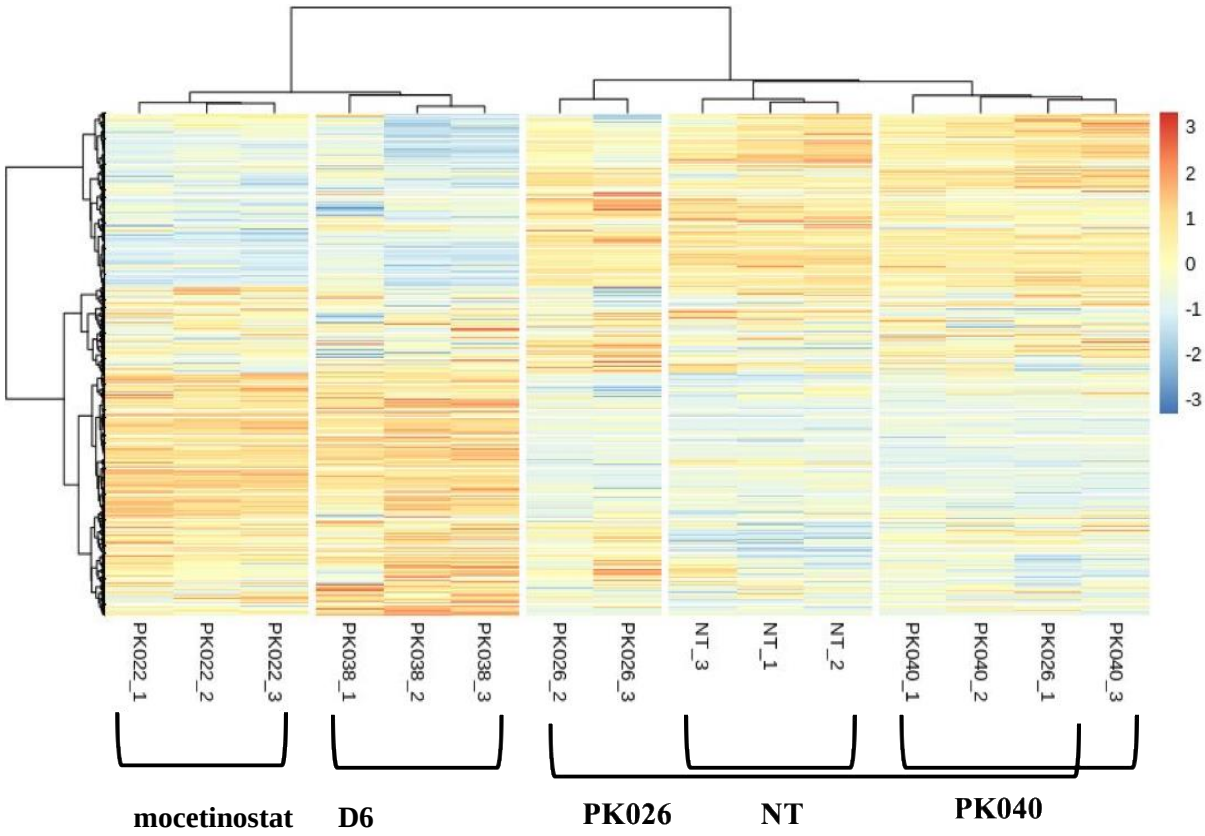


Figure 5.9: Heatmap of hierarchical clustering indicate differentially expressed genes (rows) between NT, D6, mocetinostat (PK022), PK040 and PK026 samples (fold-change > 1, P < 0.05). Orange indicates up-regulation and blue indicates down-regulation.

Since D6 is structurally similar to mocetinostat, it was decided to look closely for the number of genes that overlapped between the two compounds. As two compounds have already been established as HDAC inhibitors, a vast difference between their transcriptional activation/repression was not expected. The data indeed suggested that there were roughly 3500 genes commonly expressed between the two. However, there were also a few hundred genes that were differentially expressed in D6. Further analysis would be required to look into these genes in detail and understand if there were certain factors unique to D6.

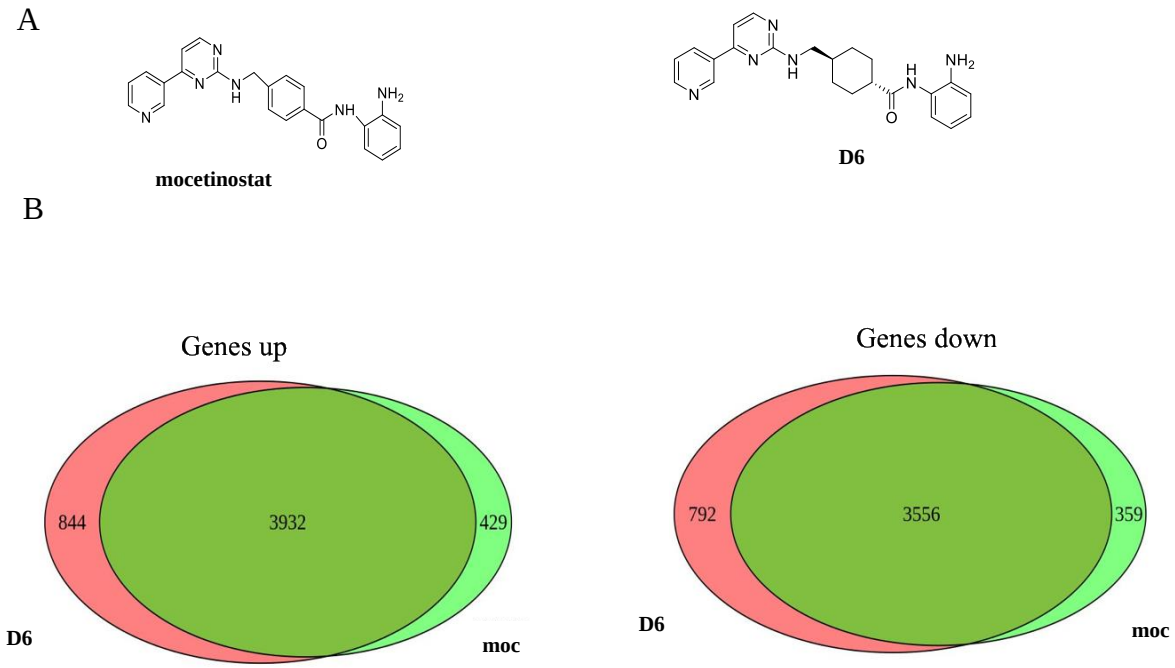


Figure 5.10: (A) Structure of mocetinostat and D6. (B)The overlap study between mocetinostat treated and D6 treated samples showing differentially expressed genes shown as up-regulated or down-regulated.

Enrichment analysis is a popular method for analysing gene sets generated by genome wide experiments for the given set of samples. Differentially expressed genes are obtained from the RNA seq data and then used as input for computing enrichment with existing knowledge from the gene libraries (Moiyadi and Sridhar, 2015) .

Enrichr is one common web-based enrichment analysis tool. It computes three types of enrichment scores to assess the significance of overlap between the input list and the gene sets in each gene-set library for ranking a term's relevance to the input list. These tests are: 1) the Fisher exact test 2) z-score of the deviation from the expected rank by the Fisher exact test and 3) a combined score that multiplies the log of the p-value computed with the Fisher exact test by the z-score computed by the correction to the test (Kuleshov et al., 2016).

With the help of this tool it was possible to analyse the gene signatures for the four compounds. The results from the Enrichr data showed (Figure 5.12 A) that PK022 had the highest combined score for mocetinostat confirming the reliability of the test and the purity of the compound whereas for D6 the results indicated entinostat or MS-275 as the closest match (Figure 5.12 B). The two compounds also upregulate genes which overlap with the macrophage signatures confirming differentiation (Figure 18 B in appendices).

The gene signatures for *meta* analogues, PK026 and PK040 closely matched with a few kinase inhibitors (Figure 5.11). The *meta* analogues are currently being tested against B-raf, EGFR, ATM/ATR, Aurora and GSK3alpha in a kinase inhibitory assay.

Index	Name	P-value	Adjusted p-value	Odds Ratio	Combined score
1	LJP006_HME1_24H-HG-6-64-01-0.04	1.592e-36	5.275e-32	9.88	814.15
2	LJP006_HA1E_24H-HG-6-64-01-0.04	5.068e-27	1.199e-23	11.67	706.87
3	LJP006_HME1_24H-KIN001-043-1.11	1.723e-32	1.903e-28	9.17	670.34
4	LJP008_PC3_24H-CGK-733-10	1.752e-34	2.902e-30	8.24	640.28
5	LJP006_HCC515_24H-KIN001-043-10	2.318e-27	6.982e-24	9.71	595.52
6	LJP005_A375_24H-erlotinib-10	2.676e-29	1.266e-25	8.99	591.65
7	LJP006_HME1_3H-PD-173074-10	4.539e-25	8.352e-22	10.49	587.85
8	LJP005_A375_24H-pelitinib-0.37	8.420e-29	3.486e-25	9.07	586.50
9	LJP005_PC3_24H-pelitinib-3.33	1.396e-21	1.101e-18	11.98	575.10
10	LJP006_HME1_24H-HG-6-64-01-0.12	3.228e-30	2.673e-26	8.32	564.75

Figure 5.11: Enrichr analysis table for PK026 and PK040

A

Index	Name	P-value	Adjusted p-value	Odds Ratio	Combined score
1	LJP008_A549_24H-mocetinostat-10	2.651e-33	8.782e-29	2.90	217.87
2	LJP008_MCF7_24H-vorinostat-10	3.393e-28	1.249e-24	3.08	194.89
3	LJP008_A549_24H-pracinostat-3.33	6.166e-31	1.021e-26	2.80	194.86
4	LJP007_MCF7_24H-vorinostat-10	8.455e-31	9.335e-27	2.76	190.87
5	LJP008_A549_24H-entinostat-10	3.715e-29	2.461e-25	2.88	188.34
6	LJP005_HT29_24H-XMD16-144-10	4.285e-29	2.028e-25	2.67	174.62
7	LJP008_MCF7_24H-belinostat-10	1.562e-29	1.294e-25	2.63	174.23
8	LJP008_A549_24H-vorinostat-10	3.805e-29	2.101e-25	2.65	173.59
9	LJP009_MCF7_24H-vorinostat-10	5.532e-29	2.291e-25	2.66	172.83
10	LJP006_MCF7_24H-BI-2536-10	1.082e-26	2.988e-23	2.77	165.52

B

Index	Name	P-value	Adjusted p-value	Odds Ratio	Combined score
1	LJP008_A549_24H-entinostat-10	8.133e-26	1.347e-21	2.63	151.77
2	LJP007_HT29_24H-vorinostat-10	7.475e-26	2.476e-21	2.51	145.37
3	LJP007_MCF7_24H-vorinostat-10	1.097e-25	1.211e-21	2.47	142.16
4	LJP008_A549_24H-pracinostat-3.33	1.708e-24	1.131e-20	2.47	135.03
5	LJP009_MCF7_24H-vorinostat-10	1.224e-24	1.014e-20	2.40	132.41
6	LJP008_MCF7_24H-vorinostat-10	4.370e-22	1.316e-18	2.68	131.94
7	LJP008_A549_24H-mocetinostat-10	3.609e-23	1.708e-19	2.44	126.23
8	LJP008_A549_24H-pracinostat-1.11	2.207e-21	6.092e-18	2.54	120.59
9	LJP008_MCF7_24H-belinostat-10	3.325e-23	1.836e-19	2.32	120.07
10	LJP005_HT29_24H-XMD16-144-10	7.510e-23	2.764e-19	2.36	120.07

Figure 5.12: Enrichr analysis table for (A) mocetinostat (B) D6

5.7 Discussion

Cells transverse the cell cycle in several controlled phases, starting from G1, S to G2 phase where repair might occur along with preparation of mitosis. This is well established mechanism, initiated and regulated by the cell cyclins and their inhibitors. This study analysed the effect of treatment with *ortho* and *meta* analogues on HL60 cell cycle. It is well established that differentiation is marked by an arrest in the G1 phase of the cell cycle (Schnerch et al., 2012a). In here, it was confirmed that the commercial HDACi mocetinostat as well as the novel analogue D6, both caused a G1 arrest consistent with a block in proliferation and upregulation of CD11b – all hallmarks of differentiation in AML cells. However, the *meta* analogues PK026 and PK040 had caused a G2 arrest in HL60 cells concomitant with their increase of the CD11b expression.

In the literature, certain agents which cause anti proliferative effects via apoptosis and induction of G2 arrest in some cancer cell lines ((Wang et al., 2016) and there are a few studies where G2 arrest is synchronised with cell differentiation in normal cells (Ayeni et al., 2016), but compounds initiating G2 arrest in AML cell lines and causing differentiation is something not well explored before. To explore this further, a few cell cyclins known to regulate G1 and G2 arrest were chosen for a western blot study. Overall, the results for *ortho* analogues mocetinostat and D6 confirmed the downregulation of CDK1 and 2 which is in line with the previous reports ((Lim and Kaldis, 2012) confirming the change from proliferation to differentiation on loss of CDK1 and 2 expression. The expression of CDK2 however upregulated with the *meta* analogues suggesting that the role of CDK2 here at 24 h time point is to check for DNA damage and to prevent such cells from mitotic entry is in accordance with the role of CDK2 reported in the literature (Chung and Bunz, 2010). The role of the CDKs has not been explored with respect to differentiation effects in AML cells and it is interesting to observe the effects on these CDKs with the compounds initiating differentiation.

The cell cyclin inhibitor p21 was upregulated in only mocetinostat and MS-275 (also serving as the positive control for the experiment) and not in D6, suggesting the role of an alternate protein/pathway leading to the known phenotypic effects.

Finally, RNA sequencing was used to further validate the target. The batch of cells treated with the respective concentrations of the compounds and used for RNA extraction were also validated for the upregulation of CD11b expression and subsequent cell cycle arrest.

The sequencing results confirmed the *ortho* compounds to be working primarily by HDAC inhibition. Enrichr analysis confirmed that D6 inhibits only two HDACs from class 1 of HDACs, thereby having distinct profile to that of mocetinostat. The Venn diagram between D6 and mocetinostat showed 844 upregulated genes and 792 downregulated genes, unique to D6. Further studies and tests would be required to draw a detailed comparison and highlight the differences on the transcriptional level between the two compounds.

On the other hand, *meta* analogues PK026 and PK040 indicated signatures close to inhibition of kinases specifically EGFR, B-Raf, GSK3 alpha, Aurora and ATM/ATR. A kinase inhibitory assay is in progress and the results may suggest a possible mechanism of action of the *meta* analogues leading to G2 arrest. Out of the above mentioned kinases ATM/ATR has been studied for its role to cause G2 arrest in colon cancer cells ((Zhu et al., 2009), and EGFR/GSK3 beta inhibition has been linked to G2 arrest in glioblastoma cells (Kapoor et al., 2007). However inhibition of B-raf kinase and its downstream target aurora kinase have been studied to induce G1 arrest in different cancer cell lines (Toress-Collado et al., 2017).

Chapter 6: Conclusion and Future Work

6.1 Conclusion

The preliminary screening identified several HDAC inhibitors and novel derivatives which induced differentiation in genetically distinct AML cell lines. The aim of this thesis was thus to understand whether or not HDAC inhibition induce differentiation effects.

6.1.1 Summary of the work

HDAC inhibitors have been in the literature as the epigenetic modulators which cause differentiation, cell cycle arrest and apoptosis though a variety of posttranslational modifications which primarily includes acetylation of the histone and other non-histone substrates. In this study, several HDACi and novel derivatives with unknown HDAC inhibitory activity were identified to cause differentiation in a variety of genetically distinct AML cell lines. The HDAC inhibitors have an anilide ring with a chelating group (NH_2 or OH) at the *ortho* position that binds potently to the zinc ion at the catalytic site *via* bidentate coordination mode to exert HDAC inhibitory effects. To confirm if HDAC inhibition leads to differentiation, potential inactive analogues were prepared to preclude the binding at the zinc ion active site binding motif. Commercial HDACi – mocetinostat and its *meta* analogue PK026 and novel analogue D6 and its *meta* version PK040 were synthesized successfully (Table 6.1). The following compounds were retested for CD11b expression in HL60 cells, and surprisingly, this time, there was an upregulation of CD11b expression even with the *meta* analogues PK026 and PK040 albeit with lower potency. EC_{80} values were chosen to confirm the differentiation effects. 2.5 μM of D6, 625 nM of mocetinostat and 30 μM of PK026 and PK040 confirmed upregulation of CD11b, block in proliferation, change in cell morphology marked by multiple nuclei, the presence of vacuoles and the distorted shape of the cytoplasm- all hallmarks of differentiation to myeloid lineage cells. Further to this, cell cycle distribution was analysed

using flow cytometry. Intriguingly, the results indicated G1 arrest with the *ortho* analogues mocetinostat and D6 and G2 arrest with the *meta* analogues PK026, PK040. Next, a western blot showed upregulation in the acetylation level of histone 3 for the cells treated with *ortho* analogue D6 but not with *meta* analogue PK040 implying that D6 works as an HDACi and not PK040. Overall, these data suggest that potential inactive analogues devoid of their zinc binding motif also induce differentiation and further studies were done to understand the targets leading to the known effects.

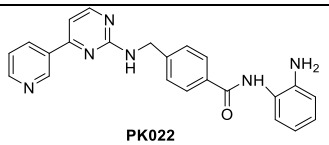
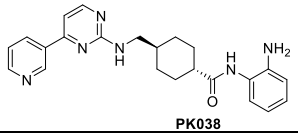
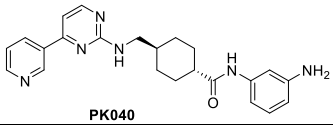
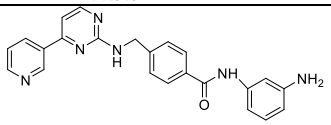
Analogue	Structure
PK022 aka mocetinostat	 PK022
D6 (D6)	 PK038
PK040	 PK040
PK026	 PK026

Table 6.1: Structures of the *ortho* analogues (D6 and mocetinostat) and their *meta* analogues (PK040 and PK026).

The next chapter discussed recombinant assays with the aim to get a better profile of the compounds. The compounds were tested against different HDACs belonging to different groups but all Zn^{2+} dependent enzymes. It was confirmed that HDAC1, 2 and 11 were inhibited by mocetinostat at an IC_{50} of 170 nM, 2.0 μM and 800 nM respectively. However, D6 inhibited only HDAC1 with an IC_{50} of 2.0 μM and not HDAC2 thereby having a distinguished profile to that of mocetinostat. Also, the *meta* analogues PK026 and PK040 failed to inhibit any of the four HDACs and thus were recognised as non HDAC inhibitors. In this chapter, an attempt was made to understand if for mocetinostat and D6, HDAC inhibition is the direct target leading to differentiation or if there is a secondary mechanism independent of HDAC inhibition, leading to differentiation. For this purpose, THP1 cells were overexpressed with HDAC1 and the overexpression of the protein was confirmed by a western blot. It was hypothesised that if the potency of D6 and mocetinostat decreases conferring resistance to the compounds then this would be consistent with HDAC1 causing differentiation. However, the experiment did not show any difference in the EC_{50} values of the HDAC1 treated cells and the control group suggesting HDAC1 may not be involved in the mechanism of action of mocetinostat and D6 although this did not rule out the involvement of other HDACs. Similar studies with other HDACs need to be performed to get a better understanding.

As had been mentioned before G1 arrest was observed with *ortho* analogues mocetinostat and D6 and a G2 arrest with *meta* analogues PK026 and PK040. In the last chapter, these effects were confirmed to be consistent across HL60 cells. G1 arrest during differentiation of AML cells is well precedented in the literature (Olsson et al., 2009) and there a few precedents of G2 arrest synchronized with differentiation in normal cells (Ayeni et al., 2016) however, there is not much evidence of G2 arrest and differentiation in leukemic cells.

In order to explore this further, a western blot was used to probe the cells treated with the four compounds against a variety of cell cyclins their inhibitors and other proteins known to play a role in cell cycle regulation. The studies showed that CDK1 and 2 were downregulated in mocetinostat and D6 treated cells but were upregulated in PK026 and PK040 treated cells. The downregulation of CDK1 and 2 is known in the literature to induce a switch from proliferation to differentiation (Lim and Kaldis, 2013) and hence is in line with the observed effects, and the upregulation of CDK2 has been found important for DNA damage checkpoint regulation and to prevent the cells from mitotic entry (Chung and Bunz, 2010). However, the role of CDK2 in AML cells is something not well explored.

The cell cyclin inhibitor p21 was shown to be upregulated only in mocetinostat and not D6 suggesting an alternate protein involved in the process of G1 arrest with this compound.

Furthermore, no change was seen in the expression of the death receptor 5 suggesting that the two HDACi trigger differentiation but not via apoptosis pathway as conventionally known in the literature (Rosato et al., 2003b).

For the target validation studies RNA sequencing was performed for the samples treated with mocetinostat, D6, PK026 and PK040. The results confirmed further that D6 was indeed an HDAC inhibitor but with a distinct profile to that of mocetinostat. Although at the global gene expression level D6 and mocetinostat looked similar, however, looking closely at the genes clustered together there were several hundred differentially expressed genes in D6. Further studies would be required to look into these genes in detail. The *meta* analogues with the RNA sequencing test gave a profile which closely matched specific kinase inhibitors. A kinase inhibitory screen is in progress to verify those targets.

6.1.2 Significance of this work

Phenotypic screen is often used as a tool to identify lead compounds for drug discovery projects. A phenotypic screen makes no assumptions about molecular target and can therefore potentially lead to compounds targeting different types of proteins (receptors, enzymes, transcription factor) and different signalling pathways. This approach when combined with target identification can lead to the discovery of novel therapeutic mechanisms. This work with the help of phenotypic screening, identified commercial HDAC inhibitors and some novel derivatives leading to differentiation in AML cell lines. HDACs are important proteins known to have an effect on the epigenetic regulation and gene expression.

HDAC inhibitors such as panobinostat, vorinostat and TSA have been shown to promote cell death, autophagy and apoptosis in preclinical AML models and are also used at various stages of clinical development, yet these compounds are not effective as monotherapies primarily due to dose limiting tolerance issue attributed to off target effects (San et al., 2019). Hence, there is a greater need to develop more specific HDAC inhibitors with improved profile and therapeutic window.

D6 is a HDAC inhibitor with a distinct profile to mocetinostat that was identified to induce differentiation across a variety of AML cell lines. These studies show that differentiation effects in AML cell lines are independent of the zinc ion binding motif. When the position of the functional group is moved from the *ortho* to *meta*, precluding the possibility of binding to the zinc ion active site binding motif then even though the HDAC inhibitory effects are lost but the phenotypic effects are still observed in AML cell lines, suggesting these act through an alternate route/mechanism. This was explored further by understanding the cell cycle arrest in the G2 phase caused by *meta* analogue and non HDACi PK026 and PK040. The role of G1 phase arrest caused by the downregulation of certain cyclins is associated with differentiation effects in AML cells and has been well described in the literature. However, the downstream

targets leading to G2 phase arrest and the concomitant increase in CD11b expression for AML cells has never been described. With the help of the RNA sequencing data this work has highlighted some specific kinases which could represent potential future targets to induce G2 arrest and differentiation. As a result, the identification of the two *meta* analogues PK026 and PK040 represents an exciting addition to the literature by expanding the available toolbox in understanding G2 arrest and differentiation effects in AML.

6.2 Future Plans

The discovery of *meta* analogues leading to G2 arrest and differentiation in HL60 cells opens up some exciting avenues to be studied in the future. A kinase inhibitory screen is in progress for *meta* analogues PK026 and PK040 against B-raf, EGFR, ATM/ATR, Aurora and GSK3 kinases. The results may support the possible molecular mechanism of action of the *meta* analogues leading to arrest. However, due to the lower potency of these compounds some SAR studies might be able to help explore other analogues close to the active hits, followed by the synthesis of those analogues.

Since in this project only a few of the recombinant HDACs from each of the HDAC group were tested, future studies might explore other HDACs to get a better insight about the profile of the compounds.

Rescue experiments with overexpression of HDAC1 plasmid did not provide a clear understanding of whether or not HDAC1 acts as a direct target to cause differentiation. Future experiments with overexpression of other HDACs might be able to provide a better understanding of this.

The RNA sequencing data has shown genes expression changes that are unique to D6 compared to mocetinostat. It would also be interesting to further understand the differences based on the different genes expressed by both D6 and mocetinostat. Lysine acetylation is a prevalent

modification in enzymes that catalyse intermediary metabolism primarily of carbohydrates, lipids, nucleotides, amino acids and secondary metabolites. Histone acetylation is widely associated with gene regulation, specifically with active genes and a more open chromatin structure and specific acetyllysines can form binding sites to recruit other effectors, suggesting distinct roles for distinct lysine residues (Crump et al., 2011)(Allfrey et al., 1964)(Eberharter and Becker, 2002).

Understanding the acetylation specificity between mocetinostat and D6 using Chip seq could further enhance knowledge between this relatively unexplored area. Chip seq studies will highlight the promoter regions in the chromatin or even the novel promoter leading to the desired effect.

Appendices

CD11b expression for the initial screen across 4 cell lines.

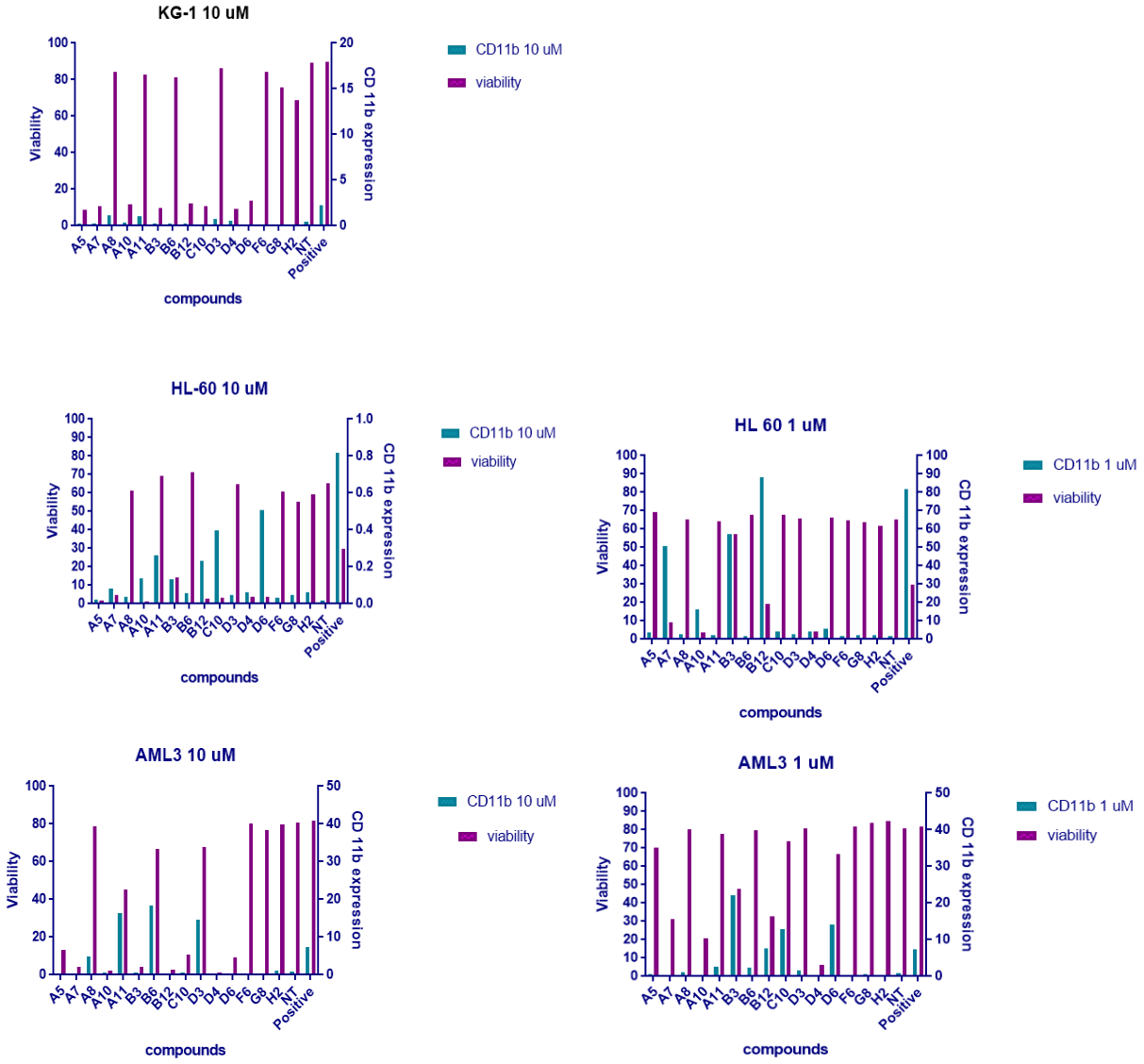


Figure 1: Effect of compounds on differentiation. HL60, OCI-AML3 and KG-1 cells were treated with 10 µM and 1 µM of the following compounds for 4 days. The percentage of cells expressing CD11b surface differentiation marker was determined by flow cytometry as described in Materials and Methods.

Retest of the active compounds in the active cell lines

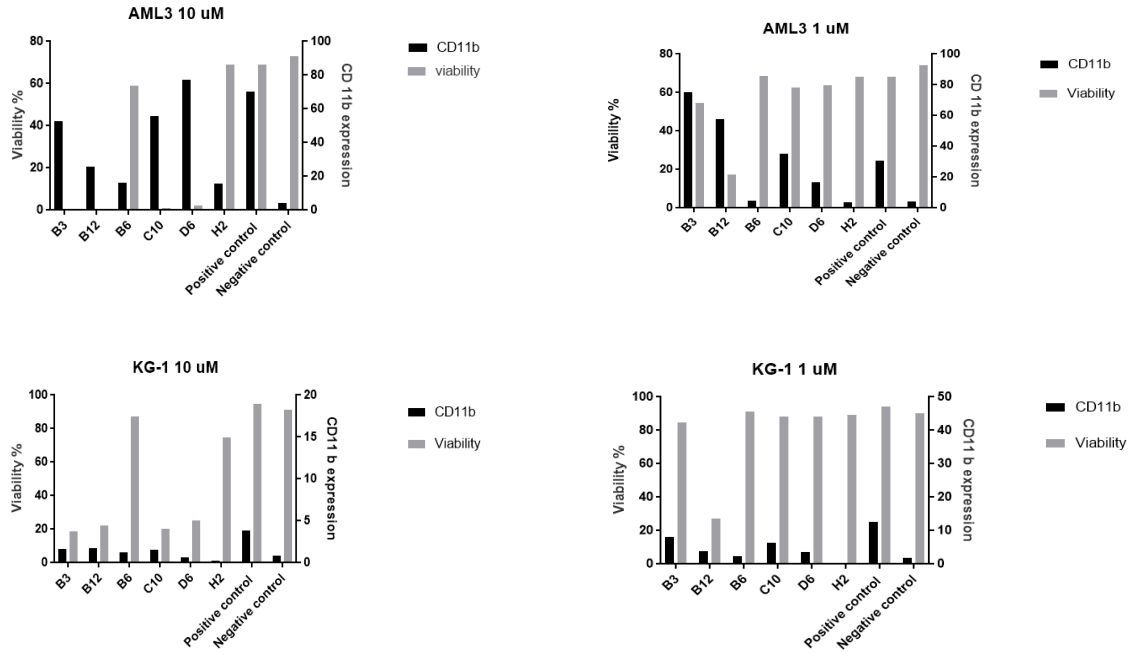


Figure 2: Retest of the active compounds at the active concentrations of 10 µM and 1 µM. OCI-AML3 and KG-1 cells were treated with the compounds at the above given concentrations for 4 days. The percentage of cells expressing CD11b surface differentiation marker was determined by flow cytometry as described in Materials and Methods. The results were consistent with the previous experiment.

Isotype Control

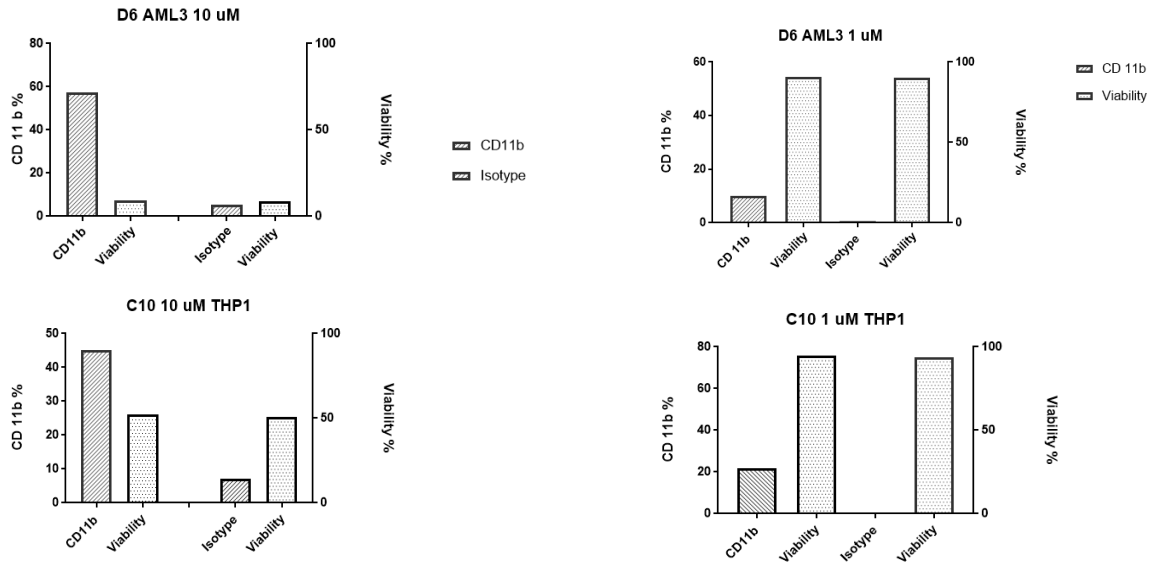


Figure 3: Novel compounds D6, C10 and B6 specifically increase CD11b expression in the three cell lines THP1, OCI-AML3 and KG-1.

Morphology analysis

KG-1

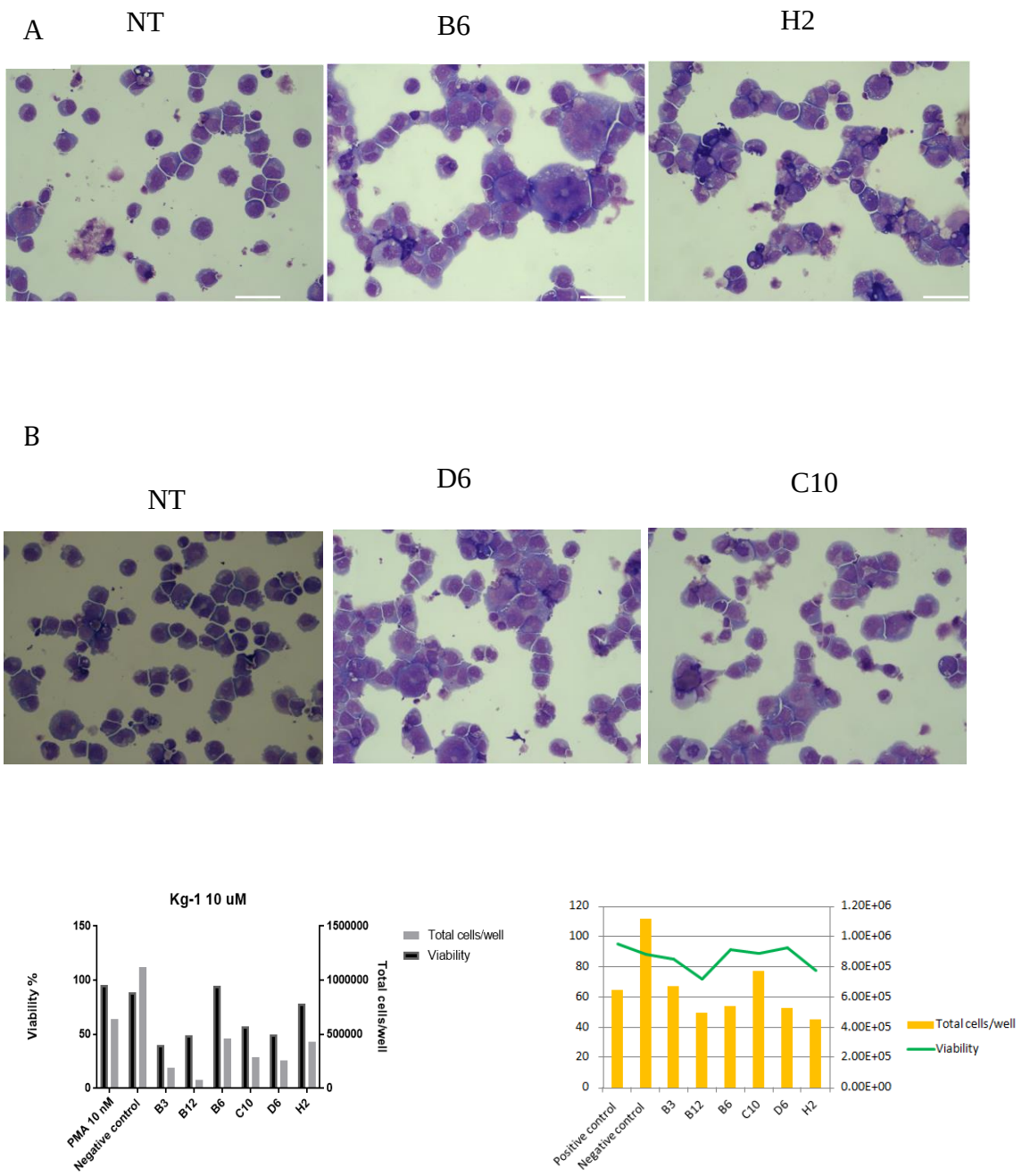


Figure 4: (A) Compound B6 and H2 at 10 µM (B) D6 and C10 at 1 µM promotes differentiation of KG-1 cells compared with non treated cells shown by extended cytoplasm, multiple nucleoli and the presence of vacuoles. Cells were stained using Wright-Giemsa Stain. Images were taken using the Olympus BX 30 camera and acquisition software Infinity, with

magnification X40 and scale bar 20 µm. (C) D6, B6, C10 and H2 inhibits cell proliferation. Equal numbers of KG-1 cells were treated with the compounds (10 µM) and (1 µM) for 4 days and the cell viability and total cells/well were counted using Nucleo Counter (NC-3000) system (described in Materials and Methods).

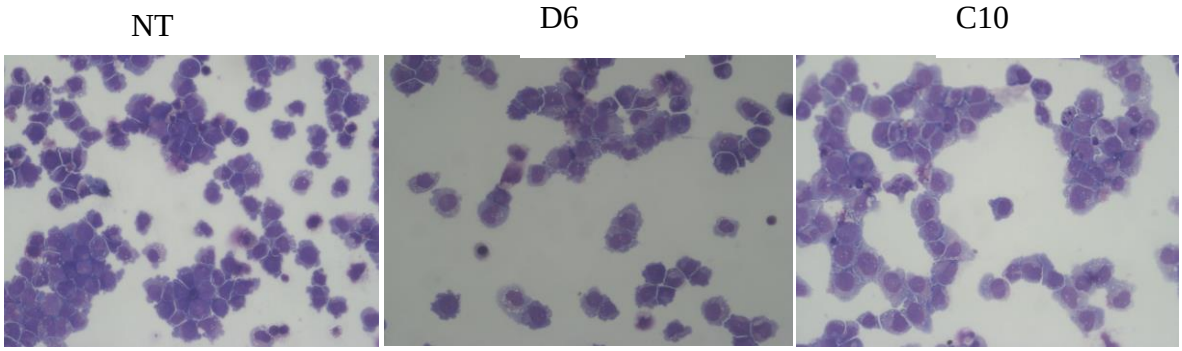


Figure 5: (A): Novel compound D6 and C10 inhibits cell proliferation. Equal numbers of OCI-AML3 cells were treated with the compounds (10 µM) and (1 µM) for 4 days and the cell viability and total cells/well were counted using Nucleo Counter (NC-3000) system. (B) Compound D6 and C10 at 1 µM promotes differentiation of OCI-AML3 cells compared with non treated cells. Cells were stained using Wright-Giemsa Stain. Images were taken using the Olympus BX 30 camera and acquisition software Infinity.

Cell cycle analysis

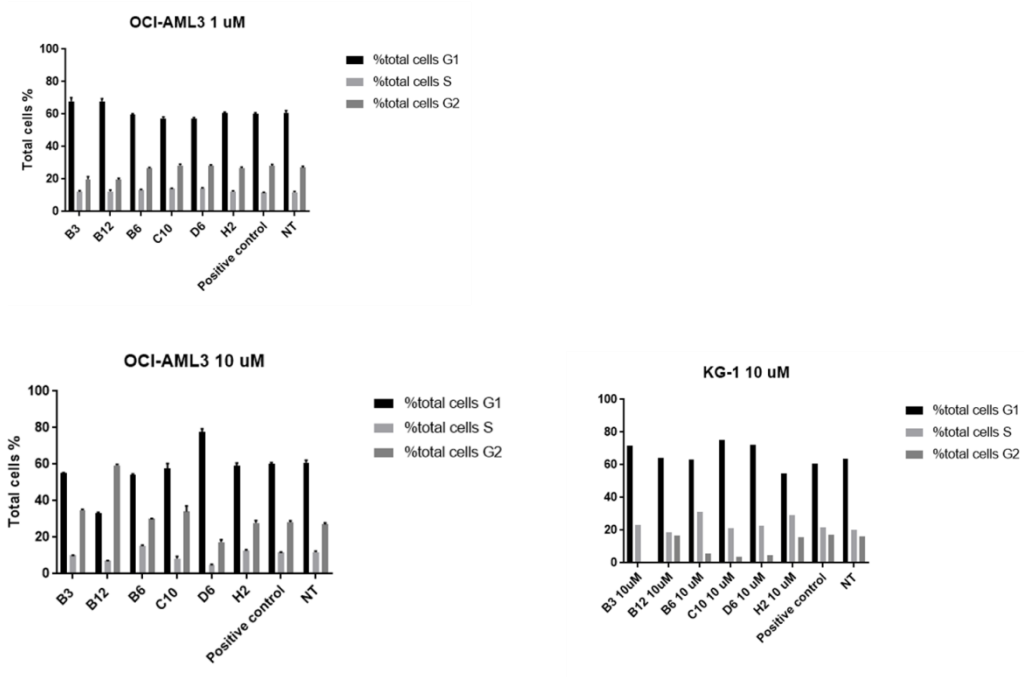
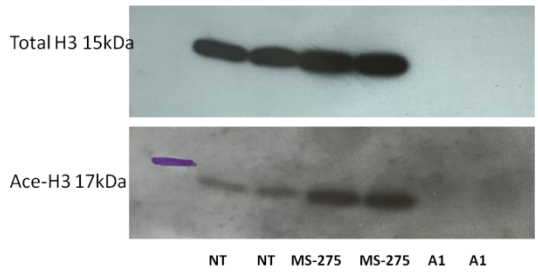
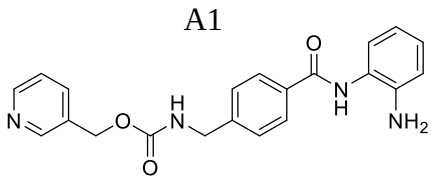


Figure 6: (A) Cell cycle analysis for OCI-AML3 and KG-1 cells after treatment with the compounds at 10 µM and 1 µM for 4 days.
Quantification of cell cycle distribution was done using propidium iodide which stains the DNA in the cell. Total n=3 for each of the samples. (The experiment would be repeated in future to confirm the results and for the consistency with the proliferation block and change in morphology.)

Western Blot analysis





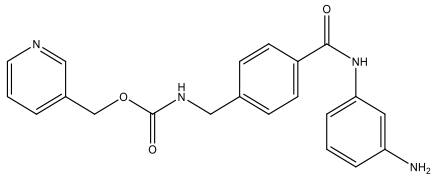


Figure 7: Western blot analysis of HDACi MS-275 and its analogue A1 (with amine at the meta position) on histone H3 acetylation after 24 hr treatment with THP1 cells. The blot needs to be repeated as the control- total H3 did not work for the inactive control hence α-tubulin would be used as the standard control for the experiment.

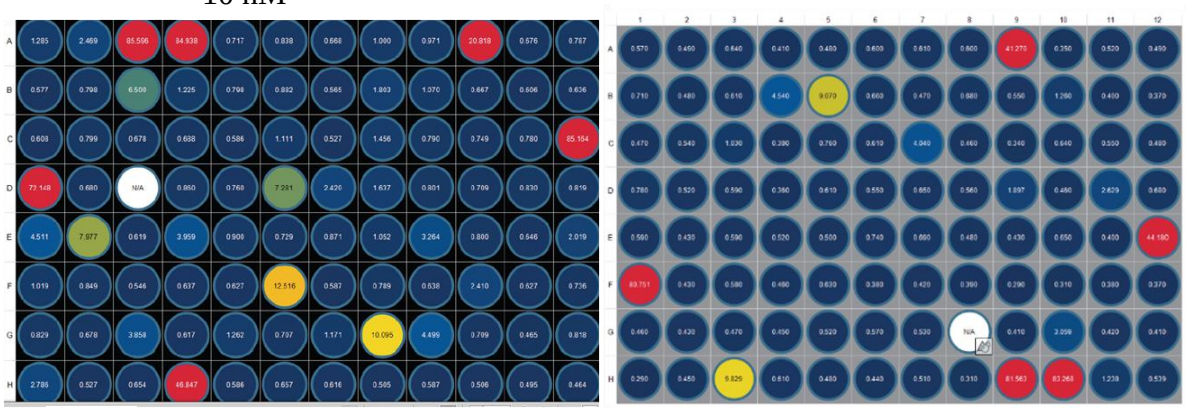
Heat Map for Initial Small Molecule Screen

HL-60 cells

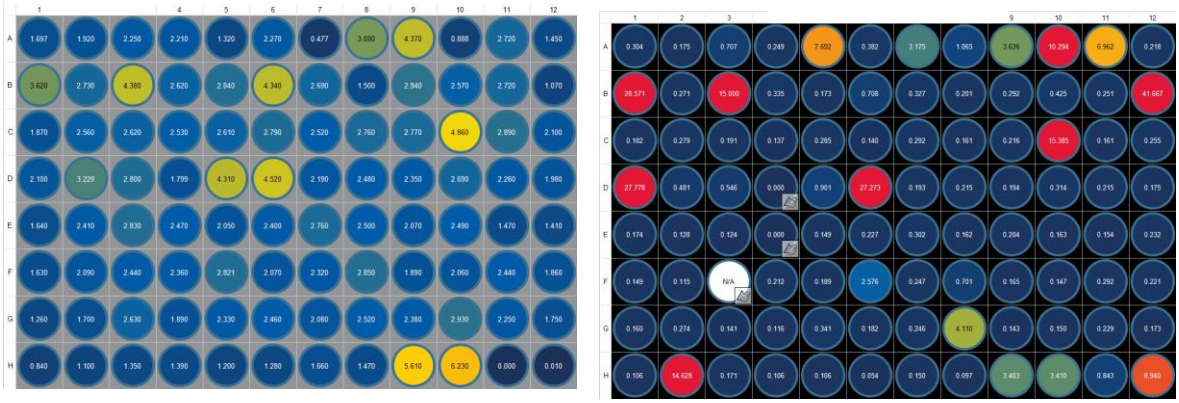
A 10 µM 1 µM



10 nM

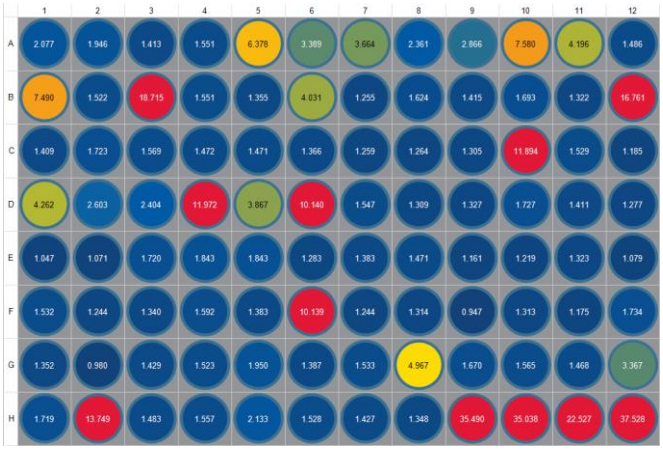


B THP1 10 Kasumi 10 µM



C

ME-1 10 µM





20 %

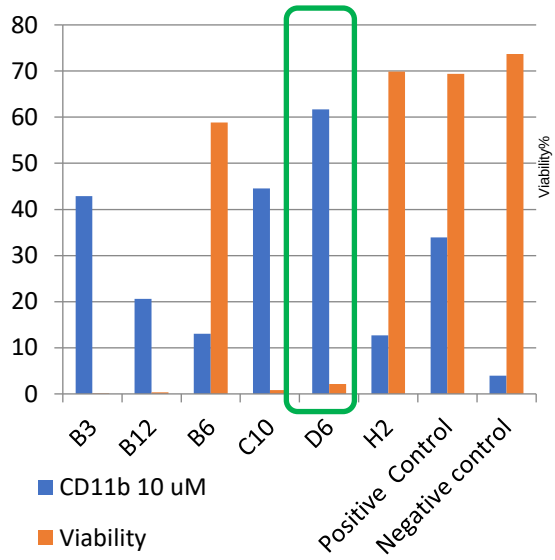
0%

Figure 8: Representative Heat maps for the initial small screen set up with 90 compounds at 4 different concentrations- 10 µM, 1 µM, 100 nM and 10 nM across five genetically different cell lines-HL-60, THP1.OCI-AML3, Kasumi, KG-1 and ME-1. (A) shows heat maps for HL-60 cells treated with the compounds (4 concentrations) for 4 days and their representative CD11b expression. (B) shows CD11b expression for THP1, Kasumi and ME-1 cell lines after treatment with the highest concentration of the compounds-10 µM (1 µM, 100 nM and 10 nM were also used) (C) shows the range of the heat map from 0% to 20%.

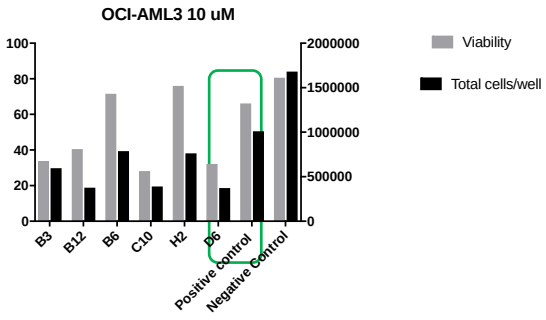
Differentiation with D6 in different cell lines

OCI-AML3

A

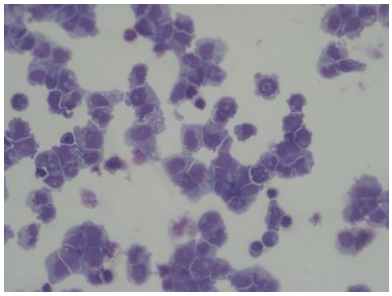


B

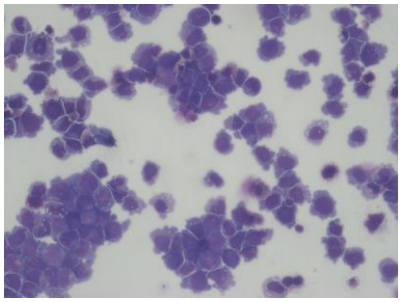


C

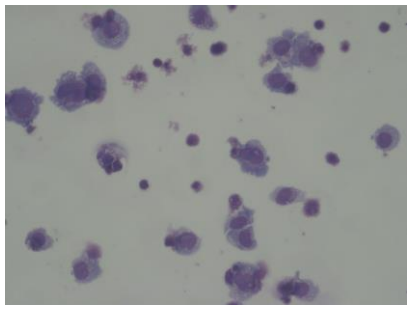
Positive control



NT



D6 (10 μM)



D

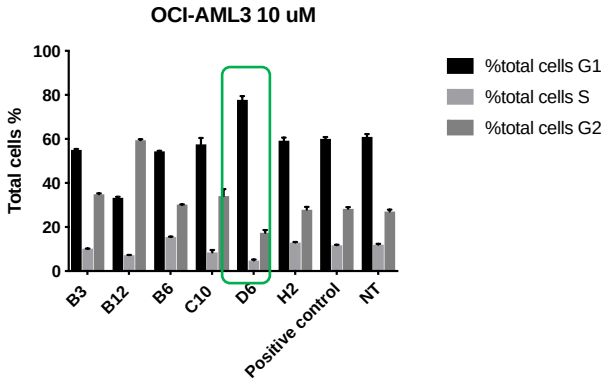
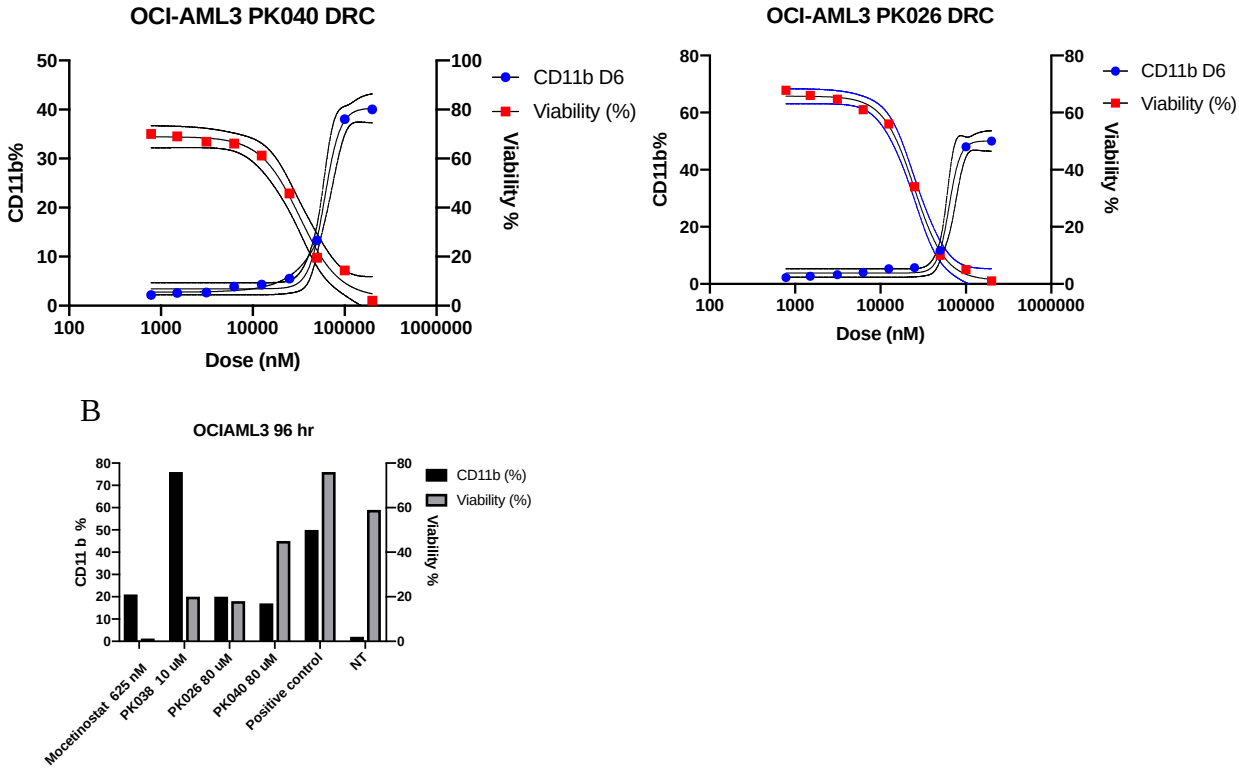


Figure 9: (A) Novel compound D6 aka D6 causes upregulation of CD11b expression. (B) There is a block in proliferation seen with D6. Equal numbers of OCI-AML3 cells were treated with the compounds (10 µM) for 4 days and the cell viability and total cells/well were counted using Nucleo Counter (NC-3000) system. (C) Compound D6 at 10 µM promotes differentiation of OCI-AML3 cells compared with non-treated cells. Cells were stained using Wright-Giemsa Stain. Images were taken using the Olympus BX 30 camera and acquisition software Infinity. (D) Cell cycle analysis for OCI-AML3 after treatment with the compounds at 10 µM for 4 days. Quantification of cell cycle distribution was done using propidium iodide which stains the DNA in the cell.

A



B

Figure 10: (A) Novel compound PK026 and PK040 causes upregulation of CD11b expression. (B) The two compounds also cause a block in proliferation. Equal numbers of OCI-AML3 cells were treated with the compounds (80 µM) for 4 days and the cell viability and total cells/well were counted using Nucleo Counter (NC-3000) system.

THP1

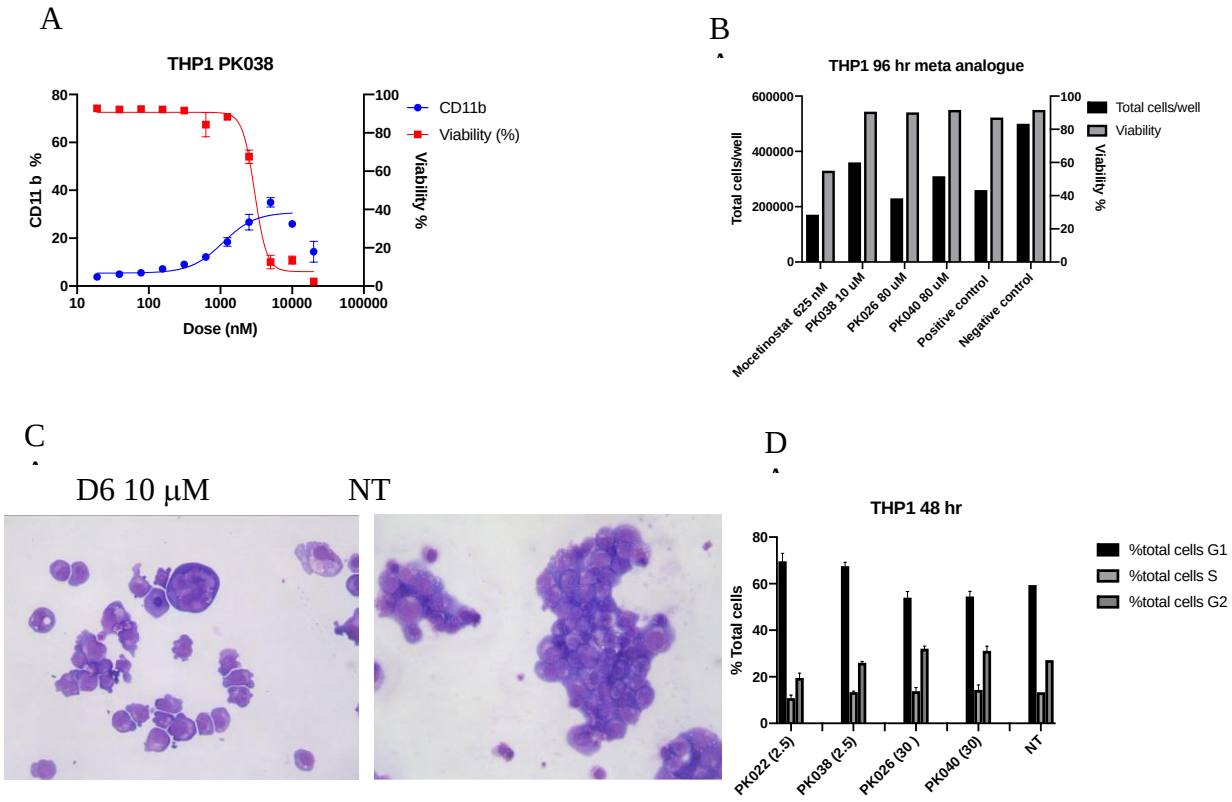


Figure 11: (A) Novel compound D6 aka D6 causes upregulation of CD11b expression. (B) There is a block in proliferation seen with D6. Equal numbers of THP1 cells were treated with the compounds (10 µM) for 4 days and the cell viability and total cells/well were counted using Nucleo Counter (NC-3000) system. (C) Compound D6 at 10 µM promotes differentiation of THP1 cells compared with non-treated cells. Cells were stained using Wright-Giemsa Stain. Images were taken using the Olympus BX 30 camera and acquisition software Infinity. (D) Cell cycle analysis for THP1 after treatment with the compounds. Quantification of cell cycle distribution was done using propidium iodide which stains the DNA in the cell.

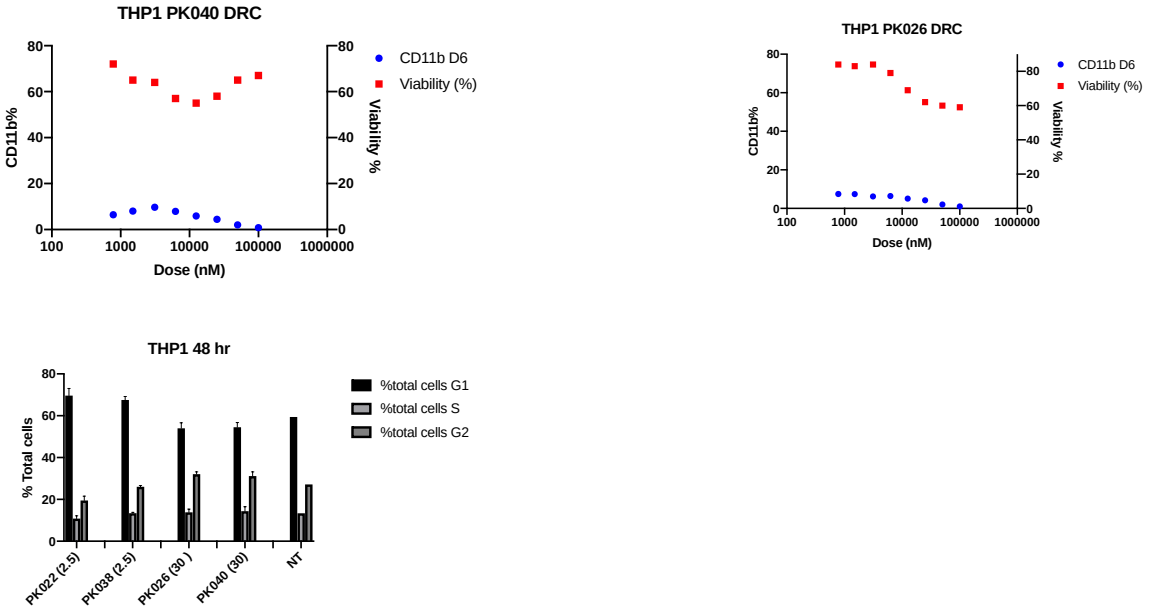


Figure 12: The dose response curves for THP1 cells treated with the meta analogues. There was no upregulation of CD11b observed with these compounds and no G2 arrest.

KG-1

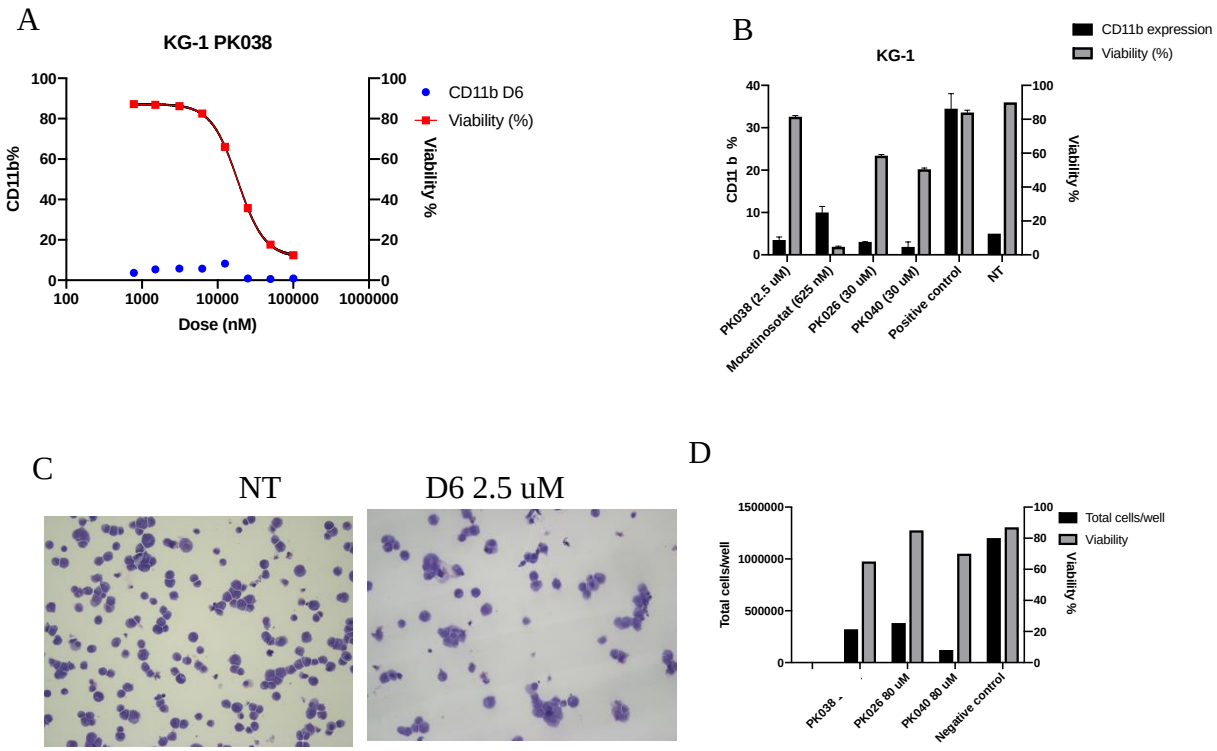


Figure 13: (A), (B) Novel compound D6 aka D6 does not cause upregulation of CD11b expression. (C) Compound D6 at 2.5 µM promotes differentiation of KG-1 cells compared with non-treated cells. Cells were stained using Wright-Giemsa Stain. Images were taken using the Olympus BX 20 camera and acquisition software Infinity. (D) However, there is a block in proliferation seen with D6. Equal numbers of KG-1 cells were treated with the compounds (2.5 µM) for 4 days and the cell viability and total cells/well were counted using Nucleo Counter (NC-3000) system.

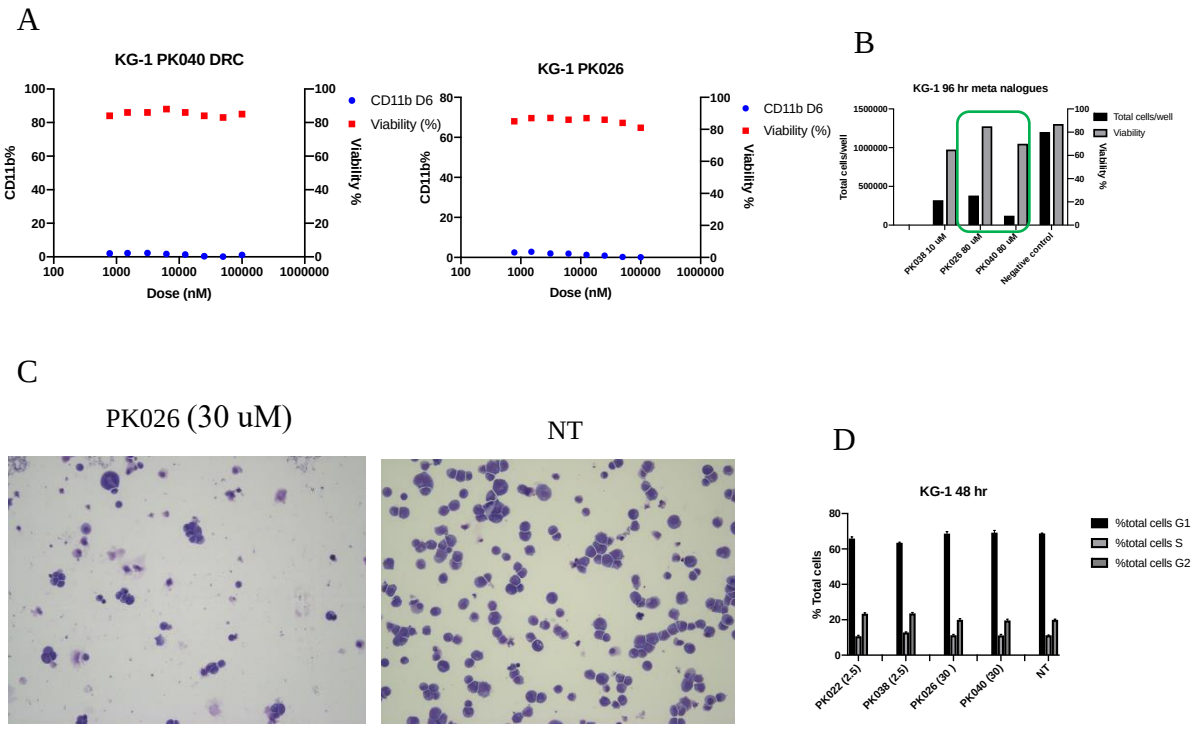


Figure 14: (A) compounds PK026 and PK040 does not cause upregulation of CD11b expression. (B) However, there is a block in proliferation seen with PK026 and PK040 at 80 µM. Equal numbers of KG-1 cells were treated with the compounds for 4 days and the cell viability and total cells/well were counted using Nucleo Counter (NC-3000) system.(C) Compound PK026 and PK040 at 30 µM promotes differentiation of KG-1 cells compared with non-treated cells. Cells were stained using Wright-Giemsa Stain. Images were taken using the Olympus BX 20 camera and acquisition software Infinity. (D) Quantification of cell cycle distribution was done using propidium iodide which stains the DNA in the cell. However no change in the percentage of G1, S and G2 phase was seen.

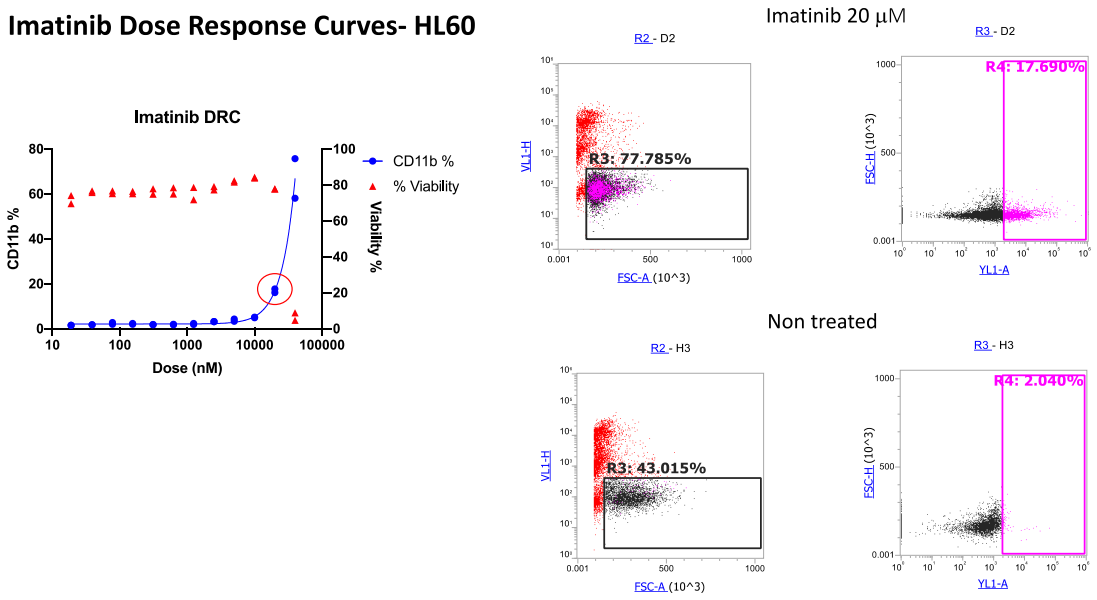


Figure 15: Representative flow cytometric analyses for HL60 cells treated with different concentrations of (A) Imatinib. (B) The representative FACS plots for 20 µM Imatinib show the cells expressing the % of CD11b in pink. The compound was done in technical triplicates for each of the concentrations and the experiments had been performed in biological triplicates.

RNA samples phenotypic effects confirmation

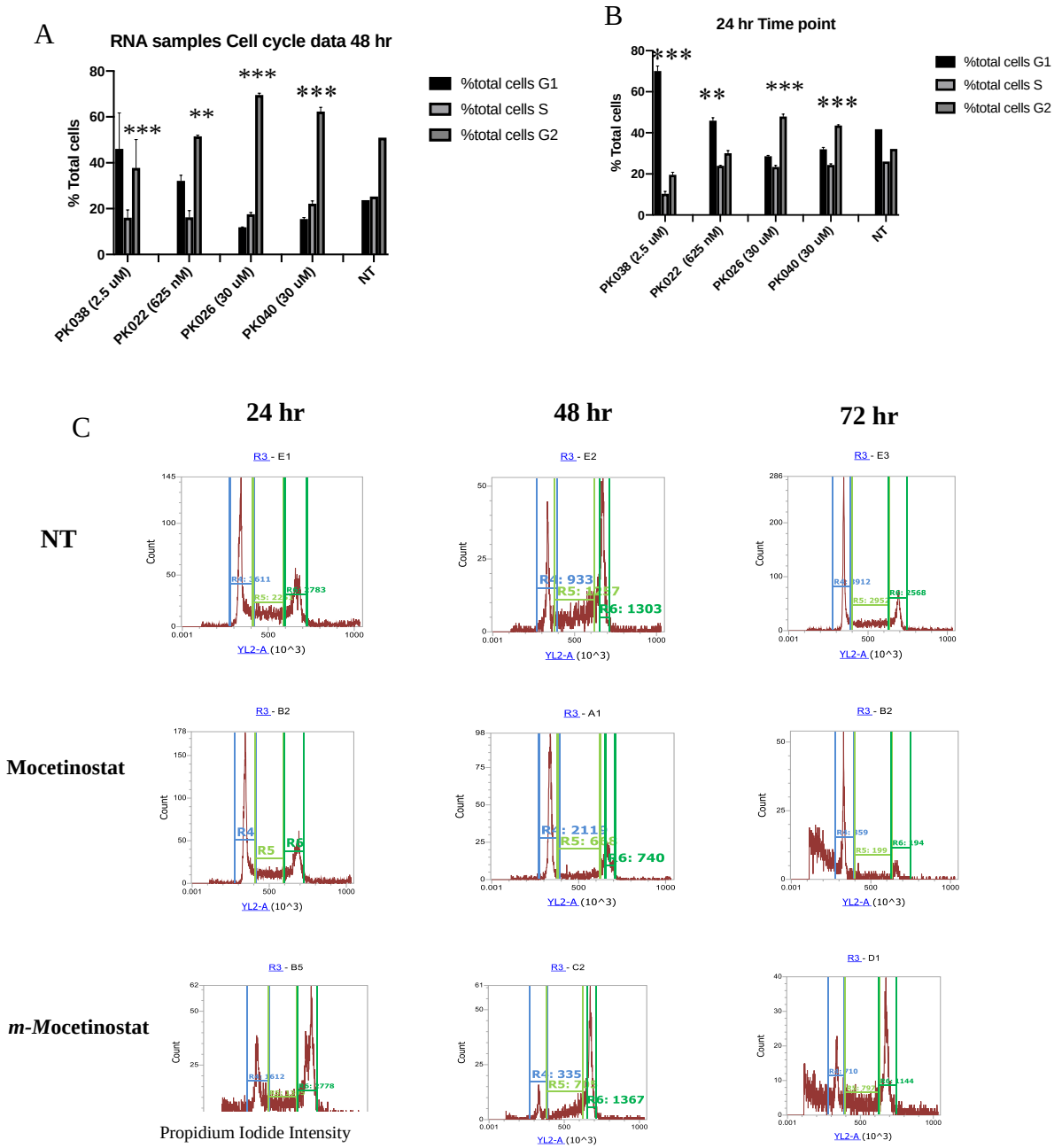
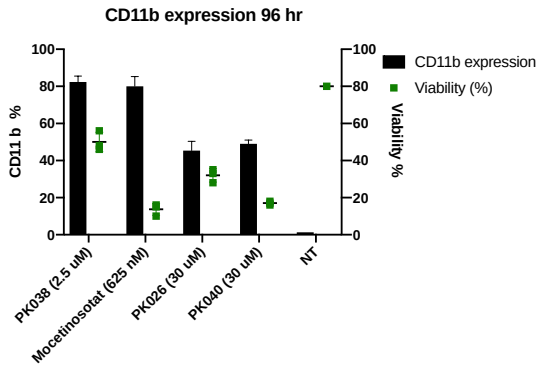


Figure 16: Effect of the compound PK026, PK040, Mocetinostat (PK022), D6 on cell cycle and distribution. HL60 were exposed to the following concentration of compounds for (A) 48 hr and (B) 24 hr after which they were treated with PI and subjected to cell cycle analysis

A



B

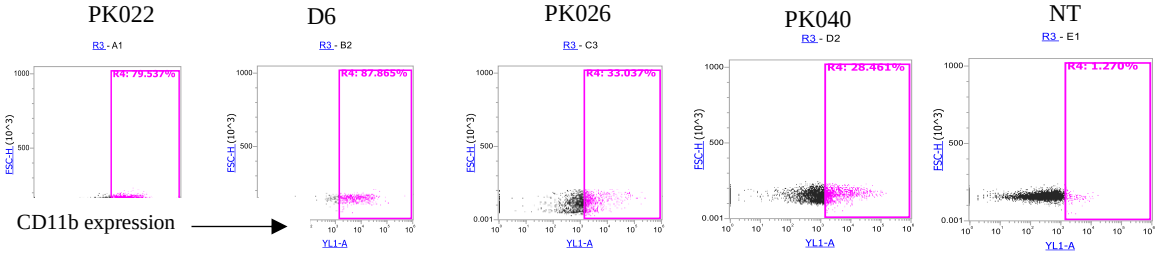
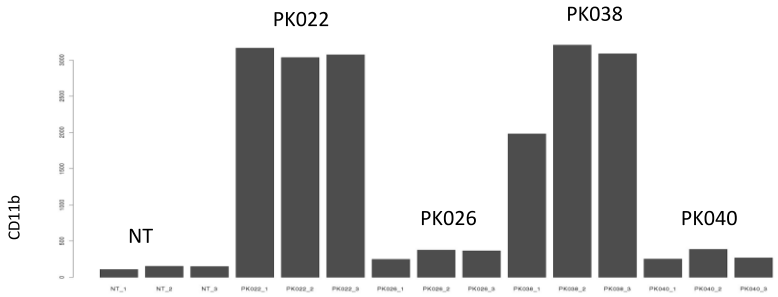


Figure 17: Effect of compounds on differentiation. HL60 cells were treated with respective concentrations of the following compounds for 4 days. The negative control for all cells were DMSO treated cells but the positive control was PMA. The percentage of cells expressing CD11b surface differentiation marker was determined by flow cytometry as described in Materials and Methods. (B) Representative FACS plots for the 4 compounds where R4 denotes the live cells expressing the marker of interest in pink.

RNA sequencing data analysis

A



B

Index	Name	P-value	Adjusted p-value	Odds Ratio	Combined score
1	MACROPHAGE	2.945e-64	3.181e-62	1.66	242.74
2	NEUTROPHIL	9.864e-30	5.327e-28	1.43	95.75
3	PERIPHERAL BLOOD	1.047e-20	3.771e-19	1.35	62.31
4	FIBROBLAST	1.302e-11	3.515e-10	1.25	31.42
5	PLASMACYTOID DENDRITIC CELL	4.623e-9	9.985e-8	1.22	23.37
6	GRANULOCYTE	8.448e-9	1.521e-7	1.21	22.56
7	BLOOD PBMC	2.049e-8	3.161e-7	1.21	21.38
8	NATURAL KILLER CELLS	3.338e-7	0.000004506	1.19	17.72
9	ALVEOLAR MACROPHAGE	5.661e-7	0.000006793	1.18	17.03
10	SPLEEN (BULK TISSUE)	0.0002186	0.002361	1.13	9.55

C

Index	Name	P-value	Adjusted p-value	Odds Ratio	Combined score
1	MACROPHAGE	3.303e-68	3.567e-66	1.64	254.54
2	NEUTROPHIL	2.767e-22	1.494e-20	1.35	66.87
3	PERIPHERAL BLOOD	1.607e-18	5.787e-17	1.31	53.78
4	FIBROBLAST	2.755e-15	7.438e-14	1.28	42.92
5	BLOOD PBMC	6.674e-8	0.000001442	1.19	19.63
6	LUNG (BULK TISSUE)	6.674e-8	0.000001201	1.19	19.63
7	SPLEEN (BULK TISSUE)	4.271e-7	0.000006590	1.18	17.24
8	ALVEOLAR MACROPHAGE	0.000001912	0.00002581	1.16	15.33
9	PLASMACYTOID DENDRITIC CELL	0.000002434	0.00002921	1.16	15.03
10	ASTROCYTE	0.000003917	0.00004230	1.16	14.43

Figure 18: (A) CD11b sense check for the poly A RNA sequencing samples. The experiment was done with technical triplicates. Y axis denotes the CD11b % and x-axis the sample name. (B) Enrichr analysis for mocetinostat and (C) D6 showing overlap of gene signatures with macrophage.

DRC for cell cycle analysis of HL60 cells treated with Mocetinostat

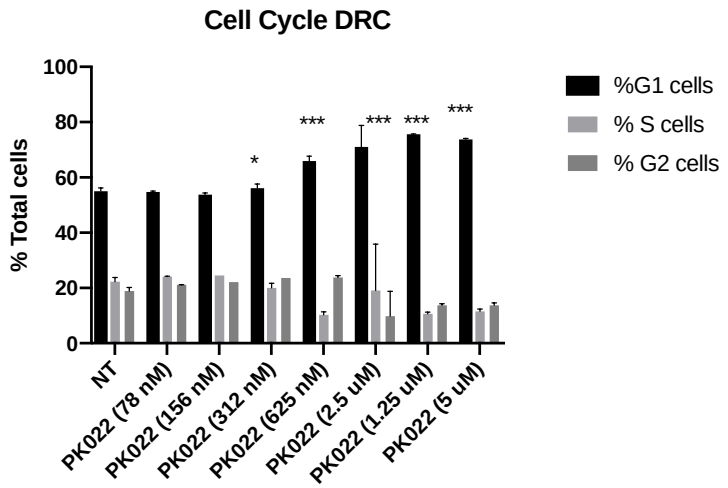
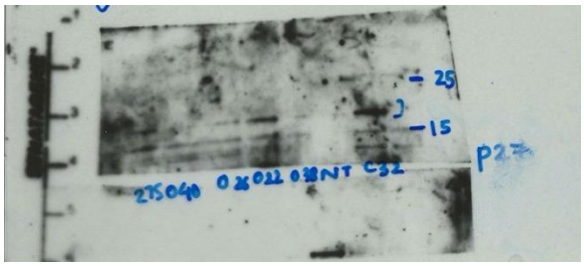
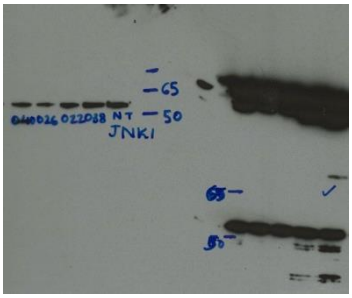
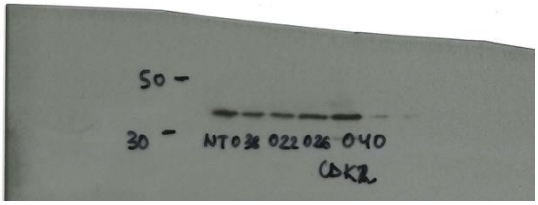


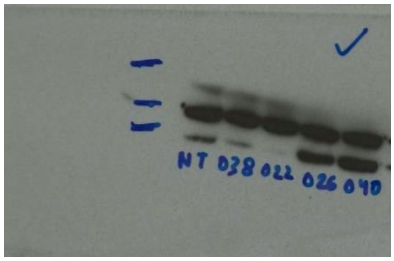
Figure19: Dose response curve for cell cycle analysis when HL60 cells were treated with different concentrations of Mocetinostat. The compound was done in technical triplicates for each of the concentrations and the experiments had been performed in biological triplicates.

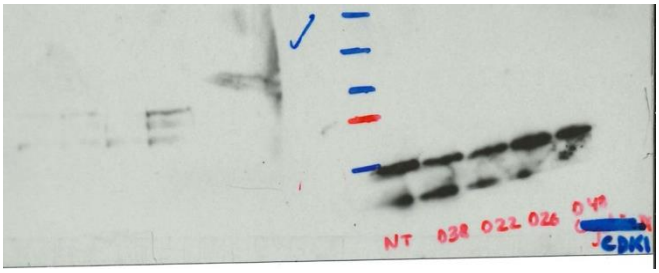
Western Blot Images

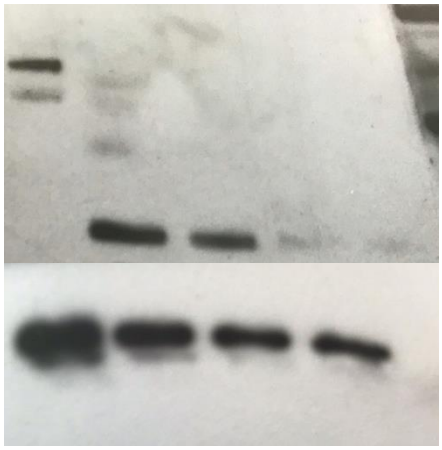












p21 MS275 2.5 uM 022 2.5 uM 038 2.5 uM NT

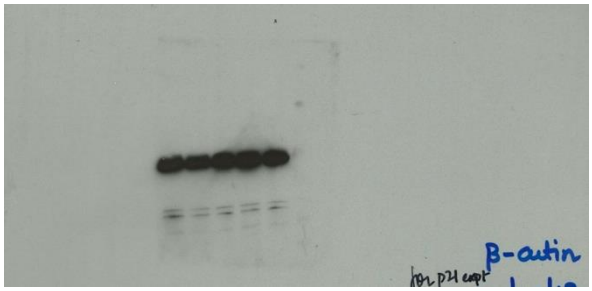


Figure 20: uncropped western blot image

Standard curve preparation using the HDAC assay standard (Color)

The HDAC assay standard (color) was diluted from 500 µM to a 2-fold dilution as described in the protocol. The HDAC Assay Standard was incubated at 37 °C for 10 minutes and the absorbance was read at 405 nm. The Standard was used in the range of 0 to 500 µM. The average absorbance or OD value at 405 nm is plotted on the y- axis versus the nmol of HDAC on the x- axis (Figure 21). The standard curve has an R^2 greater than 0.95 in order to determine the enzymatic activity from it.

A

Concentration (µM)	Product (nmol)
500	25
250	12.5
125	6.2
62.5	3.1
31.2	1.5
15.6	0.75
7.8	0.37

B

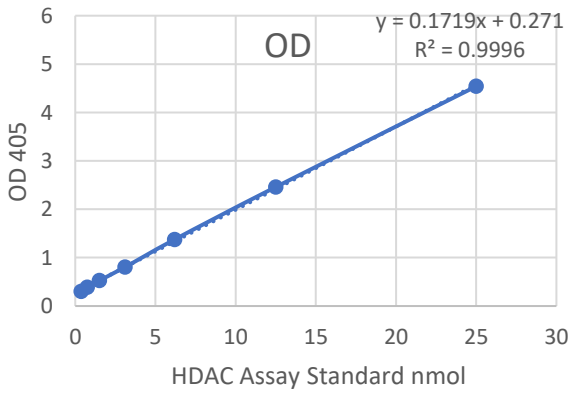


Figure 21: (A) The HDAC assay standard (colour) is made with a concentration ranging from 0 to 500 µM converted into nmol. (B) HDAC assay standard curve was prepared by testing the respective concentrations against the absorbance value of 405 nm.

A

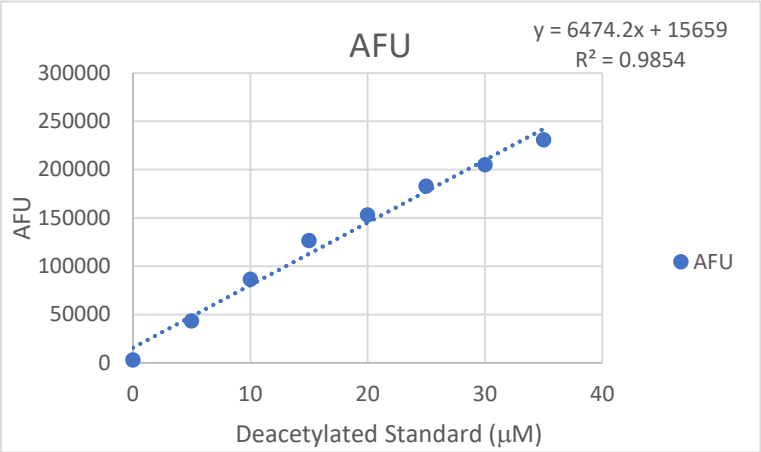


Figure 22: (A) The HDAC1 standard was prepared where the concentration on x-axis was plotted against the absorbance value measured at 460 nm.

Standard curve preparation for HL60 cells treated with compounds using the BSA assay standard

Samples	Concentration (µg/µL) 1:40 dilution
NT	1.554
D6	1.224
Mocetinostat	1.175
PK040	1.245

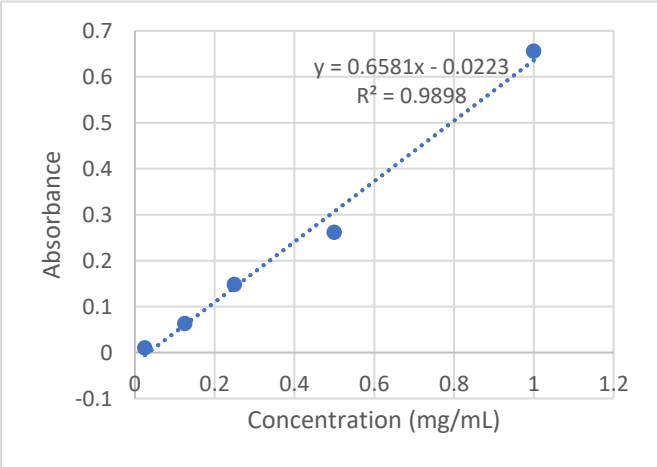


Figure 23: (A) BSA concentration of HL60 NT samples and the samples treated with the compounds D6, Mocetinostat, PK026 and PK040. (B) BSA standard curve showing the concentration of the protein in mg/mL on x – axis and the absorbance value (AU) at 595 nm on the y-axis.

Bibliography

Abdul-Hamid, G. 88+ MILLION TOP 1% MOST CITED SCIENTIST 12.2% Classification of Acute Leukemia.

Ablain, J., Nasr, R., Bazarbachi, A., and Thé, H. de (2011). The drug-induced degradation of oncoproteins: An unexpected achilles' heel of cancer cells? Cancer Discov. *1*: 117–127.

Allfrey, G., Faulkner, R., and Mirsky, A.E. (1964). Possible Role in the Regulation of Rna Synthesis *. Biochemistry *315*: 786–794.

Arber, D.A. (2017). Acute Myeloid Leukemia. In Hematopathology: A Volume in the Series: Foundations in Diagnostic Pathology, (Elsevier Inc.), pp 429-466.e5.

Ayeni, J.O., Audibert, A., Fichelson, P., Srayko, M., Gho, M., and Campbell, S.D. (2016). G2 phase arrest prevents bristle progenitor self-renewal and synchronizes cell division with cell fate differentiation. Dev. *143*: 1160–1169.

Bandyopadhyay, D., Mishra, A., and Medrano, E.E. (2004). Overexpression of histone deacetylase 1 confers resistance to sodium butyrate-mediated apoptosis in melanoma cells through a p53-mediated pathway. Cancer Res. *64*: 7706–7710.

Benedetti, R., Conte, M., and Altucci, L. (2015). Targeting Histone Deacetylases in Diseases: Where Are We? Antioxidants Redox Signal. *23*: 99–126.

Breitman, T.R., Collins, S.J., and Keene, B.R. (1981). in Response in accelerated. Blood *57*: 1000–1005.

Breitman, T.R., Selonick, S.E., and Collins, S.J. (1980). Induction of differentiation of the human promyelocytic leukemia cell line (HL-60) by retinoic acid. Proc. Natl. Acad. Sci. U. S. A. *77*: 2936–2940.

Bruserud, O. (2000). Induction of Differentiation and Apoptosis-- A Possible Strategy in the Treatment of Adult Acute Myelogenous Leukemia. Oncologist *5*: 454–462.

Burrows, F., Zhang, H., and Kamal, A. (2004). Hsp90 activation and cell cycle regulation. Cell Cycle *3*: 1530–1536.

Chen, S.M., Sun, H., Liu, Y.F., Ma, J., Zhang, Q.T., Zhu, J., et al. (2015). Expression of TRAIL and its receptor DR5 and their significance in acute leukemia cells. Genet. Mol. Res. *14*: 18562–18568.

Cherng, J.Y., Schuurmans-Nieuwenbroek, N.M.E., Jiskoot, W., Talsma, H., Zuidam, N.J., Hennink, W.E., et al. (1999). Effect of DNA topology on the transfection efficiency of poly((2-dimethylamino)ethyl methacrylate)-plasmid complexes. J. Control. Release.

Chung, J.H., and Bunz, F. (2010). Cdk2 is required for p53-independent G2/M checkpoint

control. PLoS Genet. *6*: 1–11.
Clawson, G.A. (2016). Histone deacetylase inhibitors as cancer therapeutics. Ann. Transl. Med. *4*: 1–5.
Crump, N.T., Hazzalin, C.A., Bowers, E.M., Alani, R.M., Cole, P.A., and Mahadevan, L.C. (2011). Dynamic acetylation of all lysine-4 trimethylated histone H3 is evolutionarily conserved and mediated by p300/CBP. Proc. Natl. Acad. Sci. U. S. A. *108*: 7814–7819.
Dang, L., White, D.W., Gross, S., Bennett, B.D., Bittinger, M.A., Driggers, E.M., et al. (2009). Cancer-associated IDH1 mutations produce 2-hydroxyglutarate. Nature *462*: 739–44.
Davie, J.R. (1998). Covalent modifications of histones: Expression from chromatin templates. Curr. Opin. Genet. Dev.
Dovey, O.M., Foster, C.T., and Cowley, S.M. (2010). Histone deacetylase 1 (HDAC1), but not HDAC2, controls embryonic stem cell differentiation. Proc. Natl. Acad. Sci. U. S. A. *107*: 8242–8247.
Eberharter, A., and Becker, P.B. (2002). Histone acetylation: A switch between repressive and permissive chromatin. Second in review on chromatin dynamics. EMBO Rep. *3*: 224–229.
Elmallah, M.I.Y., and Micheau, O. (2019). Epigenetic Regulation of TRAIL Signaling: Implication for Cancer Therapy. Cancers (Basel). *11*: 850.
Figueroa, M.E., Abdel-Wahab, O., Lu, C., Ward, P.S., Patel, J., Shih, A., et al. (2010). Leukemic IDH1 and IDH2 Mutations Result in a Hypermethylation Phenotype, Disrupt TET2 Function, and Impair Hematopoietic Differentiation. Cancer Cell *18*: 553–567.
Fish, K.N., Schmid, S.L., and Damke, H. (2000). Evidence that dynamin-2 functions as a signal-transducing GTPase. J. Cell Biol. *150*: 145–154.
Fisher, C.L., Pineault, N., Brookes, C., Helgason, C.D., Ohta, H., Bodner, C., et al. (2010). Loss-of-function additional sex combs like 1 mutations disrupt hematopoiesis but do not cause severe myelodysplasia or leukemia. Blood *115*: 38–46.
Fournel, M., Bonfils, C., Hou, Y., Yan, P.T., Kalita, A., Liu, J., et al. (2008). MGCD0103 , a novel isotype-selective histone deacetylase inhibitor , has broad spectrum antitumor activity in vitro and in vivo. *7*: 759–769.
Galanis, A., Ma, H., Rajkhowa, T., Ramachandran, A., Small, D., Cortes, J., et al. (2014). Crenolanib is a potent inhibitor of flt3 with activity against resistance-Conferring point mutants. Blood *123*: 94–100.
Gianní, M., Ponzanelli, I., Mologni, L., Reichert, U., Rambaldi, A., Terao, M., et al. (2000). Retinoid-dependent growth inhibition, differentiation and apoptosis in acute promyelocytic

leukemia cells. Expression and activation of caspases. Cell Death Differ. *7*: 447–460.
Gocek, E., and Marcinkowska, E. (2011). Differentiation therapy of acute myeloid leukemia. Cancers (Basel). *3*: 2402–2420.
Greenblatt, S.M., and Nimer, S.D. (2014). Chromatin modifiers and the promise of epigenetic therapy in acute leukemia. Leukemia *28*: 1396–1406.
Grimwade, D., Hills, R.K., Moorman, A. V, Walker, H., Chatters, S., Goldstone, A.H., et al. (2017). Refinement of cytogenetic classification in acute myeloid leukemia : determination of prognostic significance of rare recurring chromosomal abnormalities among 5876 younger adult patients treated in the United Kingdom Medical Research Council trials. *116*: 354–366.
Haidula, T. (2016). Windhoek Central Hospital overwhelmed. The Namibian *2015*: 5.
Hao, T., Li-Talley, M., Buck, A., and Chen, W.Y. (2019). An emerging trend of rapid increase of leukemia but not all cancers in the aging population in the United States. Sci. Rep. *9*: 1–13.
Hrgovic, I., Doll, M., Kleemann, J., Wang, X.F., Zoeller, N., Pinter, A., et al. (2012). The histone deacetylase inhibitor trichostatin a decreases lymphangiogenesis by inducing apoptosis and cell cycle arrest via p21-dependent pathways. BMC Bioinformatics *13*: 1–15.
Hsu, K.C., Liu, C.Y., Lin, T.E., Hsieh, J.H., Sung, T.Y., Tseng, H.J., et al. (2017). Novel Class IIa-Selective Histone Deacetylase Inhibitors Discovered Using an in Silico Virtual Screening Approach. Sci. Rep. *7*: 1–13.
Hu, S., Ueda, M., Stetson, L., Ignatz-Hoover, J., Moreton, S., Chakrabarti, A., et al. (2016). A novel glycogen synthase kinase-3 inhibitor optimized for acute myeloid leukemia differentiation activity. Mol. Cancer Ther. *15*: 1485–1494.
Hunt, A.G., and Walker, J.M. Polyadenylation in Plants Series Editor.
Ishihama, K., Yamakawa, M., Semba, S., Takeda, H., Kawata, S., Kimura, S., et al. (2007). Expression of HDAC1 and CBP/p300 in human colorectal carcinomas. J. Clin. Pathol. *60*: 1205–1210.
Jamaladdin, S., Kelly, R.D.W., O'Regan, L., Dovey, O.M., Hodson, G.E., Millard, C.J., et al. (2014). Histone deacetylase (HDAC) 1 and 2 are essential for accurate cell division and the pluripotency of embryonic stem cells. Proc. Natl. Acad. Sci. U. S. A. *111*: 9840–9845.
Jemal, A., Siegel, R., Ward, E., Murray, T., Xu, J., and Thun, M.J. (2007). Cancer Statistics, 2007. CA. Cancer J. Clin. *57*: 43–66.
Kapoor, G.S., Christie, A., and O'Rourke, D.M. (2007). EGFR inhibition in glioblastoma cells induces G2/M arrest and is independent of p53. Cancer Biol. Ther. *6*: 571–579.
Kim, T.K., and Eberwine, J.H. (2010). Mammalian cell transfection: The present and the

future. Anal. Bioanal. Chem. *397*: 3173–3178.
Kinigopoulou, M., Filippidou, M., Gogou, M., Giannousi, A., Fouka, P., Ntemou, N., et al. (2016). RSC Advances intermediates and analogues †‡. RSC Adv. *6*: 61458–61467.
Knight, T., Edwards, H., Taub, J.W., and Ge, Y. (2019). Evaluating venetoclax and its potential in treatment-naïve acute myeloid leukemia. Cancer Manag. Res. *11*: 3197–3213.
Kovacs, J.J., Murphy, P.J.M., Gaillard, S., Zhao, X., Wu, J.T., Nicchitta, C. V., et al. (2005). HDAC6 regulates Hsp90 acetylation and chaperone-dependent activation of glucocorticoid receptor. Mol. Cell.
Krämer, O.H., Mahboobi, S., and Sellmer, A. (2014). Drugging the HDAC6-HSP90 interplay in malignant cells. Trends Pharmacol. Sci. *35*: 501–509.
Kuleshov, M. V., Jones, M.R., Rouillard, A.D., Fernandez, N.F., Duan, Q., Wang, Z., et al. (2016). Enrichr: a comprehensive gene set enrichment analysis web server 2016 update. Nucleic Acids Res. *44*: W90–W97.
Kumar, A., D'Souza, S.S., and Thakur, A.S. (2019). Understanding the Journey of Human Hematopoietic Stem Cell Development. Stem Cells Int. *2019*: 1–13.
Lewis, T.A., Sykes, D.B., Law, J.M., Muñoz, B., Rustiguel, J.K., Nonato, M.C., et al. (2016). Development of ML390: A Human DHODH Inhibitor That Induces Differentiation in Acute Myeloid Leukemia. ACS Med. Chem. Lett. *7*: 1112–1117.
Lim, S., and Kaldis, P. (2012). Loss of Cdk2 and Cdk4 induces a switch from proliferation to differentiation in neural stem cells. Stem Cells *30*: 1509–1520.
Lim, S., and Kaldis, P. (2013). Cdks, cyclins and CKIs: roles beyond cell cycle regulation. Development *140*: 3079–3093.
Liu, F., Lin, S., Zhang, C., Ma, J., Han, Z., Jia, F., et al. (2019). The novel nature microtubule inhibitor ivalin induces G2/M arrest and apoptosis in human hepatocellular carcinoma SMMC-7721 cells in vitro. Med. *55*:.
Lo-Coco, F., Avvisati, G., Vignetti, M., Thiede, C., Orlando, S.M., Iacobelli, S., et al. (2013). Retinoic acid and arsenic trioxide for acute promyelocytic leukemia. N. Engl. J. Med. *369*: 111–121.
Lo-Coco, F., and Cicconi, L. (2014). What is the standard regimen for patients with acute promyelocytic leukemia? Curr. Hematol. Malig. Rep. *9*: 138–143.
Longo, D.L., Döhner, H., Weisdorf, D.J., and Bloomfield, C.D. (2015). Acute Myeloid Leukemia. N. Engl. J. Med. *373*: 1136–1152.
los Santos, M. De, Zambrano, A., and Aranda, A. (2007). Combined effects of retinoic acid and histone deacetylase inhibitors on human neuroblastoma SH-SY5Y cells. Mol. Cancer

Ther. *6*: 1425–1432.
Maeß, M.B., Wittig, B., and Lorkowski, S. (2014). Highly efficient transfection of human THP-1 macrophages by nucleofection. J. Vis. Exp. 1–9.
Marks, P.A., Rifkind, R.A., Richon, V.M., Breslow, R., Miller, T., and Kelly, W.K. (2001). HISTONE DEACETYLASES AND CANCER : CAUSES AND THERAPIES. *1*: 194–202.
Maurisse, R., Semir, D. De, Emamekhoo, H., Bedayat, B., Abdolmohammadi, A., Parsi, H., et al. (2010). Comparative transfection of DNA into primary and transformed mammalian cells from different lineages. BMC Biotechnol. *10*: 1–9.
Mcginniss, M.J., Kaback, M.M., Principles, R., Inheritance, A.D., Cancer, B., History, F., et al. Screening Heterozygote Testing and Carrier Genetic Heterogeneity.
Metcalf, D. (2007). On Hematopoietic Stem Cell Fate. Immunity *26*: 669–673.
Moiyadi, A. V., and Sridhar, E. (2015). δ-Aminolevulinic acid-induced fluorescence unmasks biological intratumoral heterogeneity within histologically homogeneous areas of malignant gliomas. Acta Neurochir. (Wien). *157*: 617–619.
Mughal, T.I., Ejaz, A.A., Foringer, J.R., and Coiffier, B. (2010). An integrated clinical approach for the identification, prevention, and treatment of tumor lysis syndrome. Cancer Treat. Rev. *36*: 164–176.
Nardo, C.D. Di, and Cortes, J.E. (2016). Mutations in AML: Prognostic and therapeutic implications. Hematology *2016*: 348–355.
Nebbioso, A., Clarke, N., Voltz, E., Germain, E., Ambrosino, C., Bontempo, P., et al. (2005a). Tumor-selective action of HDAC inhibitors involves TRAIL induction in acute myeloid leukemia cells. Nat. Med.
Nebbioso, A., Clarke, N., Voltz, E., Germain, E., Ambrosino, C., Bontempo, P., et al. (2005b). Tumor-selective action of HDAC inhibitors involves TRAIL induction in acute myeloid leukemia cells. Nat. Med. *11*: 77–84.
Newbold, A., Falkenberg, K.J., Prince, H.M., and Johnstone, R.W. (2016). How do tumor cells respond to HDAC inhibition? FEBS J. *283*: 4032–4046.
Niu, C., Yan, H., Yu, T., Sun, H.P., Liu, J.X., Xiu-Song, L., et al. (1999). Studies on treatment of acute promyelocytic leukemia with arsenic trioxide: Remission induction, follow-up, and molecular monitoring in 11 newly diagnosed and 47 relapsed acute promyelocytic leukemia patients. Blood *94*: 3315–3324.
Olsson, I., Bergh, G., Ehinger, M., and Gullberg, U. (2009). Cell differentiation in acute myeloid leukemia. Eur. J. Haematol. *57*: 1–16.
Palmer, A.C., and Kishony, R. (2015). mechanisms. 19–21.

Pan, R., Hogdal, L.J., Benito, J.M., Bucci, D., Han, L., Borthakur, G., et al. (2014). Selective BCL-2 inhibition by ABT-199 causes on-target cell death in acute myeloid Leukemia. Cancer Discov. *4*: 362–675.

Papaemmanuil, E., Gerstung, M., Bullinger, L., Gaidzik, V.I., Paschka, P., Roberts, N.D., et al. (2016). Genomic Classification and Prognosis in Acute Myeloid Leukemia. N. Engl. J. Med. *374*: 2209–2221.

Pastore, F., and Levine, R.L. (2016). Epigenetic regulators and their impact on therapy in acute myeloid leukemia. Haematologica *101*: 269–278.

Popovici-Muller, J., Lemieux, R.M., Artin, E., Saunders, J.O., Salituro, F.G., Travins, J., et al. (2018). Discovery of AG-120 (Ivosidenib): A First-in-Class Mutant IDH1 Inhibitor for the Treatment of IDH1 Mutant Cancers. ACS Med. Chem. Lett. *9*: 300–305.

Quek, L., David, M.D., Kennedy, A., Metzner, M., Amatangelo, M., Shih, A., et al. (2018). Clonal heterogeneity of acute myeloid leukemia treated with the IDH2 inhibitor enasidenib. Nat. Med. *24*: 1167–1177.

Quek, L., Otto, G.W., Garnett, C., Lhermitte, L., Karamitros, D., Stoilova, B., et al. (2016). Genetically distinct leukemic stem cells in human CD34 - acute myeloid leukemia are arrested at a hemopoietic precursor-like stage. J. Exp. Med. *213*: 1513–1535.

Quentmeier, H., Reinhardt, J., Zaborski, M., and Drexler, H.G. (2003). FLT3 mutations in acute myeloid leukemia cell lines. Leukemia *17*: 120–124.

Radomska, H.S., Bassères, D.S., Zheng, R., Zhang, P., Dayaram, T., Yamamoto, Y., et al. (2006). Block of C / EBP ? function by phosphorylation in acute myeloid leukemia with FLT3 activating mutations. *203*: 371–381.

Rau, R.E., Rodriguez, B., Luo, M., Jeong, M., Rosen, A., Rogers, J.H., et al. (2016). DOT1L as a therapeutic target for the treatment of DNMT3A-mutant acute myeloid leukemia. Blood *128*: blood-2015-11-684225.

Redner, R.L. (2002). Variations on a theme: the alternate translocations in APL. Leuk. Off. J. Leuk. Soc. Am. Leuk. Res. Fund, U.K *16*: 1927–1932.

Rego, E.M., Ruggero, D., Tribioli, C., Cattoretti, G., Kogan, S., Redner, R.L., et al. (2006). Leukemia with distinct phenotypes in transgenic mice expressing PML/RARα, PLZF/RARα or NPM/RARα. Oncogene *25*: 1974–1979.

Riva, L., Luzi, L., and Pelicci, P.G. (2012). Genomics of acute myeloid leukemia: The next generation. Front. Oncol. *2 MAY*: 1–12.

Rosato, R.R., Almenara, J.A., and Grant, S. (2003a). The Histone Deacetylase Inhibitor MS-275 Promotes Differentiation or Apoptosis in Human Leukemia Cells through a Process

Regulated by Generation of Reactive Oxygen Species and Induction of p21 CIP1/WAF1 1. CANCER Res. *63*: 3637–3645.
Rosato, R.R., Almenara, J.A., and Grant, S. (2003b). The Histone Deacetylase Inhibitor MS-275 Promotes Differentiation or Apoptosis in Human Leukemia Cells through a Process Regulated by Generation of Reactive Oxygen Species and Induction of p21 CIP1 / WAF1 1. 3637–3645.
Rosato, R.R., Almenara, J.A., and Grant, S. (2003c). The histone deacetylase inhibitor MS-275 promotes differentiation or apoptosis in human leukemia cells through a process regulated by generation of reactive oxygen species and induction of p21CIP1/WAF1. Cancer Res. *63*: 3637–3645.
Ru, F.G. (2006). Molecular profiling reveals myeloid leukemia cell lines to be faithful model systems characterized by distinct genomic aberrations. 994–1001.
Sachs, L. (1987). Cell Differentiation and Bypassing of Genetic Defects in the Suppression of Malignancy Perspectivesin CancerResearch Cell Differentiation and Bypassing of Genetic Defects in the Suppression of. 1981–1986.
Sahakian, E., Powers, J., Chen, J., Distler, A., Rock-Klotz, J., Deng, S., et al. (2013). A Novel Role For Histone Deacetylase 11 (HDAC11) As a Regulator Of Neutrophil Function and Differentiation In Normal and Malignant Hematopoesis. Blood *122*: 2267.
San, E., Gimenez-camino, N., and Agirre, X. (2019). HDAC Inhibitors in Acute Myeloid Leukemia. 1–24.
Santos, F.P.S. (2011). Histone deacetylase inhibitors for the treatment of myelodysplastic syndrome and acute myeloid leukemia. 226–235.
Schnerch, D., Yalcintepe, J., Schmidts, A., Becker, H., Follo, M., Engelhardt, M., et al. (2012a). Cell cycle control in acute myeloid leukemia. Am. J. Cancer Res. *2*: 508–28.
Schnerch, D., Yalcintepe, J., Schmidts, A., Becker, H., Follo, M., and Wäsch, R. (2012b). Cell cycle control in acute myeloid leukemia. *2*: 508–528.
Schroeder, A., Mueller, O., Stocker, S., Salowsky, R., Leiber, M., Gassmann, M., et al. (2006). The RIN: An RNA integrity number for assigning integrity values to RNA measurements. BMC Mol. Biol. *7*: 1–14.
Schutte, B., Nuydens, R., Geerts, H., and Ramaekers, F. (1998). Annexin V binding assay as a tool to measure apoptosis in differentiated neuronal cells. J. Neurosci. Methods.
She, S., Wei, Q., Kang, B., and Wang, Y.J. (2017). Cell cycle and pluripotency: Convergence on octamer-binding transcription factor 4 (Review). Mol. Med. Rep. *16*: 6459–6466.
Shlush, L.I., Zandi, S., Mitchell, A., Chen, W.C., Brandwein, J.M., Gupta, V., et al. (2014).

Identification of pre-leukaemic haematopoietic stem cells in acute leukaemia. Nature *506*: 328–333.

Singh, A.M., Chappell, J., Trost, R., Lin, L., Wang, T., Tang, J., et al. (2013). Cell-cycle control of developmentally regulated transcription factors accounts for heterogeneity in human pluripotent cells. Stem Cell Reports.

Soignet, S.L., Maslak, P., Wang, Z.G., Jhanwar, S., Calleja, E., Dardashti, L.J., et al. (1998). Complete remission after treatment of acute promyelocytic leukemia with arsenic trioxide. N. Engl. J. Med.

Soufi, A., and Dalton, S. (2016). Cycling through developmental decisions: How cell cycle dynamics control pluripotency, differentiation and reprogramming. Dev. *143*: 4301–4311.

Stroh, T., Erben, U., Kühl, A.A., Zeitz, M., and Siegmund, B. (2010). Combined pulse electroporation - A novel strategy for highly efficient transfection of human and mouse cells. PLoS One *5*:.

Sykes, D.B., Kfoury, Y.S., Mercier, F.E., Wawer, M.J., Law, J.M., Haynes, M.K., et al. (2016). Inhibition of Dihydroorotate Dehydrogenase Overcomes Differentiation Blockade in Acute Myeloid Leukemia. Cell *167*: 171-186.e15.

Tanaka, S., Miyagi, S., Sashida, G., Chiba, T., Yuan, J., Mochizuki-Kashio, M., et al. (2012). Ezh2 augments leukemogenicity by reinforcing differentiation blockage in acute myeloid leukemia. Blood *120*: 1107–1117.

Testa, U., and Riccioni, R. (2007). Deregulation of apoptosis in acute myeloid leukemia. Haematologica *92*: 81–94.

Toress-Collado, A.X., Nazarian, R., and Jazirehi, A.R. (2017). Rescue of cell cycle progression in BRAFV600E inhibitor–resistant human melanoma by a chromatin modifier. Tumor Biol. *39*:.

Traore, K., Trush, M.A., George, M., Spannhake, E.W., Anderson, W., and Asseffa, A. (2005). Signal transduction of phorbol 12-myristate 13-acetate (PMA)-induced growth inhibition of human monocytic leukemia THP-1 cells is reactive oxygen dependent. Leuk. Res. *29*: 863–879.

Tsai, S., Bartelmez, S., Heyman, R., Damm, K., Evans, R., and Collins, S.J. (1992). A mutated retinoic acid receptor-alpha exhibiting dominant- negative activity alters the lineage development of a multipotent hematopoietic cell line. Genes Dev. *6*: 2258–2269.

Tsai, S.C., and Seto, E. (2002). Regulation of histone deacetylase 2 by protein kinase CK2. J. Biol. Chem. *277*: 31826–31833.

Tseng, C.J., Wang, Y.J., Liang, Y.C., Jeng, J.H., Lee, W. Sen, Lin, J.K., et al. (2002).

Microtubule damaging agents induce apoptosis in HL 60 cells and G2/M cell cycle arrest in HT 29 cells. Toxicology.

Wagner, F.F., Weyiwer, M., Lewis, M.C., and Holson, E.B. (2013). Small Molecule Inhibitors of Zinc-dependent Histone Deacetylases. Neurotherapeutics *10*: 589–604.

Wang, H., Zhang, T., Sun, W., Wang, Z., Zuo, D., Zhou, Z., et al. (2016). Erianin induces G2/M-phase arrest, apoptosis, and autophagy via the ROS/JNK signaling pathway in human osteosarcoma cells in vitro and in vivo. Cell Death Dis. *7*:.

Ward, P.S., Patel, J., Wise, D.R., Abdel-Wahab, O., Bennett, B.D., Coller, H.A., et al. (2010). The Common Feature of Leukemia-Associated IDH1 and IDH2 Mutations Is a Neomorphic Enzyme Activity Converting ??-Ketoglutarate to 2-Hydroxyglutarate. Cancer Cell *17*: 225–234.

Welch, J.S., Ley, T.J., Link, D.C., Miller, C.A., Larson, D.E., Koboldt, D.C., et al. (2012). The origin and evolution of mutations in acute myeloid leukemia. Cell *150*: 264–278.

Woalder (2017). 乳鼠心肌提取 HHS Public Access. Physiol. Behav. *176*: 139–148.

Xu, W.S., Parmigiani, R.B., and Marks, P.A. (2007). Histone deacetylase inhibitors: Molecular mechanisms of action. Oncogene *26*: 5541–5552.

Yang, F., Zhao, N., Ge, D., and Chen, Y. (2019). Next-generation of selective histone deacetylase inhibitors. RSC Adv. *9*: 19571–19583.

Yang, Y., Wang, G., Wu, W., Yao, S., Han, X., He, D., et al. (2018). Camalexin induces apoptosis via the ROS-ER stress-mitochondrial apoptosis pathway in AML cells. Oxid. Med. Cell. Longev. *2018*:.

Zhang, J., Jagannathan, S., Aban, A., Okerberg, E., Herring, C., and Kozarich, J.W. (2012). of Native Kinases. *18*: 699–710.

Zhang, L., Zheng, Y., Deng, H., Liang, L., and Peng, J. (2014). Aloperine induces G2/M phase cell cycle arrest and apoptosis in HCT116 human colon cancer cells. Int. J. Mol. Med. *33*: 1613–1620.

Zhao, K.W., Li, X., Zhao, Q., Huang, Y., Li, D., Peng, Z.G., et al. (2004). Protein kinase Cδ mediates retinoic acid and phorbol myristate acetate-induced phospholipid scramblase 1 gene expression: Its role in leukemic cell differentiation. Blood *104*: 3731–3738.

Zhu, H., Miao, Z.H., Huang, M., Feng, J.M., Zhang, Z.X., Lu, J.J., et al. (2009). Naphthalimides induce G2 arrest through the ATM-activated Chk2-executed pathway in HCT116 cells. Neoplasia *11*: 1226–1234.